



THESIS APPROVAL

GRADUATE SCHOOL, KASETSART UNIVERSITY

Master of Science (Biochemistry)

DEGREE

Biochemistry

FIELD

Biochemistry

DEPARTMENT

TITLE: Protein Engineering of a β -Glucosidase for Hydrolysis of Soybean Isoflavonoids

NAME: Mr. Satrawut Charoenla

THIS THESIS HAS BEEN ACCEPTED BY

THESIS ADVISOR

(Assistant Professor Prachumporn T. Kongsaree, Ph.D.)

THESIS CO-ADVISOR

(Assistant Professor Nonlawat Boonyalai, Ph.D.)

DEPARTMENT HEAD

(Assistant Professor Amornrat Promboon, Ph.D.)

APPROVED BY THE GRADUATE SCHOOL ON

DEAN

(Associate Professor Gunjana Theeragool, D.Agr.)

THESIS

PROTEIN ENGINEERING OF A β -GLUCOSIDASE FOR HYDROLYSIS OF SOYBEAN ISOFLAVONOIDS



SATRAWUT CHAROENLA

A Thesis Submitted in Partial Fulfillment of
the Requirements for the Degree of
Master of Science (Biochemistry)
Graduate School, Kasetsart University

2014

Satrawut Charoenla 2014: Protein Engineering of a β -Glucosidase for Hydrolysis of Soybean Isoflavonoids. Master of Science (Biochemistry), Major Field: Biochemistry, Department of Biochemistry. Thesis Advisor: Assistant Professor Prachumporn T. Kongsaree, Ph.D. 134 pages.

Three leguminous isoflavone β -glucosidases, namely dalcocinase (from *Dalbergia cochinchinensis* Pierre), Dnbglu2 (from *Dalbergia nigrescen* Kruz) and GmICHG (from *Glycine max*), share about 60-80% sequence identity, but their catalytic efficiencies toward soybean isoflavone glucosides are different. Previous study revealed that changing single amino acid residues in the binding pocket of dalcocinase to the corresponding residues of GmICHG, namely A454F, E455A and S459V, could increase the catalytic efficiency for hydrolysis of soybean isoflavone glucosides, when compared with the wild-type dalcocinase. So, this study aims to construct the corresponding double and triple mutations in order to determine the interaction of amino acid residues, which may influence the hydrolytic efficiency toward soybean isoflavone glucosides. All dalcocinase mutants were approximately 66 kDa, which were similar to the wild-type enzyme. All double mutants showed improved hydrolytic efficiencies toward *p*-nitrophenyl- β -D-glucoside and dalcocinin-8'-*O*- β -D-glucoside when compared with the wild-type enzyme. For the hydrolysis of soybean isoflavone glucosides, the A454F/E455A mutant showed high hydrolytic efficiencies toward daidzin, genistin, malonyldaidzin and malonylgenistin. The A454F/S459V and E455A/S459V mutants showed increases in hydrolytic efficiencies toward genistin, malonyldaidzin and malonylgenistin. However, none of the triple mutants showed improved hydrolytic efficiencies toward those substrates. Moreover, the E455A/S459V mutant showed high ability for hydrolysis of soybean flour suspension. Therefore, the E455A/S459V mutant may be applied in food industry for releasing free isoflavone aglycones to improve the nutritional values of soybean food products.

Student's signature

Thesis Advisor's signature

ACKNOWLEDGEMENTS

I would like to express my sincere gratitude to my thesis advisor, Assistant Professor Dr. Prachumporn Kongsaree, for her invaluable suggestions and constant encouragement throughout this research. I am very impressed by her worthy advices, not only for my research progress, but also for my future career goals.

I would like to express my sincere thank to my thesis co-advisor, Assistant Professor Dr. Nonlawat Boonyalai for his valuable suggestions and Assistant Professor Patchreenart Saparpakorn from the department of chemistry, Kasetsart University for teaching me to operate the GOLD docking software.

I also thank the Center for Advanced Studies in Tropical Natural Resources under the project of National Research Universities, Kasetsart University, Bangkok, Thailand for providing the scholarship.

Finally, I would like to sincerely acknowledge my beloved parents who always stand by my side and provide me the support, faith, and inner strength. I would like to extend my thanks to all members in the PK's laboratory and my BC14th friends for their suggestions and friendship. I would not have achieved as far and this research would not have been completed without these people whose supports are much appreciated.

Satrawut Charoenla

July 2014

TABLE OF CONTENTS

	Page
TABLE OF CONTENTS	i
LIST OF TABLES	ii
LIST OF FIGURES	iv
LIST OF ABBREVIATIONS	ix
INTRODUCTION	1
OBJECTIVES	4
LITERATURE REVIEW	5
MATERIALS AND METHODS	24
Materials	24
Methods	28
RESULTS AND DISCUSSION	38
CONCLUSION	80
LITERATURE CITED	82
APPENDICES	88
Appendix A: DNA and protein techniques	89
Appendix B: Standard curves	96
Appendix C: Sequencing results of dalcochinase mutants	101
Appendix D: Kinetic results	110
Appendix E: HPLC chromatograms	127
CIRRICULUM VITAE	134

LIST OF TABLES

Table		Page
1	Hydrolysis of isoflavone glucosides by natural GmICHG	13
2	Hydrolysis of isoflavone glucosides by the recombinant GmICHG	14
3	Kinetic efficiencies of different β -glucosidases toward isoflavone glucosides	18
4	Kinetic parameters of dalcochinase, Dnbglu2 and GmICHG toward soybean isoflavone glucosides	19
5	Kinetic efficiencies of dalcochinase and its mutant forms toward soybean isoflavone glucosides	21
6	List of chemicals and reagents used in this study and their manufacturers	24
7	Mutagenic primers used in this study	28
8	Screening primers used in this study	30
9	Hydrogen fixed for docking	37
10	Absorbance at 400 nm measuring β -glucosidase activities of 50 colonies of each dalcochinase mutant toward <i>p</i> NP-Glc	44
11	Purification table of the A454F/E455A mutant	47
12	Purification table of the A454F/S459V mutant	47
13	Purification table of the E455A/S459V mutant	47
14	Purification table of the A454F/E455A/S459V mutant	48
15	Kinetic parameters of the wild-type and mutant forms of dalcochinase toward <i>p</i> NP-Glc	51
16	Kinetic parameters of the wild-type and mutant forms of dalcochinase toward dalcochinin-8'- <i>O</i> - β -D-glucoside	52
17	Kinetic parameters of the wild-type and mutant forms of dalcochinase toward daidzin	54
18	Kinetic parameters of the wild-type and mutant forms of dalcochinase toward genistin	55

LIST OF TABLES (Continued)

Table		Page
19	Kinetic parameters of the wild-type and mutant forms of dalcochinase toward malonyldaidzin	57
20	Kinetic parameters of the wild-type and mutant forms of dalcochinase toward malonylgenistin	59
21	Relative amount of soybean isoflavone glucosides after incubation with β -glucosidase from almond	62
22	Relative amount of soybean isoflavone glucosides after incubation with the wild-type dalcochinase	63
23	Relative amount of soybean isoflavone glucosides after incubation with the E455A mutant	64
24	Relative amount of soybean isoflavone glucosides after incubation with the A454F/E455A mutant	65
25	Relative amount of soybean isoflavone glucosides after incubation with the E455A/S459V mutant	66
26	Evaluation of the structural models of the wild-type dalcochinase, the A454F/E455A mutant, and GmICHG	69
27	Summary of distances between residues of dalcochinase and malonylgenistin	73
28	Summary of distances between residues of GmICHG and malonylgenistin	74

Appendix Table

A1	Preparation of 10 % SDS-polyacrylamide gel	93
A2	Preparation of 8 % Non-denaturing polyacrylamide gel	94
E1	Area under peaks of the soybean isoflavone glucoside standards	128

LIST OF FIGURES

Figure		Page
1	Mechanisms of β -glucosidases including inverting mechanism (A) and retaining mechanism (B)	7
2	Three-dimensional structures of β -glucosidases from different GH families	8
3	Structures of dalcochinin-8'-O- β -D-glucoside (left) and rotenone (right)	9
4	Structures of dalpatein diglycoside (R_1 - R_2 = O-CH ₂ -O) and dalnigreïn diglycoside (R_1 , R_2 = OMe)	11
5	Hydrolysis of isoflavone glucoside substrates by GmICHG to yield aglycone forms	12
6	Schematic diagram of isoflavone glucoside biosynthesis and its activity	16
7	Diagram of pPICZ α A, B and C	22
8	Diagram of pPICZ-His ₈ -trncTRBG	27
9	Restriction digestion of pPICZ-His ₈ -trncTRBG by <i>Pst</i> I, <i>Xba</i> I and <i>Bam</i> HI restriction endonucleases	38
10	PCR products of all dalcochinase mutants generated by site-directed mutagenesis approach	39
11	Screening of <i>E. coli</i> colonies harboring dalcochinase mutants by using colony PCR method and specific screening primers	40
12	Chromatogram of the wild-type dalcochinase	41
13	Chromatograms of the dalcochinase mutants	42
14	Comparison of nucleotide sequences of the wild-type dalcochinase and the double and triple mutants	43
15	Analysis of sizes and identities of all dalcochinase mutants	48
16	Analysis of the native forms of wild-type dalcochinase and the mutant forms	49

LIST OF FIGURES (Continued)

Figure	Page
17 HPLC profiles of soybean isoflavone glucoside standards and soybean isoflavone glucoside from soybean flour extract	61
18 Relative amount of soybean isoflavone glucosides after incubation with various enzymes	67
19 Overall structural models of the wild-type dalcochinase and GmICHG	70
20 The docking result of malonylgenistin in the wild-type dalcochinase model	71
21 The docking result of malonylgenistin in the GmICHG model	72
22 The interactions between malonylgenistin and the residues in the aglycone binding pocket of the wild-type dalcochinase and GmICHG	75
23 The interactions between malonylgenistin and the residues in the binding pocket of the wild-type dalcochinase and GmICHG	77
24 The interactions between malonyldaidzin and the residues in the binding pocket of the A454F/E455A mutant	78
25 Sequence alignment of four β -glucosidases	79
 Appendix Figure	
A1 The orientation of PVDF membrane and polyacrylamide gel	95
B1 Standard curve of protein	97
B2 Standard curve of <i>p</i> NP for determination of β -glucosidase activities during expression and purification steps	97
B3 Standard curve of <i>p</i> NP for determination of β -glucosidase activities for kinetic study	98
B4 Standard curve of glucose	98
B5 Standard curve of daidzein	99
B6 Standard curve of genistein	100

LIST OF FIGURES (Continued)

Appendix Figure		Page
D1	Michaelis-Menten plot of the A454F/E455A dalcochinase mutant toward <i>p</i> -NP-Glc	111
D2	Michaelis-Menten plot of the A454F/S459V dalcochinase mutant toward <i>p</i> -NP-Glc	111
D3	Michaelis-Menten plot of the E455A/S459V dalcochinase mutant toward <i>p</i> -NP-Glc	112
D4	Michaelis-Menten plot of the A454F/E455A/S459V dalcochinase mutant toward <i>p</i> -NP-Glc	112
D5	Michaelis-Menten plot of the A454F/E455A dalcochinase mutant toward dalcochinin-8'- <i>O</i> - β -D-glucoside	113
D6	Michaelis-Menten plot of the A454F/S459V dalcochinase mutant toward dalcochinin-8'- <i>O</i> - β -D-glucoside	113
D7	Michaelis-Menten plot of the E455A/S459V dalcochinase mutant toward dalcochinin-8'- <i>O</i> - β -D-glucoside	114
D8	Michaelis-Menten plot of the A454F/E455A/S459V dalcochinase mutant toward dalcochinin-8'- <i>O</i> - β -D-glucoside	114
D9	Michaelis-Menten plot of the A454F/E455A dalcochinase mutant toward daidzin	115
D10	Michaelis-Menten plot of the A454F/S459V dalcochinase mutant toward daidzin	115
D11	Michaelis-Menten plot of the E455A/S459V dalcochinase mutant toward daidzin	116
D12	Lineweaver-Burk plot of the E455A/S459V dalcochinase mutant toward daidzin	116
D13	Michaelis-Menten plot of the A454F/E455A/S459V dalcochinase mutant toward daidzin	117

LIST OF FIGURES (Continued)

Appendix Figure	Page
D14 Lineweaver-Burk plot of the A454F/E455A/S459V dalcochinase mutant toward daidzin	117
D15 Michaelis-Menten plot of the A454F/E455A dalcochinase mutant toward genistin	118
D16 Michaelis-Menten plot of the A454F/S459V dalcochinase mutant toward genistin	118
D17 Michaelis-Menten plot of the E455A/S459V dalcochinase mutant toward genistin	119
D18 Michaelis-Menten plot of the A454F/E455A/S459V dalcochinase mutant toward genistin	119
D19 Michaelis-Menten plot of the A454F/E455A dalcochinase mutant toward malonyldaidzin	120
D20 Michaelis-Menten plot of the A454F/S459V dalcochinase mutant toward malonyldaidzin	120
D21 Lineweaver-Burk plot of the A454F/S459V dalcochinase mutant toward malonyldaidzin	121
D22 Michaelis-Menten plot of the A454F/S459V dalcochinase mutant toward malonyldaidzin	121
D23 Lineweaver-Burk plot of the E455A/S459V dalcochinase mutant toward malonyldaidzin	122
D24 Michaelis-Menten plot of the A454F/E455A/S459V dalcochinase mutant toward malonyldaidzin	122
D25 Lineweaver-Burk plot of the A454F/E455A/S459V dalcochinase mutant toward malonyldaidzin	123
D26 Michaelis-Menten plot of the A454F/E455A dalcochinase mutant toward malonylgenistin	124
D27 Michaelis-Menten plot of the A454F/S459V dalcochinase mutant toward malonylgenistin	124

LIST OF FIGURES (Continued)

Appendix Figure	Page
D28 Michaelis-Menten plot of the E455A/S459V dalcochinase mutant toward malonylgenistin	125
D29 Michaelis-Menten plot of the A454F/E455A/S459V dalcochinase mutant toward malonylgenistin	125
D30 Lineweaver-Burk plot of the A454F/E455A/S459V dalcochinase mutant toward malonylgenistin	126
E1 HPLC chromatogram of control reaction	128
E2 HPLC chromatogram of reaction incubated with almond β -glucosidase at 10 min	129
E3 HPLC chromatogram of reaction incubated with almond β -glucosidase at 4 h	129
E4 HPLC chromatogram of reaction incubated with the wild-type dalcochinase at 10 min	130
E5 HPLC chromatogram of reaction incubated with the wild-type dalcochinase at 4 h	130
E6 HPLC chromatogram of reaction incubated with the E455A mutant at 10 min	131
E7 HPLC chromatogram of reaction incubated with the E455A mutant at 4 h	131
E8 HPLC chromatogram of reaction incubated with the A454F/E455A mutant at 10 min	132
E9 HPLC chromatogram of reaction incubated with the A454F/E455A mutant at 4 h	132
E10 HPLC chromatogram of reaction incubated with the E455A/S459V mutant at 10 min	133
E11 HPLC chromatogram of reaction incubated with the E455A/S459V mutant at 4 h	133

LIST OF ABBREVIATIONS

ABTS	2,2'-Azino-bis(3-ethylbenzothiazoline-6-sulphonic acid)
dNTP	Deoxyribonucleotide triphosphate
DMSO	Dimethyl sulfoxide
EDTA	Ethylenediaminetetraacetic acid
GmICHG	<i>Glycine max</i> isoflavone conjugate-hydrolyzing β -glucosidase
HPLC	High performance liquid chromatography
K_m	Michaelis constant
k_{cat}	Turnover number
k_{cat}/K_m	Catalytic efficiency
4MU-Glc	4-Methylumbelliferyl- β -D-glucoside
Non-denaturing PAGE	Non-denaturing polyacrylamide gel electrophoresis
<i>p</i> NP	<i>para</i> -nitrophenol
<i>p</i> NP-Glc	<i>para</i> -nitrophenyl- β -D-glucopyranoside
SDS-PAGE	Sodium dodecyl sulfate-polyacrylamide gel electrophoresis
TEMED	N,N,N',N'-tetramethylethylenediamine

PROTEIN ENGINEERING OF A β -GLUCOSIDASE FOR HYDROLYSIS OF SOYBEAN ISOFLAVONOIDS

INTRODUCTION

β -Glucosidases (EC 3.2.1.21) catalyze the hydrolysis of β -glucosidic bonds between glucose (glycone) and another glycone or noncarbohydrate moiety (aglycone) such as isoflavone. The molecular mass of most β -glucosidase is approximately 55 – 65 kDa, and the optimal pH is approximately 5.0 – 6.0. Moreover, β -glucosidases from different sources have different substrate specificities because of the differences in amino acid sequences (Ketudat Cairns and Esen, 2010). For this reason, β -glucosidases catalyze the hydrolysis of various glucoside substrates, such as cyanogenic glucoside, cellobiose, isoflavone glucoside, phenolic glucoside and thioglucoside (Svasti *et al.*, 1999).

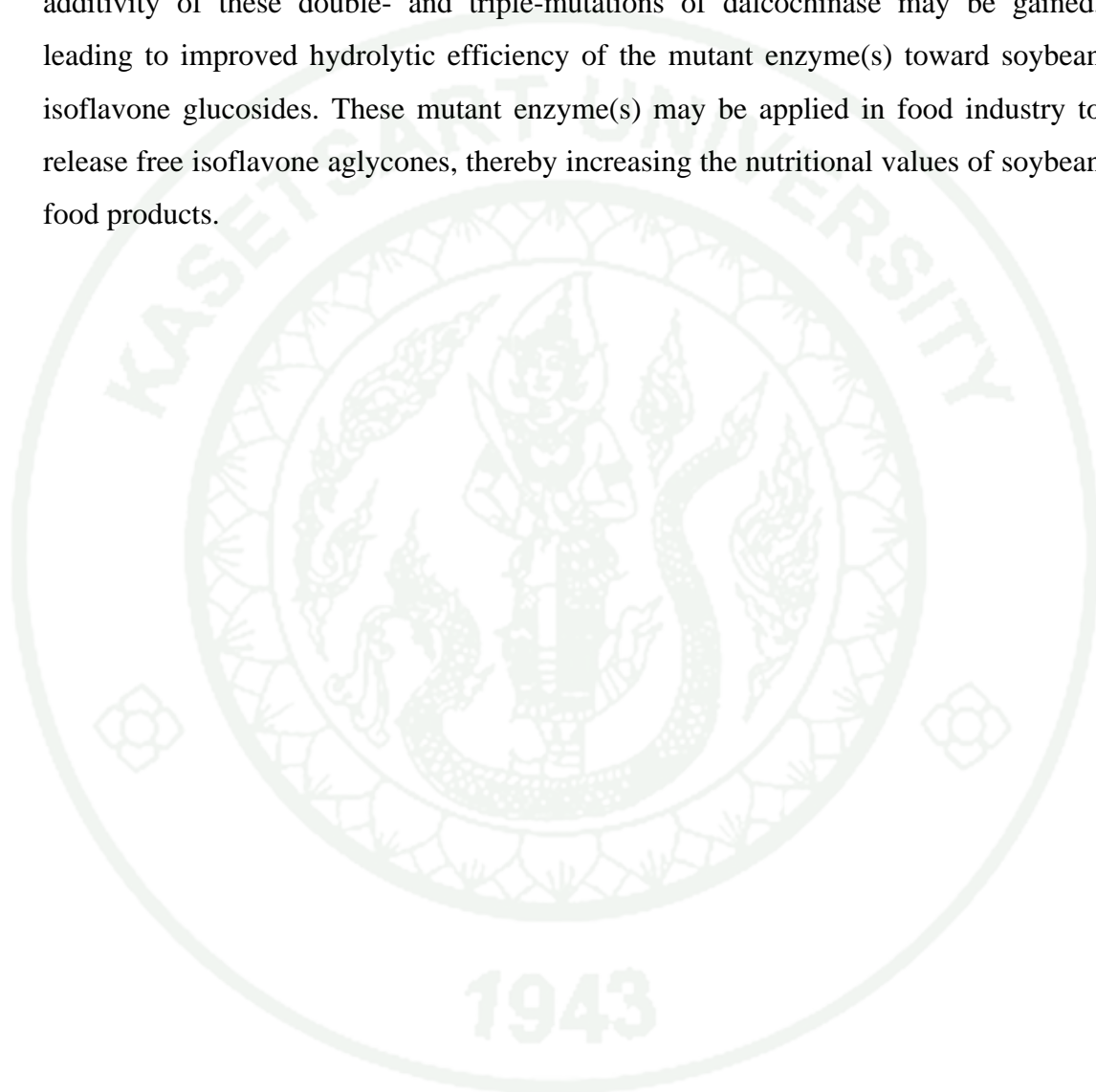
Isoflavone glucosides are important substrates of β -glucosidases. Isoflavone glucosides are hydrolyzed to yield isoflavone aglycones. Soybean isoflavones are important phytohormones. Their structures are similar to estrogen in human. For this reason, soybean isoflavones show beneficial activities against cancer, heart disease, menopausal symptom and osteoporosis (Pyo *et al.*, 2005). Isoflavones, such as genistein, daidzein, and glycitein, are mostly found in soybean and soybean food products. However, these soybean isoflavones are often conjugated with glucose, to form isoflavone glucosides, such as genistin, daidzin and glycitin, respectively. Moreover, the glucosyl group of the isoflavone glucosides may be modified at the C-6 position by a malonyl group to form malonylgenistin, malonyldaidzin, malonylglycitin, respectively, or by an acetyl group to form acetylgenistin, acetyldaidzin and acetylglycitin, respectively (Chuankhayan *et al.*, 2007a). However, soybean isoflavone glucosides exhibit less bioactivity and are not readily absorbed in the small intestine when compared with the corresponding free isoflavones because of their bulk and high polarity. In addition, isoflavone glucosides are minimally hydrolyzed by β -glucosidase from residential bacteria in the intestine. Thus,

isoflavone glucosides should be hydrolyzed into free isoflavones before consumption in order to increase the nutritional values of soybean food products (Pyo *et al.*, 2005).

Previous studies have reported the activities of three leguminous plant β -glucosidases toward soybean isoflavone glucosides. β -Glucosidase from *Dalbergia cochinchinensis* Pierre, or dalcochinase, is specific to its natural substrate, which is dalcochinin-8'-O- β -glucoside (Ketudat Cairns *et al.*, 2000). Moreover, dalcochinase also hydrolyze daidzin and genistin, which are soybean isoflavone glucoside substrates, with good catalytic efficiencies (Chuankhayan *et al.*, 2007a). In addition, β -glucosidase from *D. nigescens* Kurz, or Dnbglu2, shows the high catalytic efficiency to its natural substrates, which are dalpatein 7-O- β -D-apiofuranosyl-(1 \rightarrow 6)- β -D-glucopyranoside and dalnigreïn 7-O- β -D-apiofuranosyl-(1 \rightarrow 6)- β -D-glucopyranoside. Dnbglu2 also hydrolyzes the soybean isoflavone glucosides, namely daidzin and genistin, with high catalytic efficiencies (Chuankhayan *et al.*, 2007a). On the contrary, β -glucosidase from *Glycine max*, or GmICHG, hydrolyzes modified isoflavone glucosides well, especially malonylgenistin and malonyldaidzin (Suzuki *et al.*, 2006).

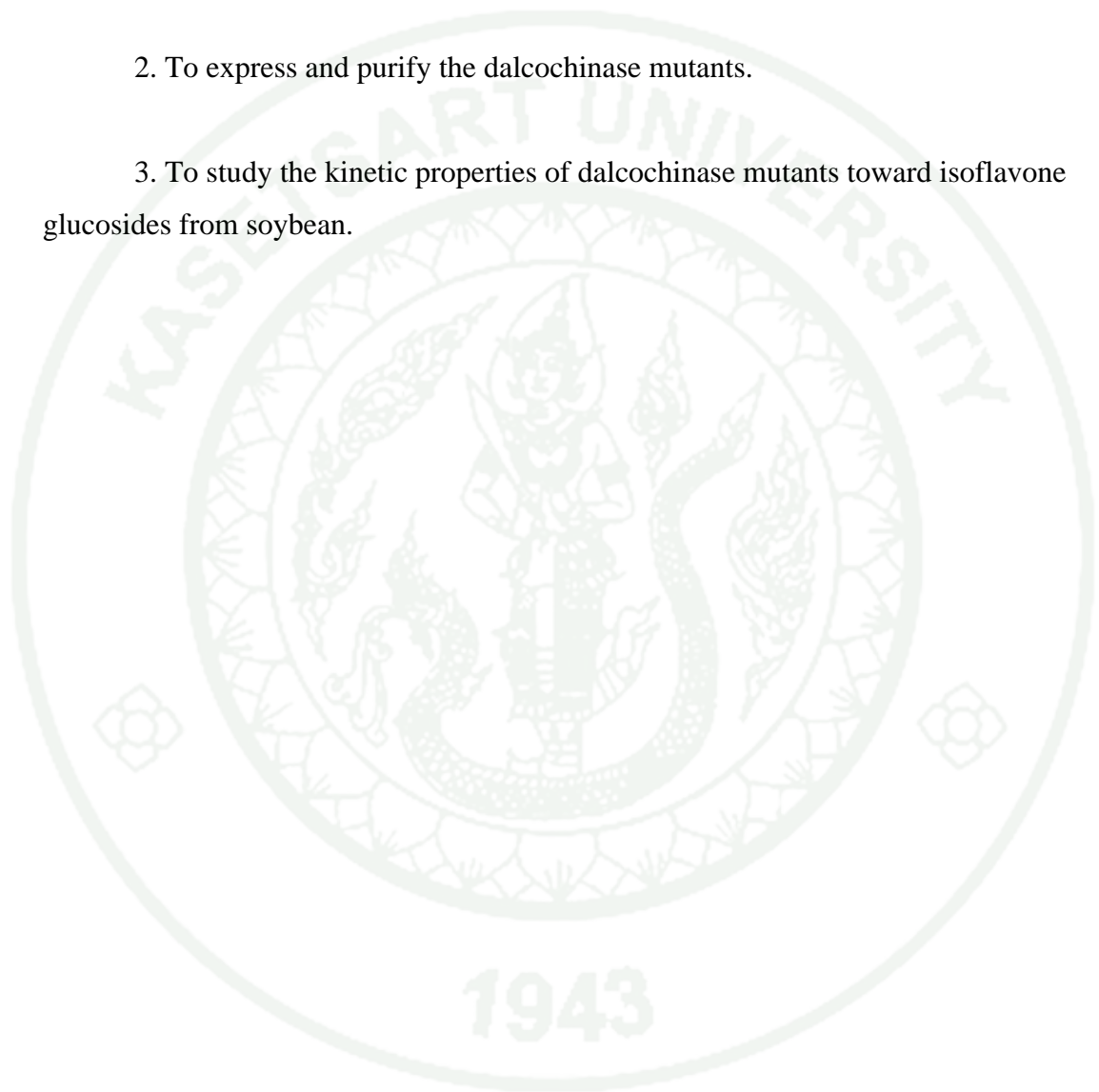
Amino acid sequence comparison showed that the afore-mentioned β -glucosidases shared 60-80% amino acid sequence identity, but exhibited variable hydrolytic efficiencies toward isoflavone glucoside substrates. Dnbglu2 is the most efficient enzyme in hydrolysis of the soybean isoflavone glucosides, whereas GmICHG is the best enzyme in hydrolysis of the modified forms of isoflavone glucosides, especially malonylgenistin. In our laboratory, the studies of Somphao (2011) and Klinkhomhom (2012) by replacing single amino acids in the binding pocket of dalcochinase to the corresponding amino acid of GmICHG, revealed that the hydrolytic efficiency toward daidzin and genistin, could be increased by the E455A and S459V mutations. For the modified isoflavone glucosides, the hydrolytic efficiency toward malonyldaidzin and malonylgenistin was increased by the A454F, E455A and S459V mutations, while that toward acetyldaidzin and acetylgenistin was increased by the afore-mentioned mutations plus the D400N mutation.

Therefore, this research project aims to construct double- and triple-mutations in the binding pocket of dalcochinase to the corresponding amino acids of GmICHG, in order to investigate the interaction of amino acid residues, which may influence the hydrolytic efficiency toward soybean isoflavone glucosides. Furthermore, the additivity of these double- and triple-mutations of dalcochinase may be gained, leading to improved hydrolytic efficiency of the mutant enzyme(s) toward soybean isoflavone glucosides. These mutant enzyme(s) may be applied in food industry to release free isoflavone aglycones, thereby increasing the nutritional values of soybean food products.



OBJECTIVES

1. To construct 3 double mutants and 1 triple mutant of dalcochinase, namely A454F/E455A, A454F/S459V, E455A/S459V and A454F/E455A/S459V.
2. To express and purify the dalcochinase mutants.
3. To study the kinetic properties of dalcochinase mutants toward isoflavone glucosides from soybean.



LITERATURE REVIEW

1. General features of β -Glucosidases

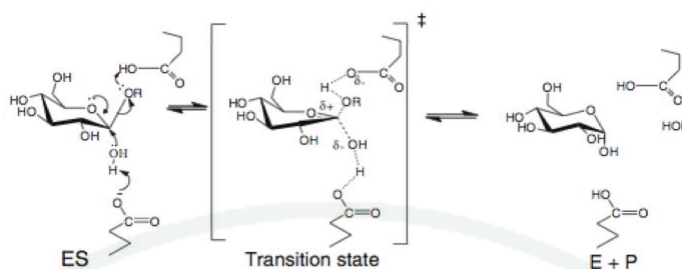
β -Glucosidases (β -D-glucopyranoside glucohydrolases, E.C. 3.2.1.21) are enzymes, which catalyze the hydrolysis of glycosidic bonds between glucose and aglycone or another sugar. These enzymes are normally found in all living organisms including Archaea, Eubacteria and Eukaryotes. β -Glucosidases in various organisms perform a variety of biological functions, which include biomass conversion in microorganism, hydrolysis of glycolipids and exogenous glucosides in animals, and lignification, defense, activation of phytohormone, catabolism of cell wall oligosaccharides and scent release in plants. In general, most β -glucosidases have the subunit molecular weights about 55-65 kDa, pH optima between pH 4.0-7.5 depending on their source and cellular location, and temperature optima vary from 30-65 °C. However, β -glucosidases from *Thermotoga maritime* which is a thermophilic bacterium may show temperature optima about over 100 °C (Ketudat Cairns and Esen, 2010).

In general, most β -glucosidases are divided into three groups depending on the basis of their substrate specificity, which are (1) aryl- β -glucosidases that show high specificity to aryl- β -D-glucosides, (2) cellobiases that hydrolyze cellobiose with high specificity, and (3) broad-specificity β -glucosidases that hydrolyze both types of substrates (Saha and Bothast, 1996). However, a classification system for glycoside hydrolases (GH) based on amino acid sequence and structural similarity was widely accepted (Henrissat, 1991). The enzymes with overall amino acid sequence similarity and conserved motifs are grouped into the same family. Therefore, this classification has grouped these enzymes into 131 GH families, some of which are grouped into 14 GH clans (GH-A to GH-N). The database of GH enzymes are updated regularly by the Carbohydrate Active enZYme (CAZY) web site (http://www.cazy.org/fam/acc_GH.html) (Ketudat Cairns and Esen, 2010). β -

Glucosidases that have been reported thus far belong to families GH1, GH3, GH5, GH9 and GH30, but most of them are members of GH1.

Glycoside hydrolases hydrolyze their substrates using one out of two mechanisms, which are either inverting or retaining mechanisms. Both mechanisms use a pair of acidic and nucleophilic amino acid residues, which are normally carboxylic acid residues, which are located on either side of the sugar substrates, approximately 10 Å apart in the inverting mechanism and 5 Å apart in the retaining mechanism. In an inverting mechanism, aglycone group of substrate is replaced by an activated water molecule in a single step. A water molecule is deprotonated by the catalytic base residue to generate the hydroxyl molecule for attacking the anomeric carbon in concomitant with the protonation of the glycosidic oxygen by the catalytic acid residue. The anomeric outcome is inverted from the substrate (Figure 1, A). In a retaining mechanism, the enzymes hydrolyze the substrate in 2 steps. In the glycosylation step, the catalytic nucleophile directly attacks the anomeric carbon and the catalytic acid residue protonates the leaving group aglycone to give a glucosyl-enzyme intermediate. Then in the deglycosylation step, the water molecule is deprotonated by the catalytic base residue to generate hydroxyl molecule for attacking the anomeric carbon of the intermediate in the concomitant with the release of glucose and the free enzyme. Therefore, the anomeric outcome is retained in the product (Figure 1, B) (Ketudat Cairns and Esen, 2010). Most β -glucosidases hydrolyze their substrates through a retaining mechanism, but the GH9 β -glucosidases hydrolyze their substrates through an inverting mechanism (Ketudat Cairns and Esen, 2010).

(A) Inverting mechanism



(B) Retaining mechanism

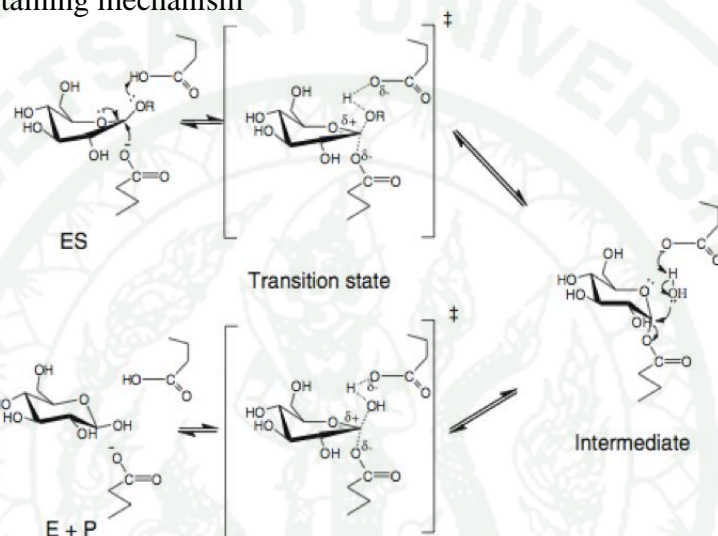


Figure 1 Mechanisms of β -glucosidases including inverting mechanism (A) and retaining mechanism (B).

Source: Ketudat Cairns and Esen (2010)

β -Glucosidases have various structures, depending on their GH families. The overall folding of the catalytic domain in each GH family is similar (Fig. 2). The families GH1, GH5 and GH30 belonging to Clan GH-A share a common $(\beta/\alpha)_8$ -barrel domains. Their catalytic residues are located on β -strand 4 and β -strand 7. On the contrary, the family GH3 has two domains, which are a $(\beta/\alpha)_8$ -barrel domain followed by an α/β sandwich domain. However, the two catalytic residues of the active site are located on each domain to serve as catalytic acid/base and catalytic nucleophile. The overall structure of GH9 enzymes have $(\alpha/\alpha)_6$ -barrel domain (Ketudat Cairns and Esen, 2010).



Figure 2 Three-dimensional structures of β -glucosidases from different GH families. The structures are colored in a spectrum from blue to red corresponding to their N-termini to C-termini. The catalytic nucleophile and acid/base residues are shown in stick. The ligands are shown in pink ball-and-sticks. (GH1 = *Zea mays* ZmGlu1, PDB code 1E1E; GH3 = *Hordeum vulgare* Exo I β -glucan glucohydrolase, PDB code 1E1X; GH5 = *Candida albicans* exo- β -(1,3)-glucanase Exg exoglucanase, PDB code 1C1Z; GH9 = *Vibrio parahaemolyticus* putative exoglucanase, PDB code 3H7L; and GH30 = *Homo sapiens* acid β -glucosidase/glucoerebrosidase GBA1, PDB code 2V3D)

Source: Ketudat Cairns and Esen (2010)

2. β -Glucosidase from *Dalbergia cochinchinensis* Pierre

β -Glucosidase from *Dalbergia cochinchinensis* Pierre (Thai rosewood), or dalcochinase, has a native molecular weight about 330 kDa, consisting of 4-6 subunits of 66 kDa. The enzyme showed dual activities against both *para*-nitrophenyl- β -D-glucopyranoside (*p*NP-Glc) and *para*-nitrophenyl- β -D-fucopyranoside (*p*NP-Fuc) with the K_m and k_{cat} of 5.4 mM and 307 s⁻¹, respectively, toward *p*NP-Glc, and 0.54

mM and 151 s^{-1} , respectively, toward *p*NP-Fuc. The pH optimum for hydrolysis of both substrates was pH 5.0. Therefore, $k_{\text{cat}}/K_{\text{m}}$ value for hydrolysis of *p*NP-Fuc ($283.1 \text{ mM}^{-1}\text{s}^{-1}$) was higher than that for hydrolysis of *p*NP-Glc ($57.3 \text{ mM}^{-1}\text{s}^{-1}$) by 5-fold (Srisomsap *et al.*, 1996). Moreover, dalcocinase was inhibited by δ -gluconolactone, HgCl_2 and *para*-chloromercuribenzoate. Also *p*NP-Fuc could inhibit the hydrolysis of *p*NP-Glc with K_i of 0.42 mM. So, both types of substrates were hydrolyzed in the same active site (Surarit *et al.*, 1997).

The natural substrate of dalcocinase was found to be 12-dihydroamorphigenin-8'-*O*- β -D-glucoside, or dalcochinin-8'-*O*- β -D-glucoside (Fig. 3), which was isoflavone glucoside obtained from extraction of Thai rosewood's seeds (Svasti *et al.*, 1999). The K_{m} value for hydrolysis of dalcochinin-8'-*O*- β -D-glucoside was 1.68 mM, which was between the K_{m} values for hydrolysis of *p*NP-Fuc and *p*NP-Glc. The structure of the aglycone group of dalcochinin-8'-*O*- β -D-glucoside is similar to that of rotenone (Fig. 3), which is a natural toxic substrate against insects. So, the researchers predicted that the aglycone group of dalcochinin-8'-*O*- β -D-glucoside may act as a deterrent against insects in the seeds of Thai rosewood.

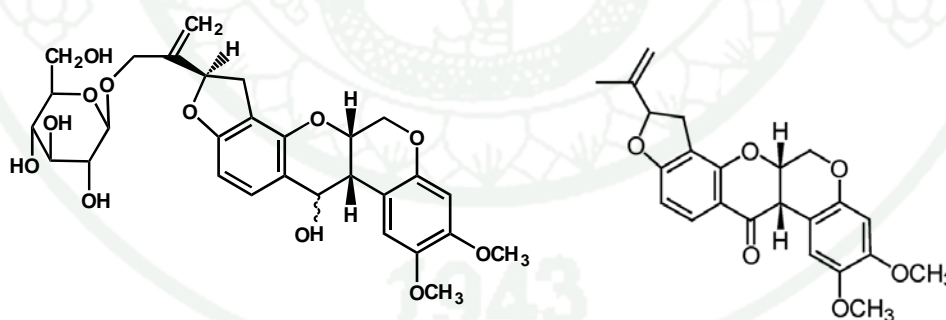


Figure 3 Structures of dalcochinin-8'-*O*- β -D-glucoside (left) and rotenone (right)

Source: Svasti *et al.* (1999)

To elucidate the structure-function relationship in dalcocinase, the gene of dalcocinase was cloned by Ketudat Cairns *et al.* (2000). The coding sequence of

dalcochinase was 1,644-bp long, which was translated into a polypeptide of 547 amino acids consisting of 23 amino acids of signal peptide and 524 amino acids for mature protein sequence (Ketudat Cairns *et al.*, 2000). Multiple sequence alignment of dalcochinase with other β -glucosidases has assigned dalcochinase as a member of GH1. Since dalcochinase and β -glucosidase from white clover shared about 60% amino acid sequence identity, thus the three-dimensional structure of dalcochinase should be similar with that of β -glucosidase from white clover, which was $(\beta/\alpha)_8$ barrel (PDB code 1CBG) (Barrett *et al.*, 1995). In addition, E182 and E396 of dalcochinase should be the site of acid/base catalyst and nucleophile, respectively, as they were conserved with E198 (the catalytic acid/base) of cassava cyanogenic β -glucosidase and E358 (the nucleophile) of β -glucosidase from *Agrobacterium*, respectively. These catalytic residues appear on the conserved motifs, TL/FNEP and I/VTENG, of GH1 enzymes, respectively. Furthermore, Toonkool *et al.*, (2006) have generated recombinant constructs of dalcochinase from both *Escherichia coli* and *Pichia pastoris*. They found that kinetic properties of the recombinant dalcochinase from *P. pastoris* were similar to those of the natural dalcochinase from Thai rosewood's seed.

3. β -Glucosidase from *Dalbergia nigrescen* Kruz

β -Glucosidase from *D. nigrescen* Kruz (Blackwood), or Dnbglu2, has a native molecular weight about 240 kDa, consisting of 4 subunits of 62 kDa. The enzyme could nicely hydrolyze both *p*NP-Glc and *p*NP-Fuc with K_m and k_{cat} of 14.7 mM and 10.4 s⁻¹, respectively, toward *p*NP-Glc, and 1.8 mM and 7.0 s⁻¹, respectively, toward *p*NP-Fuc. Hence, k_{cat}/K_m value for hydrolysis of *p*NP-Fuc (4.02 mM⁻¹s⁻¹) was higher than that for hydrolysis of *p*NP-Glc (0.88 mM⁻¹s⁻¹) by 4.6-fold. The optimal pH for hydrolysis of both substrates was pH 5.0-6.0. Its hydrolytic activities toward many substrates, including *p*NP- β -cellobioside, *p*NP- β -D-mannoside, *p*NP- β -D-thioglucoside, *p*NP- α -L-arabinoside and *p*NP- β -L-arabinoside, were lower than that toward *p*NP-Glc (Chuankhayan *et al.*, 2005).

The natural substrates of Dnbglu2 are two forms of isoflavone diglycosides, namely dalpatein-7-*O*- β -D-apiofuranosyl-(1 \rightarrow 6)- β -D-glucopyranoside (dalpatein diglycoside) and dalnigreïn-7-*O*- β -D-apiofuranosyl-(1 \rightarrow 6)- β -D-glucopyranoside (dalnigreïn diglycoside) (Fig. 4). Dnbglu2 showed good hydrolysis of both substrates with K_m , k_{cat} and k_{cat}/K_m of 0.5 mM, 465 s⁻¹ and 990 mM⁻¹s⁻¹, respectively, toward dalpatein diglycoside, and 0.7 mM, 334 s⁻¹ and 440 mM⁻¹s⁻¹, respectively, toward dalnigreïn diglycoside. So, the hydrolytic efficiency of Dnbglu2 toward dalpatein diglycoside was higher than that toward dalnigreïn diglycoside by 2-fold (Chuankhayan *et al.*, 2005).

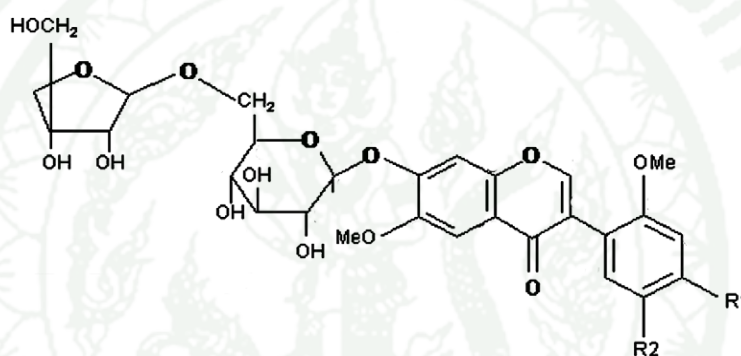


Figure 4 Structures of dalpatein diglycoside (R_1 - $R_2 = O-CH_2-O$) and dalnigreïn diglycoside ($R_1, R_2 = OMe$)

Source: Chuankhayan *et al.* (2005)

To elucidate the structure-function relationship in Dnbglu2, the gene of Dnbglu2 was cloned by Chuankhayan *et al.*, (2007b). The coding sequence of Dnbglu2 was 1,596-bp long, which was translated into a polypeptide of 531 amino acids consisting of 23 amino acids of signal peptide and 508 amino acids for mature protein. Multiple alignment of amino acid sequence of Dnbglu2 and related β -glucosidases including dalcochinase and white clover cyanogenic β -glucosidase were performed. Dnbglu2 shared the highest percent of amino acid sequence identity with dalcochinase (81%). The three-dimensional structure of Dnbglu2 should be similar with that of white clover cyanogenic β -glucosidase, which was (β/α)₈ barrel (Barrett *et al.*, 1995). Also, from multiple sequence alignment, E182 in the TINEP motif of

Dnbglu2 was conserved with the catalytic acid/base residues E182, E183 and E188 from dalcochinase, white clover cyanogenic β -glucosidase and *Zea maize* β -glucosidase, respectively. In addition, E396 in the YITENG motif of Dnbglu2 was also conserved with the catalytic nucleophile residues E396, E397 and E406 from dalcochinase, white clover cyanogenic β -glucosidase and *Zea maize* β -glucosidase, respectively. Therefore, E182 in the TINEP motif was catalytic acid/base residue and E396 in the YITENG motif was nucleophile residue of Dnbglu2. (Chuankhayan *et al.*, 2007b).

4. β -Glucosidase from *Glycine max*

Glycine max isoflavone conjugate-hydrolyzing β -glucosidase, or GmICHG, from the roots of *G. max* (soybean) seedling has a native molecular weight of 100 kDa, composing of homodimeric forms of 58 kDa. In general, the enzyme catalyzed the hydrolysis of isoflavone glucosides to release aglycone groups and glucose moiety (Fig. 5) (Suzuki *et al.*, 2006).

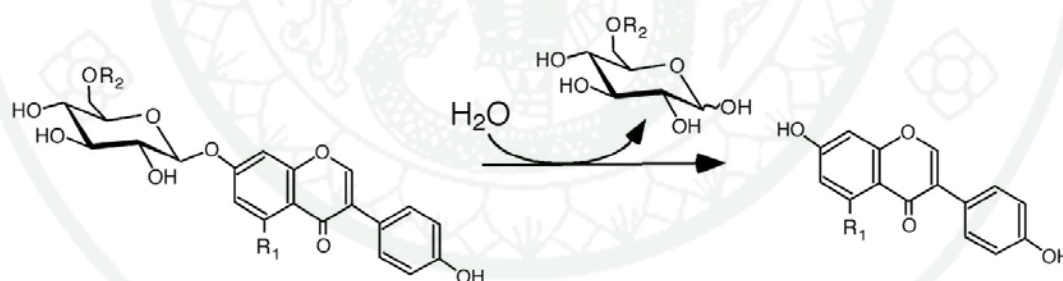


Figure 5 Hydrolysis of isoflavone glucoside substrates by GmICHG to yield aglycone forms. The isoflavone aglycones can be daidzein ($R_1 = H$) or genistein ($R_1 = OH$). The glucosyl group can be unmodified ($R_2 = H$), or modified by acetyl or malonyl group ($R_2 =$ acetyl or malonyl group, respectively).

Source: Suzuki *et al.* (2006)

When compared k_{cat}/K_m values (Table 1), the hydrolytic efficiency of GmICHG toward malonylgenistin was higher than that toward genistin by 10-fold. Similarly, the hydrolytic efficiency toward malonyldaidzin was higher than that toward daidzin by 2.7-fold. From kinetic study, GmICHG appears to be specific for malonylated isoflavone glucosides. Moreover, GmICHG showed minor activities for some substrates such as cyanidin-3-*O*-(6''-*O*-malonyl- β -D-glucosides), cyanidin-3-*O*- β -D-glucosides, quercetin-3-*O*-(6''-*O*-malonyl- β -D-glucosides), quercetin-3-*O*- β -D-glucosides, *para*-nitrophenyl- α -D-glucoside, *para*-nitrophenyl- β -D-galactoside and *p*NP-Glc, but the relative activities were less than 0.01% of activity for malonylgenistin (Suzuki *et al.*, 2006).

Table 1 Hydrolysis of isoflavone glucosides by natural GmICHG.

Substrate	k_{cat} (s^{-1})	K_m (mM)	k_{cat}/K_m ($\text{s}^{-1}\text{mM}^{-1}$)
Malonyldaidzin	46	0.019	2,400
Daidzin	22	0.025	900
Malonylgenistin	98	0.025	3,900
Genistin	13	0.032	400

Source: Suzuki *et al.* (2006)

To investigate the expression of GmICHG in different tissues, semi-quantitative real-time PCR was performed. The RNAs of GmICHG were abundantly found in the root of *G. max* seedling. Then, the immunocytochemical analysis using anti-GmICHG antibody showed that the enzyme was localized in the cell wall and intercellular space of the root hair. So, the cDNA of GmICHG was synthesized by using GmICHG RNA as a template. The full-length sequence of GmICHG cDNA was 1,545-bp long, which was translated into 514 amino acids. Multiple alignment of amino acid sequences revealed that GmICHG should be a member of the GH1 family and shares about 64% of sequence identity with dalcocinase. Its catalytic acid/base and nucleophile were placed at E209 and E420 in the motifs TLNEP and YITENG, respectively (Suzuki *et al.*, 2006). The recombinant enzyme was initially synthesized

in the precursor protein form. After that, the signal peptide of 25 amino acids was cleaved to yield the mature sequence of 489 amino acids. The recombinant GmICHG was cloned and expressed in *E. coli* with the N-terminal thioredoxin fusion. The size of recombinant GmICHG was 71 kDa and the optimal pH of recombinant enzyme was pH 5.5. The recombinant GmICHG was strongly specific for isoflavone glucoside and malonyl isoflavone glucoside (Table 2). However, its catalytic activities were lower than those of the natural enzyme, possibly due to its low stability. Moreover, the enzyme activity was inhibited by 0.1 mM Hg²⁺ (Suzuki *et al.*, 2006).

Table 2 Hydrolysis of isoflavone glucoside by the recombinant GmICHG.

Substrate	k_{cat} (s ⁻¹)	K_{m} (mM)	$k_{\text{cat}}/K_{\text{m}}$ (s ⁻¹ mM ⁻¹)
Malonyl daidzin	5.4	0.020	300
Daidzin	0.5	0.018	30
Malonyl genistin	2.7	0.041	70
Genistin	1.4	0.056	30

Source: Suzuki *et al.* (2006)

5. Soybean isoflavones

Soybean isoflavones may exist as free isoflavones, such as daidzein, genistein and glycitein. However, for storage purposes, these isoflavones are usually conjugated to glucose, forming isoflavone glucosides, namely daidzein-7-*O*-glucoside or daidzin, genistein-7-*O*-glucoside or genistin, and glycitein-7-*O*-glucoside or glycitin. Furthermore, the glucosyl moiety of isoflavone glucosides may be modified with another functional group. The acetylated forms are daidzein-7-*O*-(6''-*O*-acetyl-β-D-glucoside) or acetyldaidzin, genistein-7-*O*-(6''-*O*-acetyl-β-D-glucoside) or acetylgenistin, and glycitein-7-*O*-(6''-*O*-acetyl-β-D-glucoside) or acetylglycitin. The malonylated forms are daidzein-7-*O*-(6''-*O*-malonyl-β-D-glucoside) or

malonyldaidzin, genistein-7-*O*-(6''-*O*-malonyl- β -D-glucoside) or malonylgenistin, and glycitein-7-*O*-(6''-*O*-malonyl- β -D-glucoside) or malonylglycitin (Suzuki *et al.*, 2006).

The quantities and proportions of different forms of isoflavone glucoside in soybean are usually variable. For example, in the soybean hypocotyls, malonyldaidzin, malonylgenistin, malonylglycitin, daidzin and glycitin represented 93.2% of total isoflavone glucosides, while genistin, daidzein, genistein and glycitein were found in low amounts, but acetyldaidzin, acetylgenistin and acetylglycitin were not detected. In the cotyledons, major isoflavone glucoside forms were malonyldaidzin, malonylgenistin, daidzin and genistin, representing about 94.8% of total isoflavone glucosides, whereas daidzein and genistein were minor forms, but malonylglycitin, glycitin, glycitein, acetyldaidzin, acetylgenistin and acetylglycitin were not found (Yuan *et al.*, 2009).

The metabolism of isoflavones, which are secondary metabolites, in the cell of *G. max* is shown in Fig. 6. Flavanones are changed into isoflavone aglycone by 2-hydroxyflavanone synthase. Then, glucosylation and malonylation are successfully performed by isoflavone-7-*O*-glucosyltransferase and isoflavone-7-*O*-glucoside-6''-*O*-malonyltransferase, respectively. The modified isoflavone glucosides are transported to the vacuoles for storage. When needed, the malonylated isoflavone glucosides are mobilized to apoplast, where they will be converted by GmICHG into aglycone forms, whose actions include attracting the symbiotic organism or defending against microorganism (Suzuki *et al.*, 2006).

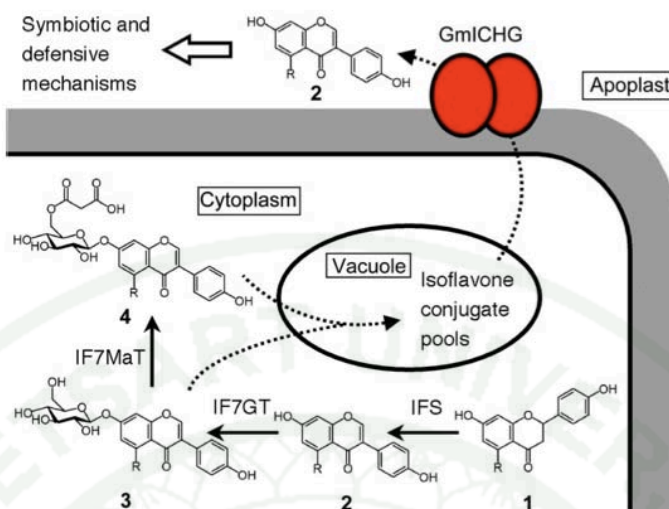


Figure 6 Schematic diagram of isoflavone glucoside biosynthesis and its activity. Name of compounds are 1 = flavanones, 2 = isoflavone aglycones (R = H, daidzein; R= OH, genistein), 3 = isoflavone-7-*O*-glucosides, 4 = isoflavone-7-*O*-(6''-*O*-malonyl-β-D-glucoside). Abbreviations of enzyme are IFS = 2-hydroxyflavanone synthase (microsomal P450 enzyme), IF7GT = isoflavone-7-*O*-glucosyltransferase and IF7MaT = isoflavone-7-*O*-glucoside-6''-*O*-malonyltransferase.

Source: Suzuki *et al.* (2006).

5.1 Biological activity of isoflavones in soybean

Soybean usually produces a large number of isoflavones for serving as both chemoattractants and defense against microorganism. For symbiotic organism, Rhizobia need isoflavone aglycones as specific chemoattractants to help them establish host-symbiont interactions, leading to nodulation in the root hair (Noguchi *et al.*, 2007; Suzuki *et al.*, 2006; Yuan *et al.*, 2009). For defense mechanism, isoflavone aglycones act as a toxic substance in the form of phytoanticipin to attack the invading microorganism (Hsieh and Graham, 2001).

5.2 Biological activity of isoflavones in human

Soybean food products are known to contain large quantities of isoflavone glucosides and free isoflavone aglycones. However, soybean isoflavone glucosides exhibit less bioactivity and are not readily absorbed in the small intestine when compared with the corresponding free isoflavones because of their bulk and high polarity. In addition, isoflavone glucosides are minimally hydrolyzed by β -glucosidase from residential bacteria in the intestine. Thus, isoflavone glucosides should be hydrolyzed into free isoflavones before consumption in order to increase the nutritional values of soybean food products (Pyo *et al.*, 2005). These isoflavones have several beneficial biological properties, such as preventing cancer and cardiovascular disease, diminishing the postmenopausal symptom, and reducing the risk of osteoporosis and antioxidant activity (Chen *et al.*, 2012). Some experimental studies have shown that isoflavones were associated with low-density lipoproteins (LDLs) and capable of preventing against oxidative modification of LDLs in our body (Tikkanen *et al.*, 1998; Zhang *et al.*, 2013). Also, black soybean has the antioxidant activity against LDL oxidation (Takahashi *et al.*, 2005). From epidemiological studies, free isoflavone aglycones (daidzein and genistein) could protect against breast cancer, prostate cancer and gastric cancer (Andres *et al.*, 2011; Magee and Rowland, 2004; Sakamoto *et al.*, 2010; Tang *et al.*, 2012). Interestingly, genistein inhibits the differentiation of preadipocytes, lipid accumulation and glucose uptake in the mature adipocytes. It increases the secretion of insulin, lipolysis and apoptosis of adipocyte, while reduces secretion of pro-inflammatory cytokines and generation of reactive oxygen species (Behloul and Wu, 2013).

6. Hydrolysis of isoflavone glucosides

Isoflavone glucosides can be hydrolyzed by β -glucosidases at the O-glucosidic bond to release free isoflavone aglycones and a glucosyl moiety. Many sources of β -glucosidases have been used in this process, some of which are shown in Table 3. Most β -glucosidases, such as those from *E. coli* (Ismail and Hayes, 2005), almond (Ismail and Hayes, 2005), *Pseudomonas* ZD-8 (Yang *et al.*, 2004), *Bacillus subtilis*

natto (Kuo and Lee, 2008), *Lactobacillus rhamnosus* CRL981 (Marazza *et al.*, 2009), *Aspergillus oryzae* (Horii *et al.*, 2009), *Pyrococcus furiosus* (Yeom *et al.*, 2012), *Dictyoglomus turgium* (Kim *et al.*, 2011b), soybean okara (Chiou *et al.*, 2010), *Paecilomyces thermophile* J18 (Yang *et al.*, 2009), *Thermoanaerobacter ethanolicus* JW200 (Song *et al.*, 2011) and *Sulfolobus solfataricus* (Kim *et al.*, 2011a), preferred to hydrolyze the unmodified isoflavone glucosides than the malonylated isoflavone glucosides. On the other hand, hydrolytic efficiencies of β -glucosidase from hyperthermophile *Thermotoga maritima* toward malonylated forms were slightly higher than those toward unmodified forms (Xue *et al.*, 2009). In addition, β -Glucosidase from *D. turgidum* showed high hydrolytic efficiency toward ononin, which is another isoflavone glucoside found in plants and herbs (Kim *et al.*, 2011b).

Table 3 Kinetic efficiencies of different β -glucosidases toward isoflavone glucosides

Source of enzyme	k_{cat}/K_m ($s^{-1}mM^{-1}$)						References
	D	G	Gly	O	MD	MG	
<i>P. ZD-8</i>	3.36	443	-	-	42	56	Yang <i>et al.</i> , 2004
<i>B. subtilis</i> natto	49.19	147.20	-	-	-	-	Kuo and Lee, 2008
<i>B. subtilis</i> natto	17.93	19.45	-	-	-	-	Kuo and Lee, 2008
<i>T. maritima</i>	60.3	82.6	-	-	93.1	103	Xue <i>et al.</i> , 2009
<i>P. furiosus</i>	4,480	12,100	1,840	-	-	-	Yeom <i>et al.</i> , 2012
<i>D. turgidum</i>	4,440	8,590	709	1,130	-	-	Kim <i>et al.</i> , 2011

Note of abbreviation: D = daidzin, G = genistin, Gly = glycitin, O = ononin, MD = malonyldaidzin and MG = malonylgenistin.

When compared the hydrolytic efficiencies of three leguminous plant β -glucosidases, namely dalcocinase, Dnbglu2 and GmICHG, toward soybean isoflavone glucosides (Table 4), Dnbglu2 hydrolyzed both daidzin and genistin with the highest efficiencies. GmICHG also hydrolyzed them with good efficiencies, while dalcocinase hydrolyzed them with low efficiencies. For the hydrolysis of

malonylgenistin, GmICHG showed the highest hydrolytic efficiencies, followed by Dnbglu2 and dalcochinase, respectively. Therefore, GmICHG appeared to be specific to malonylated isoflavone glucoside substrates, while Dnbglu2 liked to hydrolyze the unmodified forms. Nevertheless, it is difficult to compare their efficiencies because the experiments were performed under different conditions such as amount of enzyme or time of incubation.

Table 4 Kinetic parameters of dalcochinase, Dnbglu2 and GmICHG toward soybean isoflavone glucosides.

Enzyme	Kinetic parameters	Daidzin	Genistin	Malonyl-daidzin	Malonyl-genistin
Dalcochinase ^a	K_m (mM)	1.570	0.126	-	0.051
	k_{cat} (s ⁻¹)	50	208	-	1.88
	k_{cat}/K_m (s ⁻¹ mM ⁻¹)	32.2	1,700	-	37.0
Dnbglu2 ^a	K_m (mM)	0.144	0.067	-	0.052
	k_{cat} (s ⁻¹)	300	700	-	21
	k_{cat}/K_m (s ⁻¹ mM ⁻¹)	2,080	10,500	-	410
GmICHG ^b	K_m (mM)	0.025	0.032	0.019	0.025
	k_{cat} (s ⁻¹)	22	13	46	98
	k_{cat}/K_m (s ⁻¹ mM ⁻¹)	900	400	2,400	3,900

Source: ^aChuankhayan *et al.* (2007a) and ^bSuzuki *et al.* (2006).

Multiple alignment of amino acid sequences showed that Dnbglu2 and dalcochinase shared 81% identity. Therefore, previous studies have employed site-directed mutagenesis approaches in order to identify the residues responsible for substrate specificity in dalcochinase (Chuankhayan *et al.*, 2007b). Two single mutants (A454S and E455G) and one double mutant (A454S/E455G) of dalcochinase were

generated by replacing the amino acid in the substrate binding pocket of dalcochinase with the corresponding residues of Dnbglu2. The double mutant showed 2-fold increase in the hydrolytic rate for genistin and little increase for daidzin when compared with wild-type dalcochinase. The E455G mutant also showed little increases in the hydrolytic rates for both genistin and daidzin, but the A454S mutant exhibited slight decreases in the hydrolytic rates when compared with the wild-type dalcochinase (Chuankhayan *et al.*, 2007b). Therefore, changing amino acid residues, A454S and E455G, did not significantly improve the efficiencies of dalcochinase.

In our laboratory, Somphao constructed four single mutants of dalcochinase (namely D400N, A454F, E455A and S459V) by replacing the amino acid in the substrate binding pocket of dalcochinase with the corresponding residues of GmICHG. The D400N mutant showed decreased hydrolytic efficiencies toward daidzin, genistin, malonyldaidzin and malonylgenistin, but increased efficiencies toward acetyldaidzin and acetylgenistin, when compared with the wild-type dalcochinase (Table 5). Also, the A454F mutant exhibited lower hydrolytic efficiencies toward daidzin and genistin when compared with the wild-type dalcochinase, but higher efficiencies toward malonyldaidzin, malonylgenistin, acetyldaidzin and acetylgenistin. Interestingly, both the E455A and S459V mutants showed higher hydrolytic efficiencies toward all of isoflavone glucoside substrates when compared with the wild-type dalcochinase (Klin-khumhom, 2012; Somphao, 2011). Thus, changing of amino acid residues in the binding pocket of dalcochinase to those of GmICHG could influence the hydrolytic efficiencies toward isoflavone glucosides.

Table 5 Kinetic efficiencies of dalcochinase and its mutant forms toward soybean isoflavone glucosides.

Dalcochinase	k_{cat}/K_m ($s^{-1}mM^{-1}$)					
	D	G	MD	MG	AD	AG
Wild-type	95.47	45.37	0.55	1.83	0.015	0.032
D400N	47.17	9.88	0.27	0.57	0.164	0.453
A454F	75.29	19.51	0.95	4.64	0.103	0.307
E455A	302.48	236.65	2.38	65.44	0.418	1.732
S459V	221.05	109.06	1.14	2.33	0.435	0.314

Note of abbreviation: D = daidzin, G = genistin, MD = malonyldaidzin, MG = malonylgenistin, AD = acetyldaidzin and AG = acetylgenistin.

Source: Sampao (2010) and Klinkhamhom (2011).

Therefore, this study is interested in constructing the novel β -glucosidases for hydrolyzing soybean isoflavone glucosides based on the experimental results from previous studies (Table 5). By combining the effects of single mutants that improved hydrolytic efficiencies toward soybean isoflavone glucosides, the double- and triple-mutations in the binding pocket of dalcochinase will be created. The interactions between the mutated residues in the multiple mutants may yield even better hydrolytic efficiency than the single mutants.

7. Expression of recombinant dalcochinase in *P. pastoris*

At present, expression of a recombinant protein can be carried out by cloning the interested gene into a suitable expression vector and transforming it into the appropriate expression host. The most common expression host is bacteria such as *E. coli*. It has a high growth rate, and is able to provide high yield of protein in a short time. Because *E. coli* is a prokaryotic organism, it lacks the machinery needed for protein folding and protein modification. Some proteins expressed in bacterial system

may face with the problem of no biological activity if they require post-translational modifications to be fully functional. Therefore, yeast expression system, such as *P. pastoris*, is another choice for protein expression. *P. pastoris* is a single-cell, eukaryotic organism, and able to perform various posttranslational modifications, such as proteolytic cleavage, glycosylation and protein folding. Moreover, *P. pastoris* is methylotropic yeast, which uses methanol as a carbon source. Protein expression is easily induced by adding methanol under the control of *alcohol oxidase 1* (or *AOX1*) promoter in *P. pastoris*. The protein can be expressed in either intracellular or extracellular forms. For extracellular expression, the signal sequence, such as the *Saccharomyces cerevisiae* α -factor propeptide, is added to the N-terminus of the proteins to direct protein secretion to outside the cell (Invitrogen, 2008).

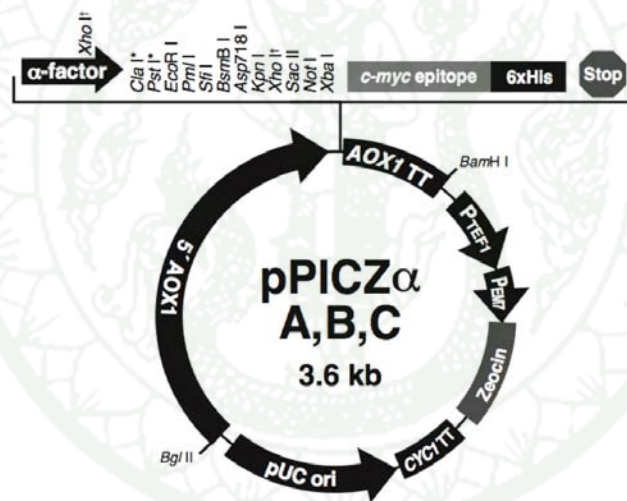


Figure 7 Diagram of pPICZ α A, B and C. The plasmid contains AOX1 promoter region (5' AOX1), α -factor signal sequence, multiple cloning sites, c-myc epitope, polyhistidine tag, AOX1 transcription termination region (AOX1 TT), the promoter for regulation of zeocin resistant gene in *P. pastoris* (P_{TEF1}), the promoter for regulation of zeocin resistant gene in *E. coli* (P_{EM7}), Zeocin resistant gene, CYC1 transcription termination region (CYC1 TT) and pUC origin of replication (pUC ori).

Source: Invitrogen (2008)

Dalcochinase was expressed in the *E. coli* at first, but the protein was insoluble and had no activities even if the protein was co-expressed with chaperonin GroESL. Then, recombinant dalcochinase was constructed with a histidine tag at either the C-terminal or N-terminal ends and expressed in *P. pastoris*. Both dalcochinase forms could be not purified by immobilized metal-ion affinity chromatography column (IMAC), due to post-translational processing at both termini. So, a new construct of recombinant dalcochinase was made without the first 13 residues of the mature dalcochinase (starting at the VPPFN sequence after the N-terminal cleavage site), and cloned into pPICZ α B following an alpha mating factor propeptide and 8 histidine residues. The resulting plasmid was named pPICZ-His₈-trncTRBG. The protein expression and purification was successful. The kinetic properties, pH and temperature optima of recombinant dalcochinase were also the same as natural dalcochinase. Therefore, this construct could be used in further study (Toonkool *et al.*, 2006).

MATERIALS AND METHODS

Materials

1. Chemical reagents

All chemicals and reagents used in this project are listed in Table 6.

Table 6 List of chemicals and reagents used in this study and their manufacturers.

Chemicals and Reagents	Manufacturer, Country
2,2'-Azino-bis(3-ethylbenzothiazoline-6-sulphonic acid) (ABTS)	Roche, USA
Acetonitrile	Duksan pure chemical, Korea
Acrylamide	Bio Basic, Canada
Agar powder, bacteriological	HiMedia laboratories, India
Agarose	1 st BASE, Singapore
Almond β -glucosidase	Sigma-Aldrich, USA
Amersham TM ECL plus western blotting detection	GE Healthcare, Sweden
Ammonium persulfate	Ajax Finechem, Australia
Ammonium sulfate	Vivantis, USA
Bio-Rad protein assay	Bio-Rad laboratories, USA
Biotin	Sigma-Aldrich, USA
Bis-acrylamide	Bio basic, Canada
Bovine serum albumin standard	Pierce, USA
Casamino acids	Bio basic INC, Canada
Casein enzyme hydrolysate, type-I (Tryptone)	HiMedia laboratories, India
Coomassie brilliant blue R 250	Panreac quimica sau, Spain
Daidzein	LC Laboratories, USA
Daidzin	LC Laboratories, USA
Dalcochinin-8'-O- β -D-glucoside	Laboratory of Professor Svasti, Mahidol University, Thailand

Table 6 (Continued)

Chemicals and Reagents	Manufacturer, Country
Deoxyribonucleotide triphosphate (dNTP)	Fermentas, USA
Dimethyl sulfoxide (DMSO)	Sigma-Aldrich, USA
Dithiothreitol	GE healthcare, Germany
<i>DpnI</i> restriction endonuclease	Fermentas, USA
Ethylenediaminetetraacetic acid (EDTA)	Ajax Finechem, Australia
Ethanol	Carlo ERBA, Italy
GeneJET™ plasmid miniprep kit	Fermentas, USA
Genistein	LC laboratories, USA
Genistin	LC laboratories, USA
D-Glucose	Ajax Finechem, Australia
Glycerol	Ajax Finechem, Australia
Glycine	Fisher Scientific, UK
HEPES free acid	Amresco, USA
Imidazole	Sigma-Aldrich, USA
Malonyldaidzin	Wako Pure Chemical, Japan
Malonylgenistin	Wako Pure Chemical, Japan
Methanol	J.T. Baker, USA
4-Methylumbelliferyl- β -D-glucopyranoside (4MU-Glc)	Sigma-Aldrich, USA
Mouse monoclonal antibody against natural dalcochinase	Laboratory of Professor Kasinrek, Chiang Mai University, Thailand
Ni ²⁺ sepharose™ 6 Fast Flow	GE healthcare, Sweden
<i>para</i> -Nitrophenol (<i>p</i> NP)	Sigma-Aldrich, USA
<i>para</i> -Nitrophenyl- β -D-glucopyranoside (<i>p</i> NP- Glc)	Sigma-Aldrich, USA
Peptone	HiMedia laboratories, India
<i>Pfu</i> DNA polymerase	Promega, USA

Table 6 (Continued)

Chemicals and Reagents	Manufacturer, Country
Phenyl sepharose™ high performance	GE healthcare, Sweden
Phosphoric acid	Merck, Germany
Polyclonal rabbit anti mouse immunoglobulin linked-HRP	Dako cytomation, Denmark
Polyoxyethylene(20)sorbitan monolaurate	Ajax Finechem, Australia
Potassium dihydrogen orthophosphate	Ajax Finechem, Australia
di-Potassium hydrogen orthophosphate	Ajax Finechem, Australia
<i>Pst</i> I restriction endonuclease	Fermentas, USA
<i>Sac</i> I restriction endonuclease	Fermentas, USA
Skim milk	HiMedia laboratories, India
Sodium acetate	Merck, Germany
Sodium carbonate	Rankem, India
Sodium chloride	Ajax Finechem, Australia
Sodium dihydrogen orthophosphate	Ajax Finechem, Australia
di-Sodium hydrogen orthophosphate	Ajax Finechem, Australia
Sodium hydroxide	Merck, Germany
Sodium lauryl sulphate	Ajax Finechem, Australia
D-Sorbitol	Ajax Finechem, Australia
<i>Taq</i> DNA polymerase	Fermentas, USA
N,N,N',N'-tetramethylethylenediamine (TEMED)	AppliChem, Germany
Tris base	Sigma-Aldrich, Germany
<i>Xba</i> I restriction endonuclease	Fermentas, USA
Yeast extract powder	HiMedia laboratories, India
Yeast nitrogen base	Bio basic INC, Canada
Zeocin	Invitrogen, USA

2. Cells and plasmid

Escherichia coli DH5 α was used as a cloning host.

Pichia pastoris Y11430 was used as an expression host.

pPICZ α B-His₈-trncTRBG was used as a template for generating dalcocinase mutants (Fig. 8).

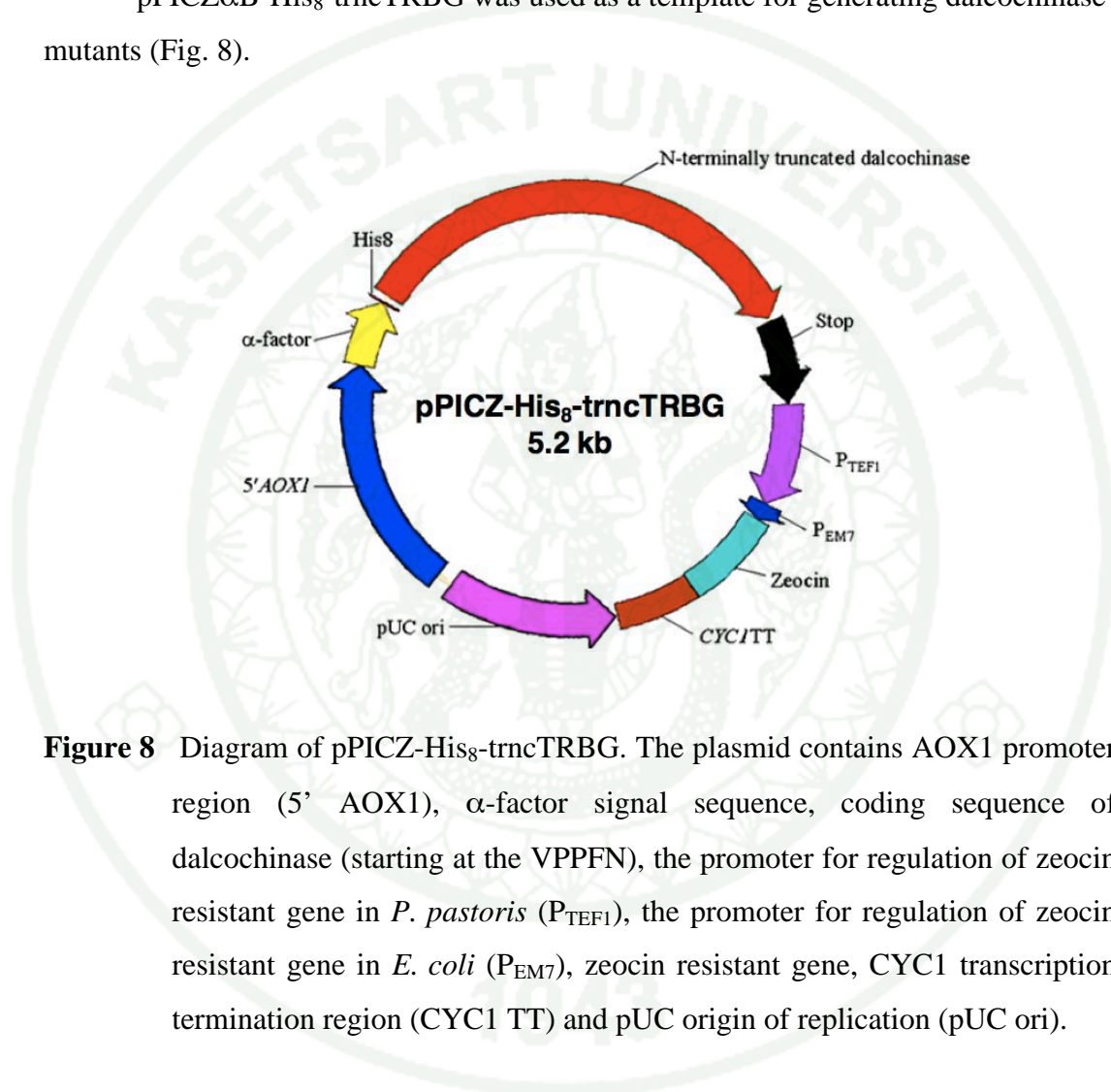


Figure 8 Diagram of pPICZ-His₈-trncTRBG. The plasmid contains AOX1 promoter region (5' AOX1), α -factor signal sequence, coding sequence of dalcocinase (starting at the VPPFN), the promoter for regulation of zeocin resistant gene in *P. pastoris* (P_{TEF1}), the promoter for regulation of zeocin resistant gene in *E. coli* (P_{EM7}), zeocin resistant gene, CYC1 transcription termination region (CYC1 TT) and pUC origin of replication (pUC ori).

Source: Toonkool *et al.* (2006)

Methods

1. Construction of four plasmids containing dalcochinase mutants

Three double mutations, namely A454F/E455A, A454F/S459V and E455A/S459V, and one triple mutation, namely A454F/E455A/S459V, of dalcochinase were constructed to replace amino acid residues in the binding pocket of dalcochinase to the corresponding residues of GmICHG. The sense and antisense mutagenic primers (Table 7) of all dalcochinase mutants were designed according to QuikChange™ site-directed mutagenesis kit (Stratagene).

Table 7 Mutagenic primers used in this study.

Name of primer	Nucleotide sequence (5' to 3')
A454F/E455A forward	GGTCATTGTTGGACAAC <u>TTTGAATGGTTTGCTGGTT</u> TATACATCAGATTTGG
A454F/E455A reverse	CCAAATCGTGATGTATAACCAGCAA <u>ACCATTCAAAGTTGTCCAACAATGA</u> CC
A454F/S459V forward	GGTCATTGTTGGACAAC <u>TTTGAATGGTTTGAGGGTT</u> TATACAG <u>TTTCGATTT</u> GGATTATATTTTGTG
A454F/S459V reverse	CACAAAATATAATCCAAATCGA <u>ACTGTATAACCCTCAAACCATTCAAAGT</u> TGTCCAACAATGACC
E455A/S459V forward	GTTGGACAAC <u>TTTGAATGGGCTGCTGGTT</u> TATACAG <u>TTTCGATTTGGATTAT</u> ATTTTGTG
E455A/S459V reverse	CACAAAATATAATCCAAATCGA <u>ACTGTATAACCAGCAGCCATTCAAAGT</u> TGTCCAAC
A454F/E455A/S459V forward	GCATGGTCATTGTTGGACAAC <u>TTTGAATGGTTTGCTGGTT</u> TATACAG <u>TTTCG</u> ATTTGGATTATATTTTGTGAAC
A454F/E455A/S459V reverse	GTTCAAAAATATAATCCAAATCGA <u>ACTGTATAACCAGCAAACCATTCAA</u> AGTTGTCCAACAATGACCATGC

Note: The mutagenic nucleotides are underlined.

The polymerase chain reaction (PCR) consisted of 500 ng of pPICZ α B-His₈-trncTRBG as a template, 125 ng of each sense and antisense mutagenic primers, 1 \times reaction buffer, 10 nmol of dNTP mix, and 3 units of *Pfu* DNA polymerase. The reaction volume was adjusted to 50 μ l by adding high pure water. The reaction cycles were set as follows: denaturation at 95 °C for 30 s; 16 cycles of denaturation at 95 °C for 30 s, annealing at 55 °C for 1 min, and extension at 68 °C for 12 min; final extension at 72 °C for 8.5 min. The size of PCR product was determined by 1% agarose gel electrophoresis (Appendix A1). Then, the reaction was incubated with 10 units of *DpnI* restriction endonuclease at 37 °C overnight in order to remove the DNA template. The mutated plasmid was then transformed into *E. coli* DH5 α by electroporation (Appendix A2) and selected on LB agar [1% (w/v) tryptone, 0.5% (w/v) yeast extract, 0.5% (w/v) sodium chloride and 1.5% (w/v) agar] containing 25 μ g/ml zeocin at 37 °C for 16 h. The clones containing correctly mutated plasmids were screened by using colony PCR method with screening primers (Table 8). The PCR mixture consisted of 5 μ l suspension of cells containing mutated plasmids as a DNA template, 20 pmol of each screening forward and reverse primers, 1 \times reaction buffer, 6 nmol of dNTP mix, 3 μ M MgCl₂, and 1.25 units of *Taq* DNA polymerase. The reaction volume was adjusted to 25 μ l by adding high pure water. The reaction cycles for screening were set as follows: denaturation at 95 °C for 5 min; 30 cycles of denaturation at 95 °C for 1 min, annealing at 50 °C for 30 s, and extension at 72 °C for 1 min; and final extension at 72 °C for 10 min. The PCR products were analyzed by 1% agarose gel electrophoresis. The correct clone of each mutant was cultured in LB broth, and its plasmid was extracted (Appendix A3). The mutations were then confirmed by DNA sequencing.

Table 8 Screening primers used in this study.

Mutant forms of dalcochinase	Name of primer	Nucleotide sequences (5' to 3')	Size of PCR product
A454F/E455A	PrimerFA_for	GACA <u>ACTTTGAATGGTTTGCT</u>	513 bp
	AOXR	GCAAATGGCATTCTGACATC	
E455A/S459V	TRF2	GATTTCCAAGACTATGCGGA	926 bp
	PrimerV_rev	ACAAAATATAATCCAAATCGA <u>AC</u>	
A454F/S459V	TRF2	GATTTCCAAGACTATGCGGA	926 bp
	PrimerV_rev	ACAAAATATAATCCAAATCGA <u>AC</u>	
A454F/E455A/S459V	TRF2	GATTTCCAAGACTATGCGGA	926 bp
	PrimerV_rev	ACAAAATATAATCCAAATCGA <u>AC</u>	

Note: The mutagenic nucleotides are underlined.

2. Cloning the plasmids containing dalcochinase mutants into *P. pastoris*

The plasmids containing the correctly mutated dalcochinase sequence were linearized by 20 units of *SacI* restriction endonuclease in 1X reaction buffer containing 1 µg/µl RNase at 37 °C overnight. The linear plasmid was precipitated with 0.1 volume of 3 M sodium acetate, pH 5.2 and 2.5 volume of absolute ethanol. The DNA pellet was washed with 70% ethanol and re-suspended with 10 µl DNase/RNase free water, before transformation into *P. pastoris* Y11430 by using electroporation (Appendix A4). Transformants were then selected on the YPDS agar containing 100 µg/ml zeocin [1% (w/v) yeast extract, 2% (w/v) peptone, 2% (w/v) glucose, 1 M sorbitol and 2% (w/v) agar] for 5 days at 30 °C. All colonies were re-streaked again on the YPD agar containing 100 µg/ml zeocin [1% (w/v) yeast extract, 2% (w/v) peptone, 2% (w/v) glucose and 2% (w/v) agar].

3. Small-scale expression

To screen for the colony with highest expression, fifty colonies of each dalcochinase mutant were cultured in 5 ml of BMGH [0.34% (w/v) yeast nitrogen base, 1% (w/v) ammonium sulfate, 0.1 M potassium phosphate, pH 6.0, and 1% (v/v) glycerol], which was supplemented with 4×10^{-5} % (w/v) biotin, at 30 °C, 200 rpm overnight. Then, the cultures were centrifuged at 3,000 rpm to collect the cell pellet. The pellets were washed in cold sterile water, centrifuged, and resuspended in BMMH [0.34% (w/v) yeast nitrogen base, 1% (w/v) ammonium sulfate, 0.1 M potassium phosphate, pH 6.0, 0.5% (v/v) methanol and 0.5% (w/v) casamino acid] supplemented with 4×10^{-5} % (w/v) biotin. The cultures were incubated at 30 °C, 200 rpm and induced by 0.5% (v/v) methanol daily for protein production for a week. β -Glucosidase activity in the culture media was measured by using *p*NP-Glc as a substrate (section 6). The colony which showed the highest β -glucosidase activity of each dalcochinase mutant would be selected for large-scale expression.

4. Large-scale expression

The selected colony of each dalcochinase mutant was grown in 20 ml of BMGH containing 4×10^{-5} % (w/v) biotin at 30 °C, 200 rpm overnight. The starter culture was transferred into 130 ml of BMGH supplemented with 4×10^{-5} % (w/v) biotin, and grown under the same condition. The culture media was removed by centrifugation at 3000 rpm, and the cells were washed once by cold sterile water. The cell pellet was resuspended in BMMH supplemented with 4×10^{-5} % (w/v) biotin to a starting OD₆₀₀ of 10. The culture was grown at 30 °C, 200 rpm and the protein production was induced by 0.5% (v/v) methanol daily until the activities did not increase further. Finally, culture media were harvested by centrifugation at 3,000 rpm, 4 °C, and β -glucosidase activity of each dalcochinase mutant was measured by using *p*NP-Glc as a substrate (section 6).

5. Purification of four recombinant dalcochinase mutants

Culture media was collected for protein purification. The large volume of culture media was reduced by using ultrafiltration membrane (30 kDa cut-off, Millipore, USA). Then, the concentrated media was added with 1 M final concentration of ammonium sulfate before applying to a phenyl sepharose column. The phenyl sepharose column was initially equilibrated with 10 mM potassium phosphate, pH 7.0, containing 1 M ammonium sulfate. The protein was loaded into the phenyl sepharose column, and eluted with 10 mM potassium phosphate, pH 7.0. The 2-ml fractions were collected and β -glucosidase activity of all fractions was determined by using *p*NP-Glc as a substrate (section 6). The fractions containing highest activity were combined and dialyzed against 50 mM sodium phosphate, pH 8.0, containing 300 mM sodium chloride and 10 mM imidazole. Then, the protein sample was applied to the Ni²⁺ sepharose column, which was previously equilibrated with 50 mM sodium phosphate, pH 8.0, containing of 300 mM sodium chloride and 10 mM imidazole. The protein was eluted with the same buffer containing 250 mM imidazole. The 1-ml fractions were collected and β -glucosidase activity of all fractions was determined by using *p*NP-Glc as a substrate (section 6). Finally, the fractions containing high β -glucosidase activity were pooled and dialyzed against 0.1 M sodium acetate, pH 5.0. The purified protein samples were stored at -20 °C.

The amount of protein was measured by using Bio-Rad protein assay kit, and compared to a standard curve of bovine serum albumin (Appendix B1). The purified enzymes were analyzed by 10 % SDS-polyacrylamide gel electrophoresis (SDS-PAGE) (Appendix A5), 8 % non-denaturing PAGE stained with 1 mM 4MU-Glc (Appendix A6) and western blotting analysis with the use of mouse monoclonal antibody against natural dalcochinase as a primary antibody, and polyclonal rabbit anti-mouse immunoglobulin linked-HRP as a secondary antibody (Appendix A7).

6. Enzyme assay for β -glucosidase activity

To measure β -glucosidase activity during expression and purification, the culture media or protein fractions were incubated with 1 mM *p*NP-Glc in 0.1 M sodium acetate, pH 5.0, at 30 °C for 30 min. The final reaction volume was adjusted to 500 μ l. The control reaction was prepared by incubating 1 mM *p*NP-Glc in 0.1 M sodium acetate, pH 5.0, under the same condition. All reactions were stopped by adding 1 ml of 2 M sodium carbonate to yield yellow solution. The amount of *p*NP released was measured by reading its absorbance at 400 nm, and compared to its standard curve (Appendix B2). One unit of enzyme was defined as the amount of enzyme that released 1 μ mole of *p*NP per min at 30 °C in 0.1 M sodium acetate, pH 5.0.

To measure β -glucosidase activity of the purified enzyme, the enzyme was incubated with 15 mM *p*NP-Glc in 0.1 M sodium acetate, pH 5.0, in a 50 μ l reaction, at 30 °C for 5 min. The control reaction was performed by incubating 15 mM *p*NP-Glc in 0.1 M sodium acetate, pH 5.0, under the same condition. Then, 100 μ l of 2 M sodium carbonate was added in order to stop the reaction. The amount of *p*NP released was then measured by reading its absorbance at 405 nm, and compared to its standard curve (Appendix B3). One unit of enzyme is defined as the amount of enzyme that releases 1 μ mol *p*NP in 1 min.

7. Kinetic analysis

7.1 Kinetic study of the dalcocinase mutants for hydrolysis of *p*NP-Glc

According to Somphao (2011), 0.01 unit of the purified enzyme was incubated with 0-45 mM *p*NP-Glc in 0.1 M sodium acetate, pH 5.0, in a 50 μ l reaction, at 30 °C for 10 min. The reaction was stopped by adding 100 μ l of 2 M sodium carbonate. The amount of *p*NP released was measured by reading its absorbance at 405 nm and compared to the standard curve of *p*NP (Appendix B3).

7.2 Kinetic study of the dalcochinase mutants for hydrolysis of dalcochinin-8'-*O*- β -D-glucoside

0.01 unit of the purified enzyme was incubated with 0-25 mM dalcochinin-8'-*O*- β -D-glucoside in 0.1 M sodium acetate, pH 5.0, containing 5 % DMSO, in a 50 μ l reaction, at 30 °C for 10 min. The reactions were stopped by boiling for 5 min, and then cooled on ice. The glucose released were reacted with 0.5 unit glucose oxidase reagent and 0.5 mg/ml ABTS at 37 °C for 15 min. The amount of product were determined by reading its absorbance at 405 nm and compared to the glucose standard curve (Appendix B4).

7.3 Kinetic study of dalcochinase mutant toward hydrolysis of soybean isoflavone glucosides

0.01 unit of the purified enzyme was incubated with 0-1 mM soybean isoflavone glucosides (daidzin, genistin, malonyldaidzin, and malonylgenistin) in 0.1 M sodium acetate, pH 5.0, containing 5 % DMSO, in a 50 μ l reaction, at 30 °C for 10 min. Then, all reactions were stopped by boiling for 5 min, and cooled on ice. These reactions were dried by speed vacuum and re-suspended in 50 μ l of 70 % solvent A [0.1 % phosphoric acid in ultrapure water] 30 % solvent B [100 % acetonitrile]. The amount of isoflavone aglycone released in the reaction was analyzed by injecting 10 μ l of reaction mixture into the HPLC system (Perkin Elmer, U.S.A.). The analytes were separated by using Venusil XBP C18 column (4.6 mm \times 250 mm) (Agela Technologies, USA), and detected at 260 nm. The elution was performed at a flow rate of 0.8 ml per min, using elution gradients as follows:

70 % Solvent A	10 min
70 % Solvent A to 35 % Solvent A	20 min
35 % Solvent A to 5 % Solvent A	5 min
5 % Solvent A	10 min
5 % Solvent A to 70 % Solvent A	5 min
Total	50 min

The amount of free isoflavone aglycones in the reaction was calculated by comparing the areas under peaks with either daidzein or genistein standard curves (Appendices B5 and B6, respectively).

7.4 Kinetic calculation

Kinetic parameters, V_{max} and K_m , are calculated from the Michaelis-Menten equation (equation 1) using KaleidaGraph program (Synergy Software).

$$V = \frac{V_{max}[S]}{K_m + [S]} \quad (1)$$

where V is the velocity of reaction, V_{max} is the maximum reaction velocity, $[S]$ is the concentration of substrate and K_m is Michaelis-Menten constant.

In case of high K_m values, the Lineweaver-Burk equation was used in order to calculate the V_{max} and K_m (equation 2).

$$\frac{1}{V} = \frac{K_m}{V_{max}} \times \frac{1}{[S]} + \frac{1}{V_{max}} \quad (2)$$

The turnover number, k_{cat} , was calculated by dividing of V_{max} with the enzyme quantity used in the reaction.

8. Hydrolysis of soybean flour

Soybean flour was purchased from a local market. 40 g of the flour was defatted by using Soxhlet extractor with 500 ml of petroleum ether as solvent for 14 h. 5 g of defatted soybean flour was extracted with 40 ml of 80 % methanol by stirring at ambient temperature overnight. The crude supernatant was collected by centrifugation at 13,000 rpm for 15 min, and concentrated 10-fold. A 5 μ l aliquot of the concentrated extract was incubated with 0.01 unit of purified enzymes (the wild-type dalcocinase, the E455A, the A4544F/E455A and the E455A/S459V mutants, or a commercial preparation of almond β -glucosidase) in 50 μ l of 0.1 M sodium acetate, pH 5.0,

containing 5% DMSO, at 30 °C for 10 min, 2 h or 4 h. The reactions were stopped by boiling for 5 min, and dried by speed vacuum. The dried products were re-suspended in 50 µl of 70 % solvent A [0.1 % phosphoric acid in ultrapure water] 30 % solvent B [100 % acetonitrile]. The amount of isoflavone glucosides and aglycones were analyzed by HPLC as described in section 7.3.

9. Molecular docking

The homology models of dalcochinase and GmICHG were generated by using Modeller 9v4 with the crystal structure of cyanogenic β -glucosidase from white clover (1CBG) as a template (Barrett *et al.*, 1995). The qualities of the models were evaluated by using 4 online programs including PROCHECK (Laskowski *et al.*, 1993), ProSA (Sippl, 1993; Wiederstein and Sippl, 2007), Verify3D (Eisenberg *et al.*, 1997), and WHATIF (Hoofst *et al.*, 1996). The docking parameters were set as default and the hydrogen bonds between ligand and protein were fixed previously published (Table 9) (Somphao, 2011). Then, malonylgenistin was docked into the binding pockets of wild-type dalcochinase and GmICHG, and malonyldaidzin was docked into the binding pocket of the A454F/E455A mutant by using GOLD (Jones *et al.*, 1995). The docking outputs were visually analyzed by using PyMOL (Schrodinger, 2010). The different residues from dalcochinase located close to malonylated group of isoflavone glucoside were compared and then mutated into the corresponding residues from GmICHG to generate four single mutations (Somphao, 2011).

Table 9 Hydrogen fixed for docking.

Protein	Residues fixed	Ligand
Dalcochinase	E395 (Oxygen 5,936)	MG (Hydrogen 47)
	W452 (Hydrogen 6,868)	MG (Oxygen 4)
GmICHG	E420 (Oxygen 6,535)	MG (Hydrogen 47)
	W477 (Hydrogen 7,453)	MG (Oxygen 4)
The A454F/E455A mutant	E483 (Oxygen 5,936)	MD (Hydrogen 37)
	W540 (Hydrogen 6,868)	MD (Oxygen 6)

Note: MG is malonylgenistin and MD is malonyldaidzin

RESULTS AND DISCUSSION

1. Cloning of dalcochinase mutants

The previous study revealed that the A454F dalcochinase mutant showed increased efficiencies toward malonylated soybean isoflavone glucosides, while the E455A and S459V mutants increased efficiencies toward both unmodified and malonylated forms (Somphao, 2011). This study therefore aimed to combine the effect of the three single mutations (A454F, E455A, and S459V) to generate the double and triple mutations in dalcochinase. This will enable us to investigate the interactions between these mutations in hydrolysis of soybean isoflavone glucosides.

1.1 Construction of double- and triple-mutants of dalcochinase

pPICZ-His₈-trncTRBG, which was used as a template for generating double and triple dalcochinase mutants, was extracted from its *E. coli* host. The plasmid was digested with *Pst*I-*Xba*I to give 3,562-bp and 1,537-bp fragments, and with *Bam*HI to give a 5,208-bp fragment. The DNA fragments were analyzed by agarose gel electrophoresis (Fig. 9).

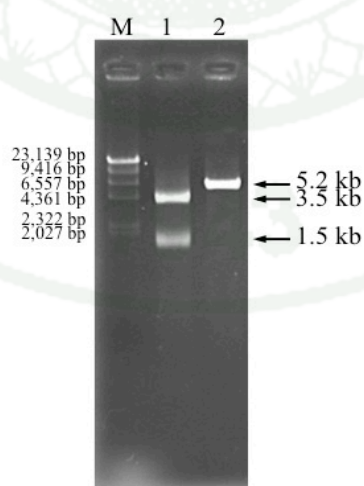


Figure 9 Restriction digestion of plasmid pPICZ-His₈-trncTRBG by *Pst*I, *Xba*I and *Bam*HI restriction endonucleases. Lane M: λ DNA cut by *Hind*III, Lane 1: the plasmid digested by *Pst*I-*Xba*I, Lane 2: the plasmid cut by *Bam*HI.

In order to construct three double and one triple mutations of dalcochinase, namely A454F/E455A, A454F/S459V, E455A/S459V, and A454F/E455A/S459V, the sense and anti-sense mutagenic primers were designed. All dalcochinase mutants were generated by site-directed mutagenesis approach. After the thermal cycles, the correct size of PCR products, which was 5.2 kb, was obtained (Fig. 10A). The PCR reaction was then incubated with 10 units of *DpnI* restriction endonuclease at 37 °C overnight in order to remove the parental double-stranded DNA (Fig. 10B).

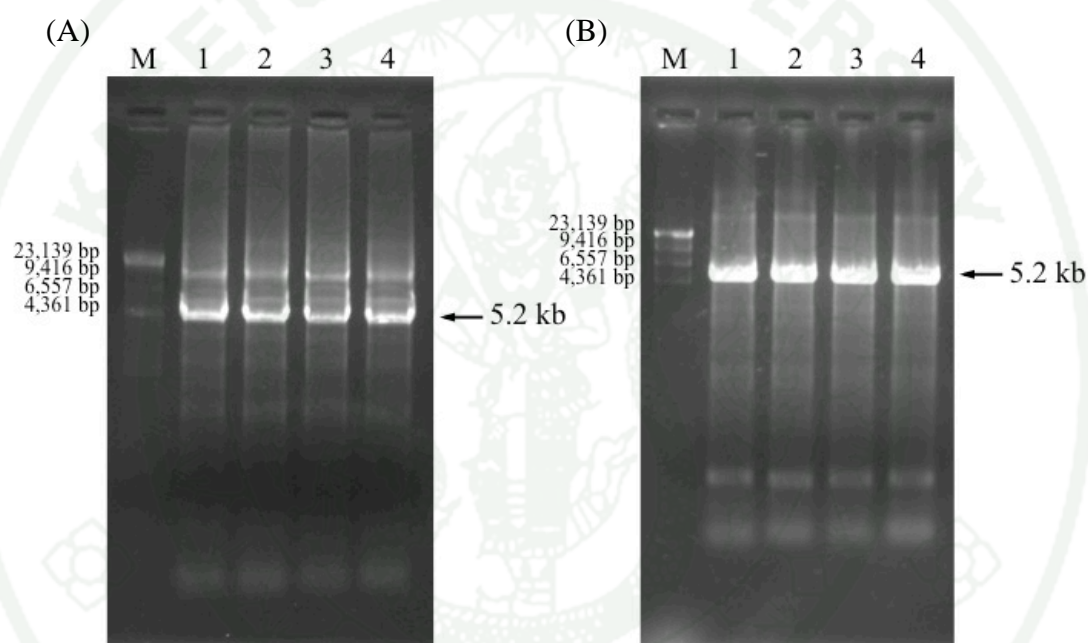


Figure 10 PCR products of all dalcochinase mutants generated by site-directed mutagenesis approach, before (A) and after (B) digestion with *DpnI* restriction endonuclease. Lane M: λ DNA cut by *HindIII*, Lane 1: A454F/E455A, Lane 2: A454F/S459V, Lane 3: E455A/S459V, Lane 4: A454F/E455A/S459V.

1.2 Plasmid transformation into the *E. coli* DH5 α

Plasmids containing dalcochinase mutants were transformed into *E. coli* DH5 α , which was the cloning host. Eight colonies of each transformant were selected and screened by using colony PCR method and specific screening primers. PCR products of all dalcochinase mutants were analyzed by 1% agarose gel electrophoresis (Fig. 11). The correct size of PCR product of A454F/E455A was 513 bp, while the correct size of PCR products of other mutants was 926 bp. Colony numbers 1, 4, 5, and 4 of A454F/E455A, A454F/S459V, E455A/S459V, and A454F/E455A/S459V, respectively, were chosen for DNA sequencing.

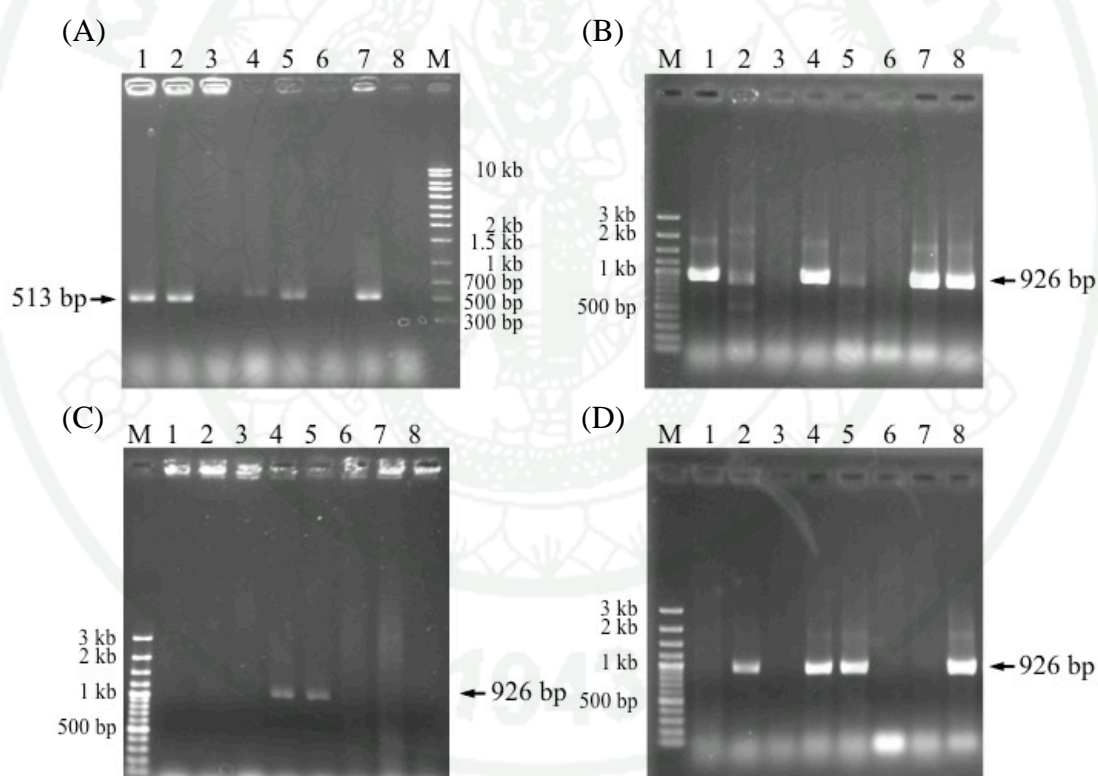


Figure 11 Screening of *E. coli* colonies harboring dalcochinase mutants by using colony PCR method and specific screening primers: A454F/E455A (A), A454F/S459V (B), E455A/S459V (C), and A454F/E455A/S459V (D). Lane M: DNA marker, Lanes 1-8: colony numbers 1 to 8.

The nucleotide sequences of all dalcochinase mutants were confirmed by DNA sequencing (Appendix C). The chromatograms of the wild-type and mutant constructs are shown in Figs. 12 and 13, respectively.

For the A454F/E455A mutant, GCT and GAG, which are codons for alanine and glutamic acid, respectively (Fig. 12), were mutated to TTT and GCT, which are codons for phenylalanine and alanine, respectively (Fig. 13A).

For the A454F/S459V mutant, GCT and TCA, which are codons for alanine and serine, respectively (Fig. 12), were mutated to TTT and GTT, which are codons for phenylalanine and valine, respectively (Fig. 13B).

For the E455A/S459V mutant, GAG and TCA, which are codons for glutamic acid and serine, respectively (Fig. 12), were mutated to GCT and GTT, which are codons for alanine and valine, respectively (Fig. 13C).

For the A454F/E455A/S459V mutant, GCT, GAG, and TCA, which are codons for alanine, glutamic acid, and serine, respectively (Fig. 12), were mutated to TTT, GCT, and GTT, which are codons for phenylalanine, alanine, and valine, respectively (Fig 13D).

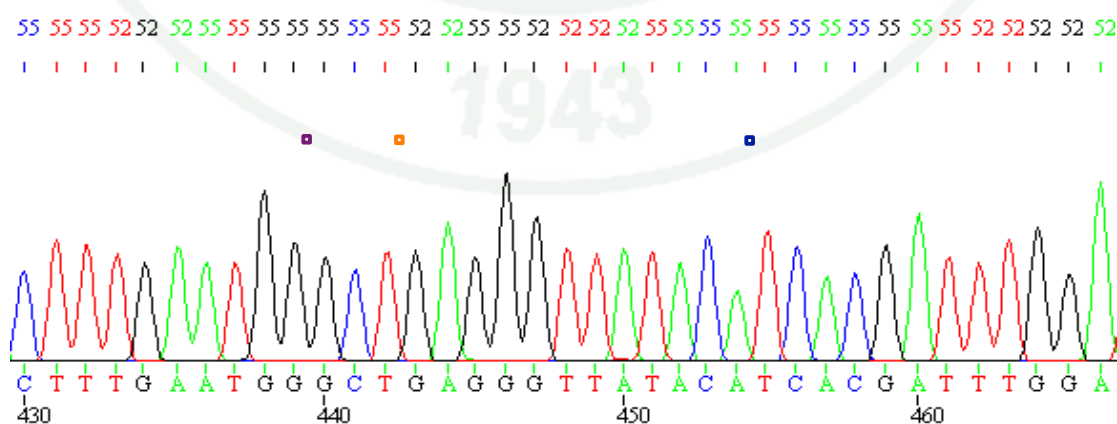


Figure 12 Chromatogram of the wild-type dalcochinase. The codons for A454, E455, and S459 are indicated in purple, orange and blue boxes, respectively.

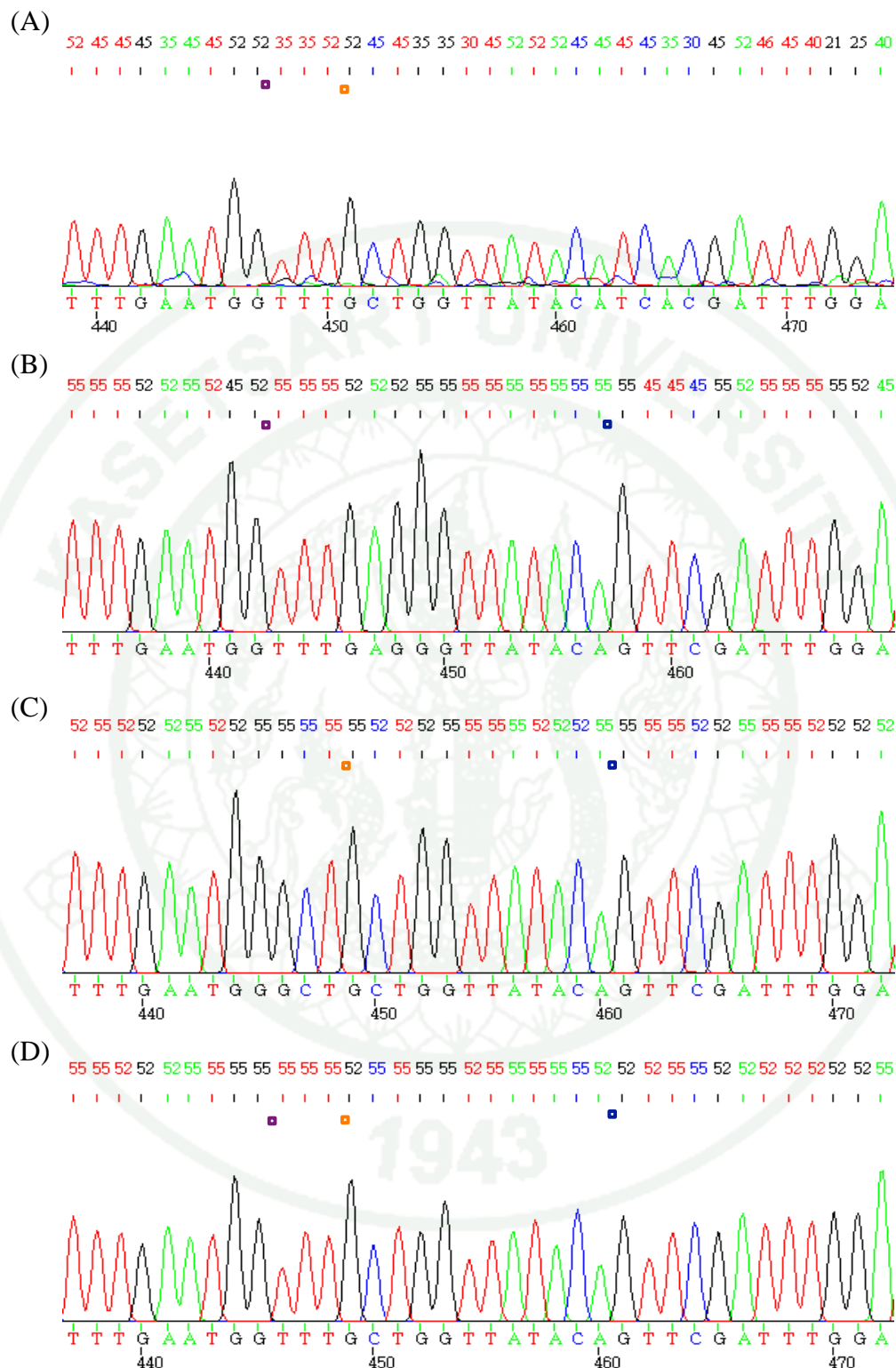


Figure 13 Chromatograms of the dalcochinase mutants: A454F/E455A (A), A454F/S459V (B), E455A/S459V (C), and A454F/E455A/S459V (D). The codons for F454, A455, and V459 are indicated in purple, orange and blue boxes, respectively

These sequences were aligned with that of the wild-type dalcichinase (Fig. 14).

Wild-type	TCATTGTTGGACAACCTTTGAATGGGCTGAGGGTTATACATCACGATTTGGATTATAT
A454F/E455A	TCATTGTTGGACAACCTTTGAATGGTTTGCTGGTTATACATCACGATTTGGATTATAT
A454F/S459V	TCATTGTTGGACAACCTTTGAATGGTTTGAGGGTTATACAGTTCGATTTGGATTATAT
E455A/S459V	TCATTGTTGGACAACCTTTGAATGGGCTGCTGGTTATACAGTTCGATTTGGATTATAT
A454F/E455A/S459V	TCATTGTTGGACAACCTTTGAATGGTTTGCTGGTTATACAGTTCGATTTGGATTATAT

Figure 14 Comparison of nucleotide sequences of the wild-type dalcichinase and the double and triple mutants. Mutated sites are underlined.

1.3 Transformation of dalcichinase mutants into *P. pastoris* Y11430 and enzyme activity screening of each mutant

Plasmids containing double and triple dalcichinase mutants were linearized by *SacI* restriction endonuclease, and transformed into *P. pastoris* Y11430 for protein expression. Because it is a single-celled eukaryotic organism, it can perform various posttranslational modifications such as glycosylation, protein folding, disulfide bond formation, and proteolytic cleavage. So, proteins can be folded correctly without forming inclusion bodies, which are generated by prokaryotic organism such as *E. coli*. *P. pastoris* system showed many advantages such as being fast, easy to handle, and cheaper than other eukaryotic expression systems. Moreover, this expression system also gave high yield of protein expression (Higgins, 1998).

There were more than 100 transformant colonies observed for each dalcichinase mutant. Fifty colonies of each dalcichinase mutant were chosen for expression screening. These colonies were grown in BMGH and induced in BMMH by adding 0.5 % methanol everyday for 7 days. The β -glucosidase activities of all colonies were tested against 1 mM *p*-NP-Glc as described in section 3 of the Methods. The colonies which showed the highest β -glucosidase activities of the A454F/E455A, A454F/S459V, E455A/S459V, and A454F/E455A/S459V mutants were colony

numbers 50, 50, 22, and 44, respectively (Table 10). Therefore, these colonies were chosen for protein expression.

Table 10 Absorbance at 400 nm measuring β -glucosidase activities of 50 colonies of each dalcochinase mutant toward *p*NP-Glc

Colony No.	OD ₄₀₀			
	A454F/E455A	A454F/S459V	E455A/S459V	A454F/E455A/S459V
1	0.363	0.131	0.201	0.203
2	0.507	0.157	0.502	0.240
3	0.358	0.149	0.765	0.151
4	0.327	0.316	0.824	0.226
5	0.329	0.454	0.677	0.207
6	0.358	0.548	0.743	0.230
7	0.349	0.465	0.796	0.222
8	0.404	0.513	0.740	0.236
9	0.337	0.518	0.636	0.246
10	0.313	0.512	0.640	0.260
11	0.450	0.555	0.910	0.208
12	0.330	0.415	0.931	0.216
13	0.359	0.599	0.652	0.275
14	0.419	0.553	0.776	0.213
15	0.298	0.597	0.808	0.253
16	0.329	0.427	0.750	0.233
17	0.408	0.629	0.711	0.202
18	0.335	0.421	0.757	0.204
19	0.398	0.406	0.563	0.222
20	0.275	0.444	0.654	0.252
21	0.484	0.569	0.731	0.266
22	0.364	0.377	0.956	0.165
23	0.414	0.504	0.669	0.195
24	0.426	0.490	0.633	0.231

Table 10 (Continued)

Colony No.	OD ₄₀₅			
	A454F/E455A	A454F/S459V	E455A/S459V	A454F/E455A/S459V
25	0.358	0.524	0.496	0.250
26	0.411	0.504	0.783	0.226
27	0.342	0.528	0.041	0.241
28	0.358	0.364	0.768	0.274
29	0.339	0.494	0.600	0.048
30	0.382	0.603	0.808	0.225
31	0.099	0.396	0.784	0.224
32	0.401	0.638	0.724	0.235
33	0.375	0.488	0.843	0.201
34	0.393	0.601	0.742	0.233
35	0.401	0.565	0.770	0.216
36	0.377	0.411	0.033	0.233
37	0.467	0.498	0.605	0.237
38	0.408	0.523	0.650	0.246
39	0.398	0.467	0.884	0.206
40	0.065	0.543	0.682	0.211
41	0.350	0.121	0.738	0.248
42	0.389	0.179	0.638	0.258
43	0.481	0.148	0.847	0.212
44	0.373	0.334	0.049	<u>0.283</u>
45	0.382	0.159	0.867	0.269
46	0.416	0.574	0.683	0.214
47	0.426	0.443	0.715	0.229
48	0.383	0.609	0.676	0.229
49	0.570	0.568	0.868	0.207
50	<u>0.580</u>	<u>0.684</u>	0.684	0.211

Note: The highest absorbance of each mutant is underlined.

2 Protein expression and purification

P. pastoris colonies of A454F/E455A, A454F/S459V, E455A/S459V, and A454F/E455A/S459V were cultured and induced for protein expression (section 4 of the Methods). In this system, all dalcokinase mutants were secreted outside the cell because they possessed the α factor signal peptide at the N-terminal sequence. The volume of culture media was reduced by ultrafiltration. The dalcokinase mutants were then purified by phenyl sepharose column and Ni²⁺ sepharose column (section 5 of the Methods). The purification tables are shown in Tables 10-13.

In the ultrafiltration step, the activities of the A454F/S459V and E455A/S459V mutants increased when compared with their activities in the culture media (Tables 11-12). It may be suggested that culture media contained some inhibitors that decreased the activities of dalcokinase mutants and were removed by ultrafiltration. So, this step is helpful not only for reducing the large volume, but also for removing small molecules that inhibited the activities of enzyme. However, the activities tended to decrease in the following purification steps, because only fractions containing high activities were pooled. Some fractions showing small activities were not collected. After Ni²⁺ sepharose column, the activities were found in all fractions collected, but only fraction numbers 3-4 that showed high activities of β -glucosidase, were collected. As a result, the purification yields of dalcokinase mutants were between 17 % and 44 % (Tables 10-13).

The amount of proteins in each step also decreased due to removal of contaminated proteins or some lost during the purification steps. So, the specific activities of all dalcokinase mutants tended to increase in each protein purification step due to large decreases in protein content but slight decreases in enzyme activities. However, different dalcokinase mutants showed different specific activities. The mutants showing high specific activities may be determined as good mutants for hydrolysis of β -glucoside substrates. In this case, The A454F/E455A mutant showed the highest specific activity, followed by the E455A/S459V, A454F/S459V, and A454F/E455A/S459V mutants, respectively (Tables 11-14).

Table 11 Purification table of the A454F/E455A mutant

Purification step	Activity (unit)	Protein (mg)	Specific activity (unit/mg)	Purification fold	% Yield
Culture media	19.49	20.32	0.96	1	100
Ultrafiltration	14.71	17.09	0.86	0.90	75.50
Phenyl column	12.41	8.32	1.49	1.56	63.66
Ni ²⁺ column	5.57	0.15	37.13	38.68	28.60

Table 12 Purification table of the A454F/S459V mutant

Purification step	Activity (unit)	Protein (mg)	Specific activity (unit/mg)	Purification fold	% Yield
Culture media	9.94	8.68	1.15	1	100
Ultrafiltration	16.79	7.04	2.39	2.08	168.86
Phenyl column	9.53	2.10	4.54	3.97	95.84
Ni ²⁺ column	4.38	0.22	19.71	17.20	44.02

Table 13 Purification table of the E455A/S459V mutant

Purification step	Activity (unit)	Protein (mg)	Specific activity (unit/mg)	Purification fold	% Yield
Culture media	15.25	26.04	0.59	1	100
Ultrafiltration	21.92	17.69	1.24	2.12	143.75
Phenyl column	10.79	10.47	1.03	1.76	70.75
Ni ²⁺ column	3.06	0.14	22.58	38.57	20.04

Table 14 Purification table of the A454F/E455A/S459V mutant

Purification step	Activity (unit)	Protein (mg)	Specific activity (unit/mg)	Purification fold	% Yield
Culture media	11.07	14.30	0.77	1	100
Ultrafiltration	7.01	6.40	1.09	1.41	63.30
Phenyl column	3.33	2.07	1.60	2.08	30.05
Ni ²⁺ column	1.98	0.40	4.95	6.39	17.87

3 The basic properties of dalcochinase mutants

All dalcochinase mutants showed the molecular weight of 66 kDa (Fig. 15A), which is the same as the wild-type dalcochinase. The identities of dalcochinase mutants were then confirmed by western blot analysis with the use of a mouse monoclonal antibody against natural dalcochinase as the primary antibody (Fig. 15B). The smear in the proteins' band may be due to heterologous glycosylation of the wild-type dalcochinase and the mutant forms.

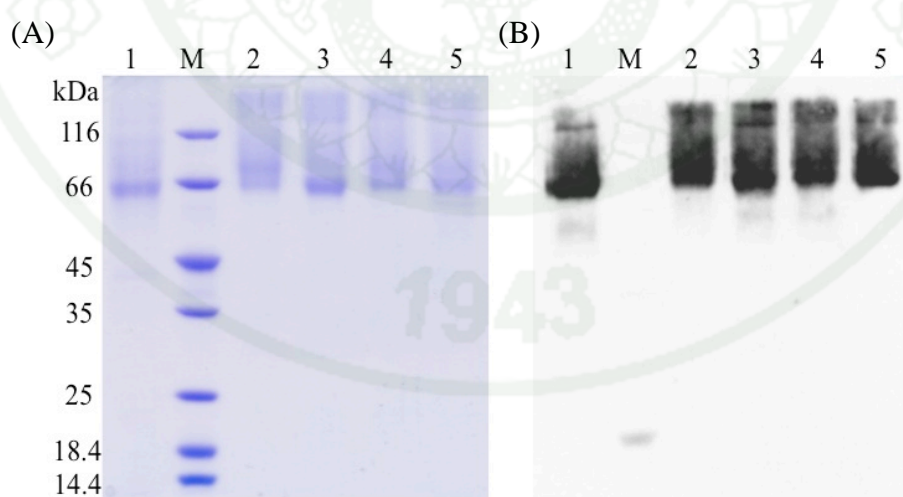


Figure 15 Analysis of sizes and identities of all dalcochinase mutants: 10% SDS-PAGE (A), and western blot analysis (B). Lane M: protein marker, Lane 1: wild-type, Lane 2: A454F/E455A, Lane 3: A454F/S459V, Lane 4: E455A/S459V, Lane 5: A454F/E455A/

The native forms of all dalcocinase mutants were analyzed by non-denaturing PAGE (Fig 16A), and their activities were stained with 1 mM 4MU-Glc (Fig 16B). The amount of each enzyme used in this experiment was 0.1 unit. The A454F/E455A/S459V mutant showed the largest protein band (Fig 16A), while it also gave the highest activity toward 4MU-Glc (Fig. 16B). The A454F/E455A, E455A/S459V and A454F/S459V mutants showed similar activities toward this substrate. However, the wild-type dalcocinase represented the lightest protein band and the lowest activity toward 4MU-Glc (Fig. 16B). So, the A454F/E455A/S459V mutant hydrolyzed the 4MU-Glc with the highest preference (with respect to the activity toward *p*NP-Glc) than other dalcocinase forms.

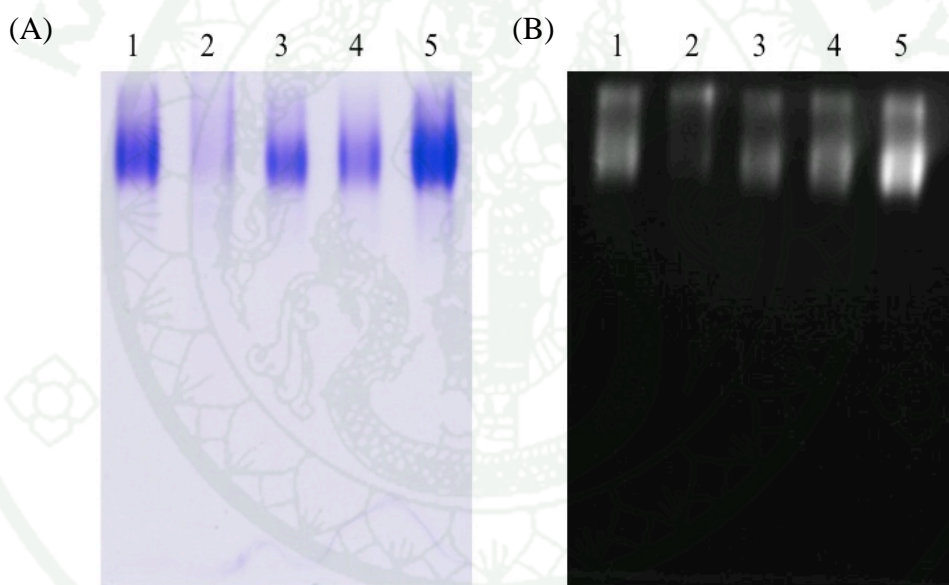


Figure 16 Analysis of the native forms of wild-type dalcocinase and the mutant forms: 8% non-denaturing PAGE stained with coomassie brilliant blue (A), and stained with 1 mM 4MU-Glc and visualized under the ultraviolet light (B). Lane 1: A454F/E455A, Lane 2: wild-type, Lane 3: E455A/S459V, Lane 4: A454F/S459V, Lane 5: A454F/E455A/S459V.

4. Kinetic study of dalcochinase mutants

The kinetic study of all dalcochinase mutants was determined against *p*NP-Glc, which is the chromogenic substrate tested for β -glucosidase activity, dalcochinin-8'-*O*- β -D-glucoside, which is the natural substrate of dalcochinase, and four soybean isoflavone glucoside substrates, namely daidzin, genistin, malonyldaidzin, and malonylgenistin. The kinetic parameters were calculated by using Michaelis-Menten equation. In case of high K_m values, the Lineweaver-Burk equation was used.

4.1 Hydrolysis of *p*NP-Glc

The kinetic parameters of the wild-type dalcochinase and all dalcochinase mutants toward *p*NP-Glc are shown in Table 15, and the plots are shown in Appendices D1-D4. The A454F/E455A and E455A/S459V mutants showed improved hydrolytic efficiencies by 4-fold and 5-fold, respectively, when compared with the wild-type dalcochinase, due to their 2-fold lower K_m values, but 2-fold higher k_{cat} values. The A454F/S459V mutant showed a slight increase in the efficiency toward *p*NP-Glc, when compared with the wild-type dalcochinase, as a result of about 2-fold reductions in both the K_m and the k_{cat} values. On the contrary, the A454F/E455A/S459V mutant showed a 2-fold decrease in the efficiency toward *p*NP-Glc, when compared with the wild-type enzyme because of 2- and 5-fold reductions in the K_m and the k_{cat} values, respectively.

Table 15 Kinetic parameters of the wild-type and mutant forms of dalcochinase toward *p*NP-Glc

Dalcochinase	K_m (mM)	k_{cat} (s^{-1})	k_{cat}/K_m ($mM^{-1}s^{-1}$)
Wild-type	5.82 ± 0.47	110.76 ± 2.55	19.03 ± 1.58
A454F ^a	8.18 ± 0.88	132.17 ± 4.90	16.16 ± 1.84
E455A ^a	7.73 ± 0.61	242.55 ± 6.77	31.38 ± 2.63
S459V ^a	5.45 ± 0.40	27.10 ± 0.58	4.97 ± 0.38
A454F/E455A	2.61 ± 0.14	183.14 ± 2.35	70.15 ± 3.94
A454F/S459V	2.90 ± 0.20	73.61 ± 1.18	25.41 ± 1.76
E455A/S459V	2.11 ± 0.12	196.74 ± 2.26	93.17 ± 5.40
A454F/E455A/S459V	2.39 ± 0.14	21.64 ± 0.27	9.06 ± 0.53

Note: ^a Data obtained from Somphao, 2011

The previous study revealed that the E455A mutant could improve its efficiency toward *p*NP-Glc by 2-fold, while the efficiencies of the A454F and S459V mutants were lower when compared with the wild-type enzyme (Somphao, 2011). So, the combination of A454F/E455A and E455A/S459V mutations could significantly increase its efficiency, compared with the corresponding single mutants. Therefore, these results suggest that for hydrolysis of *p*NP-Glc, there may be synergistic interaction between the residues in all double mutants, but antagonistic interaction in the triple mutant, when compared with the corresponding single mutants.

In this experiment, replacing A454, E455, and S459 with F, A, and V, respectively, in the double and triple mutants created hydrophobic environment around the binding pocket. These hydrophobic residues interacted tightly with the *p*NP-Glc resulting in the reduction of the K_m values in the double and triple mutants. Moreover, the negative charge of glutamate residue in the wild-type enzyme may have obstructed the binding between *p*NP-Glc and catalytic residues.

4.2 Hydrolysis of dalcochinin-8'-O-β-D-glucoside

The kinetic parameters of the wild-type dalcochinase and all dalcochinase mutants toward dalcochinin-8'-O-β-D-glucoside are shown in Table 16, and the plots are shown in Appendices D5-D8. The A454F/E455A, A454F/S459V, and E455A/S459V mutants showed improved efficiencies toward dalcochinin-8'-O-β-D-glucoside by 13-, 3-, and 6-fold, respectively, when compared with the wild-type dalcochinase. The K_m value of the A454F/E455A decreased 2-fold, while those of the other 2 double mutants increased slightly, when compared with the wild-type dalcochinase. Their k_{cat} values increases 6-, 4-, and 8-fold, for the A454F/E455A, A454F/S459V, and E455A/S459V mutants, respectively, when compared with the wild-type dalcochinase. Although the k_{cat} value of the E455A/S459V mutant was the highest, the mutant that showed the highest efficiency was the A454F/E455A mutant because of the largest reduction in the K_m value. On the other hand, the A454F/E455A/S459V mutant showed a decrease in its efficiency toward dalcochinin-8'-O-β-D-glucoside, due to a 2-fold increase in the K_m value and a slight increase in the k_{cat} value.

Table 16 Kinetic parameters of the wild-type and mutant forms of dalcochinase toward dalcochinin-8'-O-β-D-glucoside

Dalcochinase	K_m (mM)	k_{cat} (s ⁻¹)	k_{cat}/K_m (mM ⁻¹ s ⁻¹)
Wild-type	0.87 ± 0.07	25.68 ± 0.60	29.65 ± 2.53
A454F ^a	2.36 ± 0.21	24.82 ± 0.72	10.53 ± 1.00
E455A ^a	2.42 ± 0.39	122.52 ± 8.22	50.66 ± 8.89
S459V ^a	1.40 ± 0.17	59.3 ± 2.36	42.44 ± 5.45
A454F/E455A	0.39 ± 0.04	152.97 ± 3.79	393.52 ± 41.94
A454F/S459V	1.22 ± 0.10	109.84 ± 3.26	89.95 ± 8.06
E455A/S459V	1.09 ± 0.10	206.73 ± 6.45	190.17 ± 17.80
A454F/E455A/S459V	1.86 ± 0.20	37.19 ± 1.83	19.99 ± 2.34

Note: ^a Data obtained from Somphao, 2011

The previous study revealed that only the E455A and S459V mutants could improve their efficiencies toward dalcochinin-8'-*O*- β -D-glucoside by 2-fold and 1.5-fold, respectively, while the A454F mutant showed the opposite effect (Somphao, 2011). All double mutants showed higher efficiencies than their corresponding single mutants, due to increases in the k_{cat} values but decreases in the K_m values. On the other hand, the A454F/E455A/S459V mutant showed a decrease in its efficiency because of a high K_m value. Therefore, these results suggest that it may be synergistic interaction in all double mutants for hydrolysis of dalcochinin-8'-*O*- β -D-glucoside, but antagonistic interaction in the triple mutant for hydrolysis of this substrate, when compared with the corresponding single mutants.

Again, replacing A454, E455, and S459 with F, A, and V, respectively, in the double and triple mutants built up hydrophobic environment around the binding pocket. The hydrophobic residues in the binding pocket seemed to assist in the hydrolysis of dalcochinin-8'-*O*- β -D-glucoside. However, in all dalcochinase mutants, except the A454F/E455A mutant, these residues may interact weakly with dalcochinin-8'-*O*- β -D-glucoside, resulting in increases in the K_m values.

4.3 Hydrolysis of daidzin

The kinetic parameters of the wild-type dalcochinase and all dalcochinase mutants toward daidzin are shown in Table 17, and the plots are shown in Appendices D9-D14. Only, the A454F/E455A mutant exhibited a slight increase in its efficiency, when compared with the wild-type dalcochinase, due to 3-fold increases in both the k_{cat} and K_m values. On the other hand, the efficiencies of the other double mutants decreased, when compared with the wild-type dalcochinase, due to larger increases in the K_m values than the k_{cat} values. In the triple mutant, the K_m value increased by 5-fold, while the k_{cat} value decreased slightly, when compared with the wild-type enzyme. Thus, the increases in the K_m values lowered the efficiencies of double and triple mutant enzymes.

Table 17 Kinetic parameters of the wild-type and mutant forms of dalcochinase toward daidzin

Dalcochinase	K_m (mM)	k_{cat} (s^{-1})	k_{cat}/K_m ($mM^{-1}s^{-1}$)
Wild-type	0.07 ± 0.007	7.07 ± 0.17	95.47 ± 9.43
A454F ^a	0.07 ± 0.008	5.17 ± 0.17	75.29 ± 9.41
E455A ^a	0.04 ± 0.003	11.04 ± 0.19	302.48 ± 27.34
S459V ^a	0.08 ± 0.008	18.13 ± 0.44	221.05 ± 21.55
A454F/E455A	0.24 ± 0.02	24.22 ± 0.62	100.43 ± 7.58
A454F/S459V	0.32 ± 0.03	14.45 ± 0.43	45.71 ± 4.04
E455A/S459V ^b	0.45 ± 0.03	35.04 ± 2.29	78.39 ± 7.52
A454F/E455A/S459V ^b	0.33 ± 0.04	4.97 ± 0.59	15.24 ± 0.61

Note: ^a Data obtained from Somphao, 2011

^b Data obtained via the Lineweaver-Burk equation

The previous study revealed that the E455A and S459V mutants exhibited increased efficiencies toward daidzin by 3-fold and 2-fold, respectively, when compared with the wild-type dalcochinase (Somphao, 2011). In fact, the k_{cat} values of the A454F/E455A and E455A/S459V mutants were higher than those of the E455A and S459V mutants, but their K_m values were also higher. Therefore, the higher K_m values of the A454F/E455A and E455A/S459V mutants led to their lower catalytic efficiencies, when compared with the E455A and S459V mutants. So, the combination of single mutations resulted in weak binding interactions between the residues and daidzin. Therefore, these results suggest that it may be antagonistic interaction in double and triple mutants for hydrolysis of daidzin, when compared with the corresponding single mutants.

Our kinetic data suggested that the hydrophobic residues in the binding pocket of single mutants were required for hydrolysis of daidzin, but not in combination. Moreover, in double and triple dalcochinase mutants, these residues may interact weakly with daidzin, resulting in increases in the K_m values.

4.4 Hydrolysis of genistin

The kinetic parameters of the wild-type dalcochinase and all dalcochinase mutants toward genistin are shown in Table 18, and the plots are shown in Appendices D15-D18. The A454F/E455A and E455A/S459V mutants showed increases in their efficiencies toward genistin by 3- and 2-fold, respectively, when compared with the wild-type dalcochinase. For the A454F/E455A mutant, it was mainly due to an increase in the k_{cat} value, while for the E455A/S459V mutant, both the K_m and k_{cat} values increased by 4- and 7-fold, respectively, when compared with the wild-type dalcochinase. The A454F/S459V mutant also showed a slight increase in its efficiency, when compared with the wild-type enzyme, due to 2-fold increases in both the K_m and k_{cat} values. However, the A454F/E455A/S459V mutant exhibited 3.5-fold lower efficiency, when compared with the wild-type enzyme, mainly due to the 2.5-fold increase in the K_m value.

Table 18 Kinetic parameters of the wild-type and mutant forms of dalcochinase toward genistin

Dalcochinase	K_m (mM)	k_{cat} (s^{-1})	k_{cat}/K_m ($mM^{-1}s^{-1}$)
Wild-type	0.08 ± 0.01	3.67 ± 0.12	45.37 ± 5.80
A454F ^a	0.14 ± 0.02	2.77 ± 0.11	19.51 ± 2.33
E455A ^a	0.12 ± 0.02	27.96 ± 1.45	236.65 ± 44.95
S459V ^a	0.11 ± 0.01	12.19 ± 0.37	109.06 ± 12.98
A454F/E455A	0.07 ± 0.007	9.74 ± 0.25	147.36 ± 16.50
A454F/S459V	0.13 ± 0.02	6.88 ± 0.10	54.95 ± 6.63
E455A/S459V	0.29 ± 0.04	25.23 ± 1.37	87.09 ± 11.54
A454F/E455A/S459V	0.20 ± 0.02	2.64 ± 0.08	13.04 ± 1.24

Note: ^a Data obtained from Somphao, 2011

The previous study revealed that the E455A and S459V mutants showed higher hydrolytic efficiencies toward genistin by 5-fold and 2-fold, respectively, when

compared with the wild-type dalcochinase (Somphao, 2011). The combination of E455A/S459V mutation resulted in only a 2-fold increase in the efficiency, due to a 7-fold increase in the k_{cat} value (similar to the E455A mutant) but also almost 4-fold increase in K_{m} value. So, even though the E455A and the S459V mutations could improve hydrolytic efficiencies toward genistin, the combinations of these single mutations did not improve the efficiencies, when compared with the corresponding single mutants. Therefore, these results suggest that it may be antagonistic interaction in double and triple mutants for hydrolysis of genistin, when compared with the corresponding single mutants.

Our results suggested that, in the single mutants, replacing E455 and S459 with A and V, respectively, created hydrophobic environment around the binding pocket, which appeared to be beneficial for the hydrolysis of genistin. The negative charge of glutamate residue and the polarity of serine residue may have obstructed the binding between the residues and genistin. However, the combination of hydrophobic residues showed negative effects in the double and triple mutants, when compared with the corresponding single mutants. Moreover, in all dalcochinase mutants, except the A454F/E455A mutant, these residues may interact weakly with genistin, resulting in increases in the K_{m} values.

4.5 Hydrolysis of malonyldaidzin

The kinetic parameters of the wild-type dalcochinase and all dalcochinase mutants toward malonyldaidzin are shown in Table 19, and the plots are shown in Appendices D19-D25. All double mutants exhibited between 5- to 18-fold higher efficiencies toward malonyldaidzin, when compared with the wild-type dalcochinase. The A454F/E455A mutant showed the highest increase in the efficiency (18-fold) due to an 8-fold increase in the k_{cat} value, and a 2.5-fold decrease in the K_{m} value, when compared with the wild-type dalcochinase. On the other hand, the E455A/S459V mutant showed the highest increase in the k_{cat} value (26-fold), but its K_{m} value also increased 3-fold, resulting in only an 8-fold increase in the efficiency, when compared with the wild-type dalcochinase. The K_{m} value of the A454F/S459V mutant was

similar to the wild-type enzyme, while its k_{cat} value increased by 5-fold. However, the A454F/E455A/S459V mutant showed a very high K_m value, such that it could not be accurately determined by the present method.

The previous study revealed that the A454F, E455A, and S459V mutants showed increases in the hydrolytic efficiencies toward malonyldaidzin by 1.4-fold, 4-fold, and 2-fold, respectively, when compared with the wild-type enzyme (Somphao, 2011). The single mutants showed slight increases in the k_{cat} values, while the K_m values changed slightly, when compared with the wild-type dalcochinase. So, the double mutations performed in this study could improve hydrolytic efficiencies toward malonyldaidzin, when compared with the corresponding single mutants. Therefore, these results suggest that it may be synergistic interaction in all double mutants for hydrolysis of malonyldaidzin but antagonistic interaction in triple mutants, when compared with the corresponding single mutants.

Table 19 Kinetic parameters of the wild-type and mutant forms of dalcochinase toward malonyldaidzin

Dalcochinase	K_m (mM)	k_{cat} (s^{-1})	k_{cat}/K_m ($\text{mM}^{-1}\text{s}^{-1}$)
Wild-type	0.45 ± 0.06	0.27 ± 0.02	0.62 ± 0.09
A454F ^a	0.47 ± 0.07	0.40 ± 0.03	0.85 ± 0.13
E455A ^a	0.18 ± 0.02	0.42 ± 0.02	2.32 ± 0.31
S459V ^a	0.81 ± 0.10	0.93 ± 0.06	1.15 ± 0.16
A454F/E455A	0.18 ± 0.02	2.04 ± 0.07	11.10 ± 1.17
A454F/S459V ^b	0.41 ± 0.05	1.35 ± 0.15	3.31 ± 0.52
E455A/S459V ^b	1.35 ± 0.25	6.89 ± 1.26	5.11 ± 1.32
A454F/E455A/S459V ^c	N.D.	N.D.	N.D.

Note: ^a Data obtained from Somphao, 2011;

^b Data obtained via the Lineweaver-Burk equation;

^c Data not determined due to a very high K_m value.

The results suggested that replacing A454, E455, and S459 with F, A, and V, respectively, in the double and triple mutants created hydrophobic environment around the binding pocket. These hydrophobic residues in the binding pocket seemed to be important for hydrolysis of malonyldaidzin. Especially, the F454 and A455 residues in the A454F/E455A mutant showed tight binding with malonyldaidzin. It is likely that these positions prefer an aromatic hydrophobic residue (F454) and a small hydrophobic residue (A455) for binding and hydrolysis of malonyldaidzin.

4.6 Hydrolysis of malonylgenistin

The kinetic parameters of the wild-type dalcochinase and all dalcochinase mutants toward malonylgenistin are shown in Table 20, and the plots are shown in Appendices D26-D30. The A454F/E455A, A454F/S459V, and E455A/S459V mutants showed increased efficiencies toward malonylgenistin by 3.6-fold, 1.5-fold, and 2-fold, respectively, when compared with the wild-type dalcochinase. As described previously for the hydrolysis of malonyldaidzin, the E455A/S459V mutant showed the highest increase in the k_{cat} value (2-fold) among the double mutants, but its K_m value also increased slightly, resulting in only 2-fold increase in the efficiency, when compared with the wild-type dalcochinase. For the other 2 double mutants, their k_{cat} values were similar to the wild-type enzyme, while the K_m value slightly decreased, resulting in increases in the efficiencies. However, the A454F/E455A/S459V mutant showed decrease in the efficiency by 2-fold, when compared with the wild-type dalcochinase, because of the increase in the K_m value by 1.6-fold without affecting the k_{cat} value.

Table 20 Kinetic parameters of the wild-type and mutant forms of dalcochinase toward malonylgenistin

Dalcochinase	K_m (mM)	k_{cat} (s^{-1})	k_{cat}/K_m ($mM^{-1}s^{-1}$)
Wild-type	0.30 ± 0.02	0.60 ± 0.02	1.97 ± 0.16
A454F ^a	0.09 ± 0.01	0.43 ± 0.02	4.64 ± 0.58
E455A ^a	0.09 ± 0.01	5.84 ± 0.12	65.44 ± 5.25
S459V ^a	0.44 ± 0.01	0.99 ± 0.01	2.25 ± 0.06
A454F/E455A	0.08 ± 0.007	0.55 ± 0.01	7.02 ± 0.62
A454F/S459V	0.20 ± 0.02	0.58 ± 0.02	2.90 ± 0.34
E455A/S459V	0.37 ± 0.02	1.32 ± 0.03	3.54 ± 0.21
A454F/E455A/S459V ^b	0.68 ± 0.08	0.59 ± 0.07	0.87 ± 0.15

Note: ^a Data obtained from Somphao, 2011;

^b Data obtained via the Lineweaver-Burk equation;

The previous study revealed that the A454F and E455A mutants showed increases in the efficiencies by 2.4-fold and 33-fold, respectively, while the efficiency of the S459V mutant slightly increased, when compared with the wild-type dalcochinase (Somphao, 2011). In particular for the E455A mutant which showed the highest efficiency, its k_{cat} value increased by almost 10-fold, while its K_m value decreased by 3-fold, when compared with the wild-type enzyme. However, in the combination of A454F/E455A mutation, the k_{cat} value did not change, while the K_m value decreased 4-fold, when compared with the wild-type dalcochinase. In the combination of E455A/S459V mutation, the k_{cat} value increased 2-fold, while the K_m value also increased slightly. So, even though the single mutations at A454F, E455A and S459V could increase the hydrolytic efficiencies toward malonylgenistin, the combinations of these single mutations did not improve the efficiencies, when compared with the corresponding single mutants. Therefore, these results suggest that it may be antagonistic interaction in the double and triple mutants for hydrolysis of malonylgenistin, when compared with the corresponding single mutants.

Again, our data suggested that replacing A454, E455, and S459 with F, A, and V, respectively, created hydrophobic environment around the binding pocket. These hydrophobic residues interacted tightly with malonylgenistin in the A454F, E455A, and A454F/E455A mutants resulting in the reduction of K_m values, but showed weak binding in the A454F/E455A/S459V mutant. Moreover, the negative charge of glutamate residue in the wild-type enzyme may have obstructed the binding and hydrolysis between malonylgenistin and catalytic residues. Especially, the A455 residues in the E455A mutant showed tight binding and a high k_{cat} value with malonylgenistin. It is likely that this position prefers a small hydrophobic residue (A455) for binding and hydrolysis of malonylgenistin. However, the combination of these hydrophobic residues in the double and triple mutants showed negative effect when compared with the corresponding single mutants.

5. Hydrolysis of soybean flour extracts

In order to determine the abilities of our dalcochinase mutants in the hydrolysis of soybean isoflavone glucosides present in common food sources, such as soybean flour, the mutants that showed the highest efficiencies toward soybean isoflavone glucosides (the E455A and A454F/E455A mutants) and the highest k_{cat} value (the E455A/S459V mutant) were tested, and compared with the activities of the wild-type dalcochinase and the commercial preparation of almond β -glucosidase. In this study, the commercially available soybean flour was firstly de-fatted, and then extracted by 80% methanol. The amount of soybean isoflavone glucosides from crude soybean flour extracts was determined by reverse phase HPLC before the reactions were performed. The peaks of daidzin, genistin, malonyldaidzin, malonylgenistin, acetyldaidzin, acetylgenistin, daidzein, and genistein were identified by comparing them with those of the commercially available soybean isoflavone glucosides (Fig. 17A). Malonylgenistin, genistin, and daidzin were found to be the major forms in crude soybean flour extracts (Fig. 17B). The acetylated forms and malonyldaidzin were also present in small amounts in the extracts, but the corresponding free aglycone forms were very little. According to Coward *et al.* (1998) and Wang and Murphy (1996), the isoflavone glucosides were the dominant forms in unprocessed

soybean flour, while the amount of aglycone forms were very small. Moreover, among the gluco-conjugated forms, malonylated isoflavone glucosides were the major forms in the unprocessed soy food.

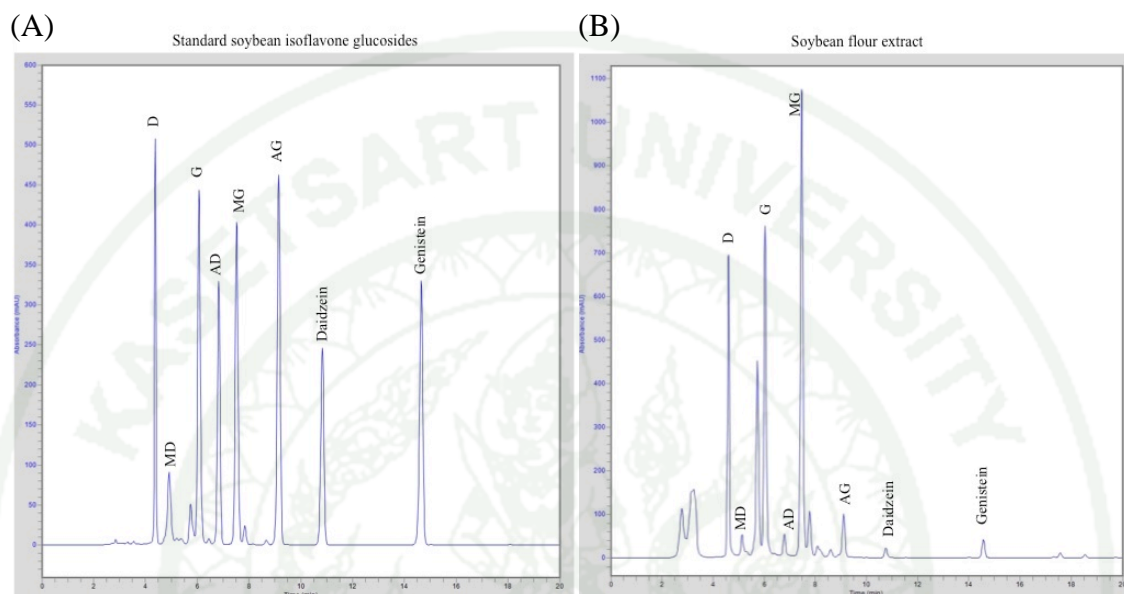


Figure 17 HPLC profiles of soybean isoflavone glucoside standards (A) and soybean isoflavone glucoside from soybean flour extract (B); D = daidzin, G = genistin, MD = malonylgenistin, MG= malonylgenistin, AD = acetyl daidzin, and AG = acetylgenistin.

For hydrolysis by almond β -Glucosidase (Table 21), the enzyme hydrolyzed 31 % of daidzin and 14 % of genistin within 10 min. After incubation for 4 h, daidzin and genistin were then hydrolyzed by 40 % and 31 %, respectively. However, β -glucosidase from almond hardly hydrolyzed malonylated and acetylated soybean isoflavone glucosides.

Table 21 Relative amount of soybean isoflavone glucosides after incubation with β -glucosidase from almond. The amount before incubation was taken as 100%. The amount at other incubation times was calculated relative to the amount before incubation.

Soybean isoflavones	Area under peaks		
	0 min	10 min	4 h
Daidzin	100	68.63	60.26
Genistin	100	85.67	69.00
Malonyldaidzin	100	111.56	0
Malonylgenistin	100	82.68	92.79
Acetyldaidzin	100	92.52	121.59
Acetylgenistin	100	90.78	117.11
Daidzein	100	189.94	1,124.10
Genistein	100	152.59	861.74

For hydrolysis by the wild-type dalcocinase (Table 22), 17 % and 5 % of daidzin and genistin were hydrolyzed, respectively, after 10 min of incubation. After incubation for 4 h, daidzin and genistin were hydrolyzed by 65 % and 70 %, respectively. Moreover, the wild-type dalcocinase also slightly hydrolyzed malonylgenistin.

Table 22 Relative amount of soybean isoflavone glucosides after incubation with the wild-type daltocchinase. The amount before incubation was taken as 100%. The amount at other incubation times was calculated relative to the amount before incubation.

Soybean isoflavones	Area under peaks		
	0 min	10 min	4 h
Daidzin	100	82.53	34.85
Genistin	100	95.28	29.57
Malonyldaidzin	100	135.51	119.50
Malonylgenistin	100	104.00	93.07
Acetyldaidzin	100	126.72	108.67
Acetylgenistin	100	114.43	104.85
Daidzein	100	326.15	1,524.68
Genistein	100	368.10	1,578.03

For hydrolysis by the E455A mutant (Table 23), only small amounts of soybean isoflavone glucosides were hydrolyzed after 10 min of the reactions. When the reactions were incubated for 4 h, the E455A mutant hydrolyzed daidzin, genistin, and malonylgenistin by 56 %, 65 %, and 9 %, respectively.

Table 23 Relative amount of soybean isoflavone glucosides after incubation with the E455A mutant. The amount before incubation was taken as 100%. The amount at other incubation times was calculated relative to the amount before incubation.

Soybean isoflavones	Area under peaks		
	0 min	10 min	4 h
Daidzin	100	86.72	43.84
Genistin	100	100.12	35.04
Malonyldaidzin	100	132.82	123.52
Malonylgenistin	100	107.61	91.46
Acetyldaidzin	100	118.22	125.04
Acetylgenistin	100	120.21	107.86
Daidzein	100	308.90	1,215.16
Genistein	100	365.69	1,332.19

For hydrolysis by the A454F/E455A mutant (Table 24), the enzyme hydrolyzed 11 % of daidzin within 10 min. After incubation for 4 h, malonyldaidzin was completely hydrolyzed, while daidzin, genistin, malonylgenistin, acetyldaidzin, and acetylgenistin were then hydrolyzed by 70 %, 77 %, 30 %, 23 %, and 28 %, respectively.

Table 24 Relative amount of soybean isoflavone glucosides after incubation with the A454F/E455A mutant. The amount before incubation was taken as 100%. The amount at other incubation times was calculated relative to the amount before incubation.

Soybean isoflavones	Area under peaks		
	0 min	10 min	4 h
Daidzin	100	89.23	30.41
Genistin	100	105.16	23.25
Malonyldaidzin	100	130.14	0
Malonylgenistin	100	109.57	70.02
Acetyldaidzin	100	107.13	77.32
Acetylgenistin	100	118.04	72.74
Daidzein	100	263.58	974.95
Genistein	100	291.02	1,037.91

For hydrolysis by the E455A/S459V mutant (Table 25), the enzyme hydrolyzed 48 % of daidzin, 52 % of genistin, 24 % of malonylgenistin, 32 % of acetyldaidzin, and 31 % of acetylgenistin within 10 min. However, some experiments, the areas under peaks of all soybean isoflavone glucosides were higher than the control. It may be because, in this experiment, all reactions were separately performed. The amount of substrates used may not be equal in all reactions. However, the E455A/S459V mutant released the highest amount of soybean isoflavone aglycones after 4 h of incubation (data not shown).

Table 25 Relative amount of soybean isoflavone glucosides after incubation with the E455A/S459V mutant. The amount before incubation was taken as 100%. The amount at other incubation times was calculated relative to the amount before incubation.

Soybean isoflavones	Area under peaks		
	0 min	10 min	4 h
Daidzin	100	52.15	12.86
Genistin	100	47.73	14.71
Malonyldaidzin	100	0	133.17
Malonylgenistin	100	75.90	96.05
Acetyldaidzin	100	68.18	87.97
Acetylgenistin	100	69.47	72.72
Daidzein	100	373.14	1451.57
Genistein	100	487.72	1503.32

To compare the abilities of these enzymes in the hydrolysis of soybean isoflavone glucosides in soybean flour extract, the relative amount of soybean isoflavone glucosides at 10 min and 4 h of incubation were plotted (Fig. 18). At 10 min, the E455A/S459V mutant appeared to be the best enzyme for hydrolysis of soybean isoflavone glucosides in soybean flour extract, as it gave the highest relative amount of free isoflavone aglycones (Fig. 18A). However at 4 h, both the wild-type dalcochianse and the E455A/S459V mutant showed similar capabilities (Fig. 18B).

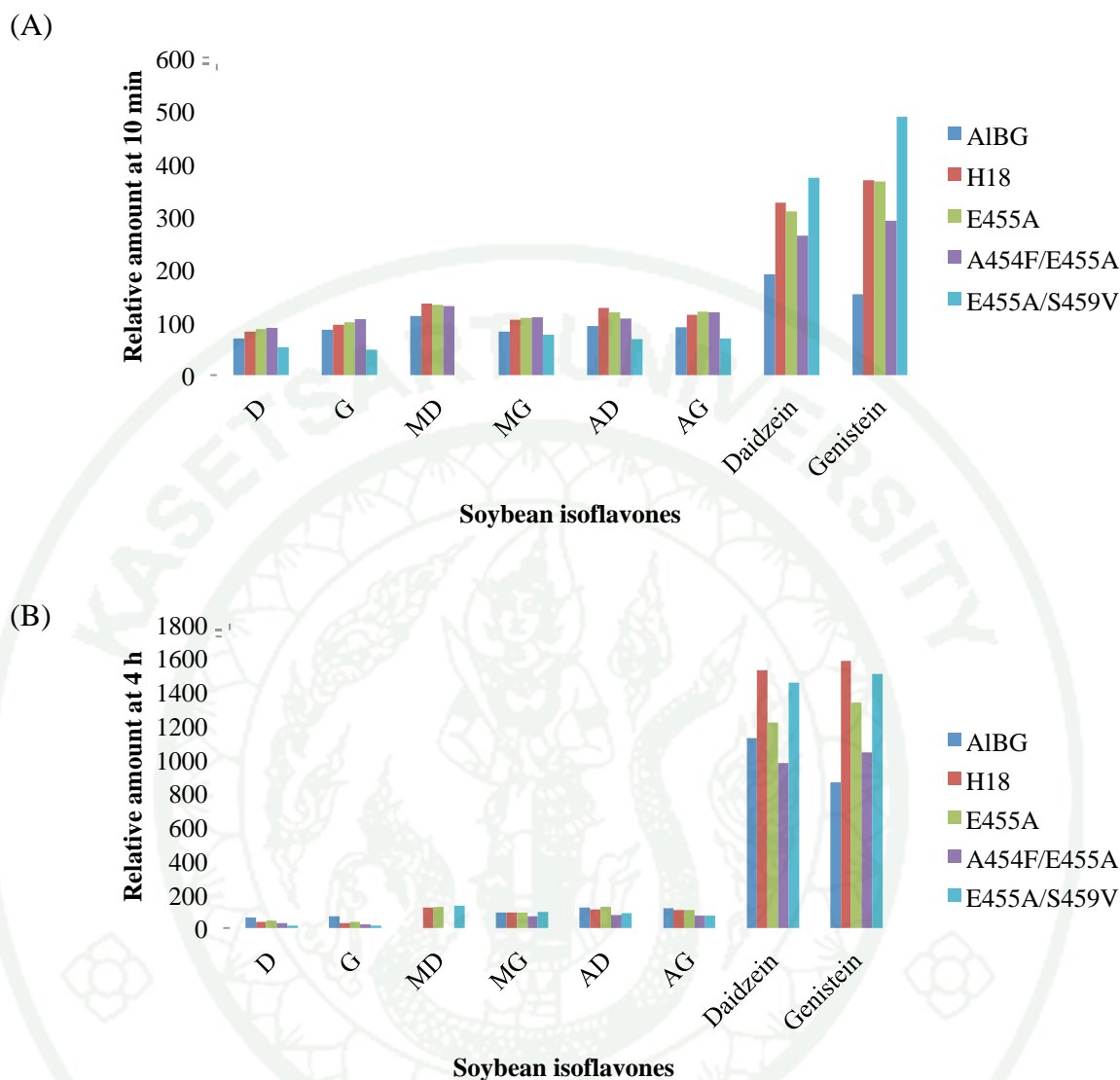


Figure 18 Relative amount of soybean isoflavone glucosides after incubation with various enzymes for 10 min (A) and 4 h (B). The amount before incubation was taken as 100%. D = daidzin, G = genistin, MD = malonylgenistin, MG= malonylgenistin, AD = acetyldaidzin, and AG = acetylgenistin.

6. Molecular docking

Since the crystal structures of dalcocinase and GmICHG have not been determined, their structural models were generated by Modeller 9v4. The wild-type dalcocinase, the A454F/E455A mutant, and the GmICHG were modeled by using cyanogenic β -glucosidase from *Trifolium repens* L. (white clover) (PDB code: 1CBG) as a template. Their quality was also evaluated by using several free online programs, namely PROCHECK, ProSA, verify 3D, and WHATIF. The high quality of the modeling structure should contain over 90 % of residues in the most favoured regions as judged by PROCHECK. Our structural models showed percentage of residues in the most favoured regions between 87 % to 89 %, which were close to 90%. Moreover, these models contained 0.2 % of the residues in the disallowed regions, which was acceptable because it should be less than 2 % of residues in disallowed regions. ProSA is a tool for evaluating the three-dimensional structure of models for potential errors. The z-scores obtained by ProSA for the three β -glucosidase models (-8.36 to -9.18), which were within an acceptable range and indicated good model qualities. Verify 3D, which checked the correctness of three-dimensional structure of these models based on low-resolution electron density maps, inadequate distance constraints, or computational procedures, gave z-scores over 90 %, indicating correct folding in most of protein structures. WHATIF evaluated several factors such as the missing unit cell, backbone and residue conformation, bond length, and etc. The z-scores obtained by WHATIF of these β -glucosidase models were all above -2.0, which were acceptable (Table 26).

Table 26 Evaluation of the structural models of the wild-type dalcochinase, the A454F/E455A mutant, and GmICHG

Program	Dalcochinase	A454F/E455A mutant	GmICHG
PROCHECK:			
- Residues in most favoured regions (%)	87.4	87.4	89.2
- Residues in additional allowed regions (%)	11.9	11.9	9.0
- Residues in generously allowed regions (%)	0.5	0.5	1.6
- Residues in disallowed regions (%)	0.2	0.2	0.2
ProSA: z-score	-8.4	-8.36	-9.18
Verify 3D: z-score (% of residues with a score over 0.2)	94.05	94.07	90.73
WHATIF: z-score	-1.356	-1.355	-0.044

The models of dalcochinase and GmICHG showed $(\beta/\alpha)_8$ -barrel of domains (Fig. 19). The length and width of the binding pocket of dalcochinase were 22 Å (measured by the distance of P347-C γ and E455-O ϵ 2) and 7.8 Å (measured by the distance of N189-N δ 2 and W368-C δ 1), respectively. The distance between two catalytic residues was 5.5 Å. The length and width of the binding pocket of GmICHG were 24.3 Å (measured by the distance of S371-O γ and A479-C β) and 10.9 Å (measured by the distance of G216-C α and W392-C δ 1), respectively. The distance between two catalytic residues was 4.2 Å

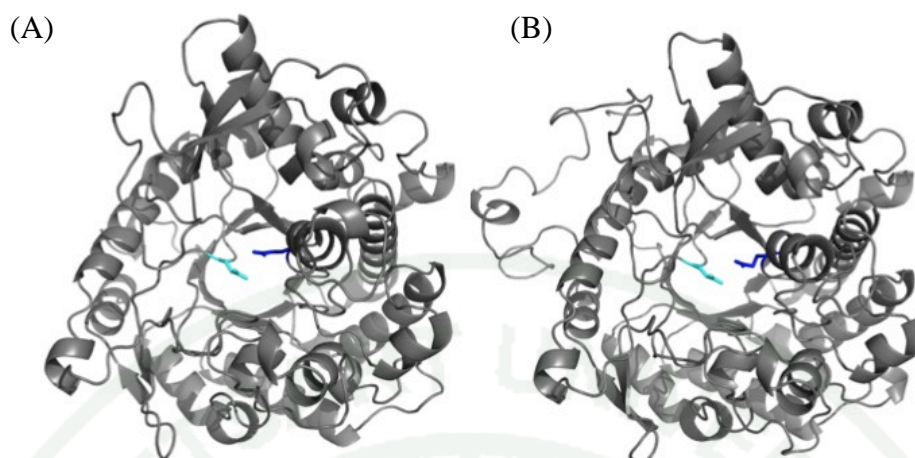


Figure 19 Overall structural models of the wild-type dalcochinase (A) and GmICHG (B). The catalytic acid/base residues, E182 and E209 in the wild-type dalcochinase and GmICHG, respectively, are shown as blue stick models. The catalytic nucleophile residues, E396 and E420 in the wild-type dalcochinase and GmICHG, respectively, are shown as cyan stick models.

A previous study revealed that the hydrolytic efficiency of the GmICHG toward malonylgenistin was higher than that of the wild-type dalcochinase by 100-fold. In order to investigate the interaction of the two β -glucosidases and malonylgenistin, malonylgenistin was docked into the binding pocket of dalcochinase and GmICHG by using GOLD. From the docking result, the subsite -1, which is the glycone binding site, was formed via the interactions between the glycone moiety and seven residues of dalcochinase (namely Q36, N181, E182, E396, W445, E452, and W453), which correspond to seven residues of GmICHG (namely Q59, N208, E209, E420, W469, E476, and W477, respectively) (Figs. 20 and 21, and Tables 27 and 28). In dalcochinase, residues E182 and E396 were catalytic acid/base and catalytic nucleophile residues, respectively. O-2 of the glycone moiety formed a hydrogen bond with E396 at a distance of 3.3 Å, and also with N181. The side-chains of Q36 and W453 were bonded with O-3 of the glycone moiety at a distance of 2.9 Å and 3.4 Å, respectively. Residue Q36 also formed a weak hydrogen bond between its NH group and O-4 of the glycone moiety. The side-chains of W445 and E452 were bonded with O-4 at hydrogen bonding distances of 2.5 Å and 2.8 Å, respectively.

Residue E452 also formed hydrogen bond with O-6 with a distance of 1.9 Å. Moreover, the side-chain of W445 of daltrocinase turned its aromatic face to C3 and C5 of the glycone group (Czjzek *et al.*, 2000; Saino *et al.*, 2014; Verdoucq *et al.*, 2004). These residues, which formed the glycone binding site, were conserved in all GH1 glycoside hydrolases.

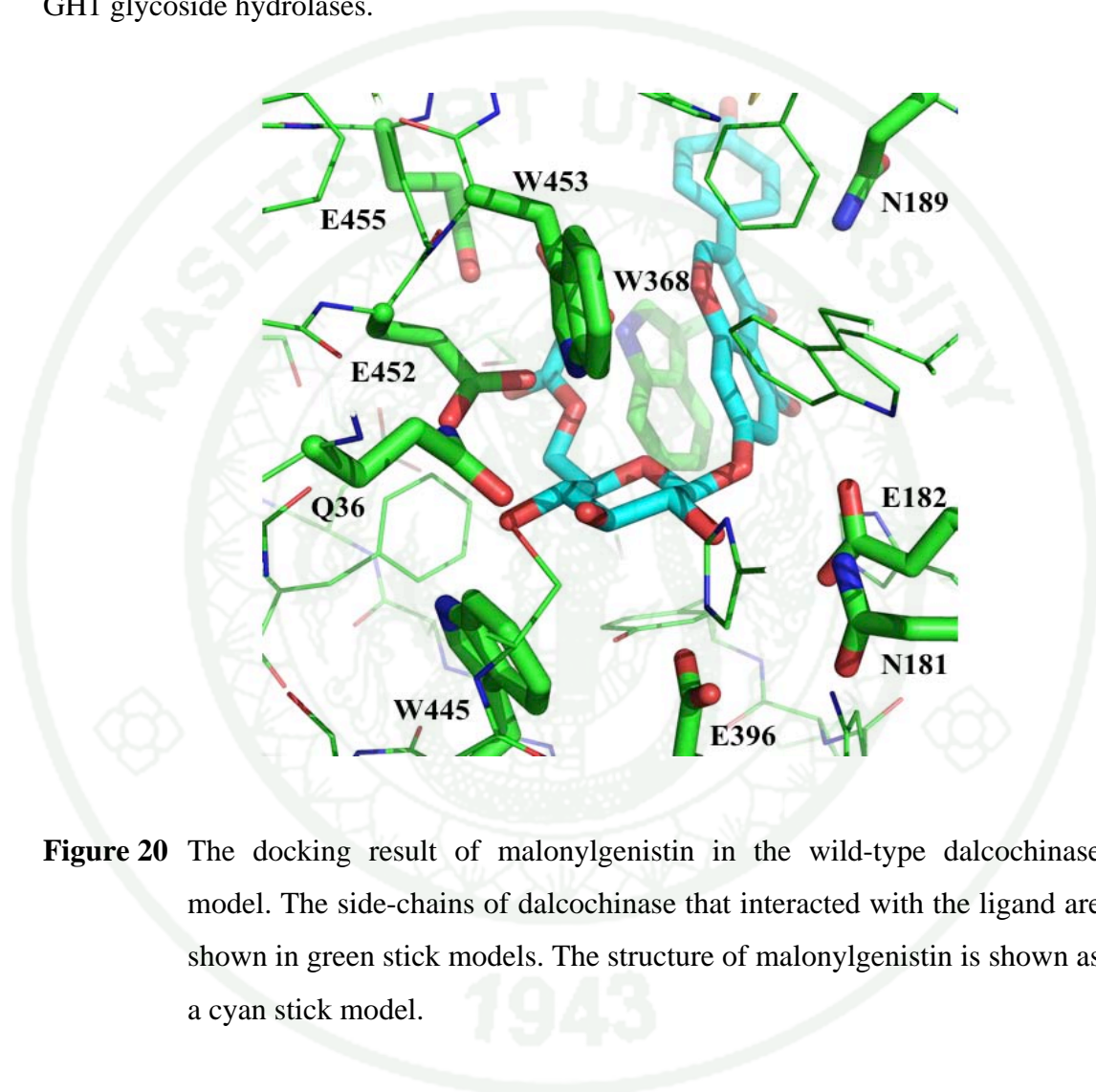


Figure 20 The docking result of malonylgenistin in the wild-type daltrocinase model. The side-chains of daltrocinase that interacted with the ligand are shown in green stick models. The structure of malonylgenistin is shown as a cyan stick model.

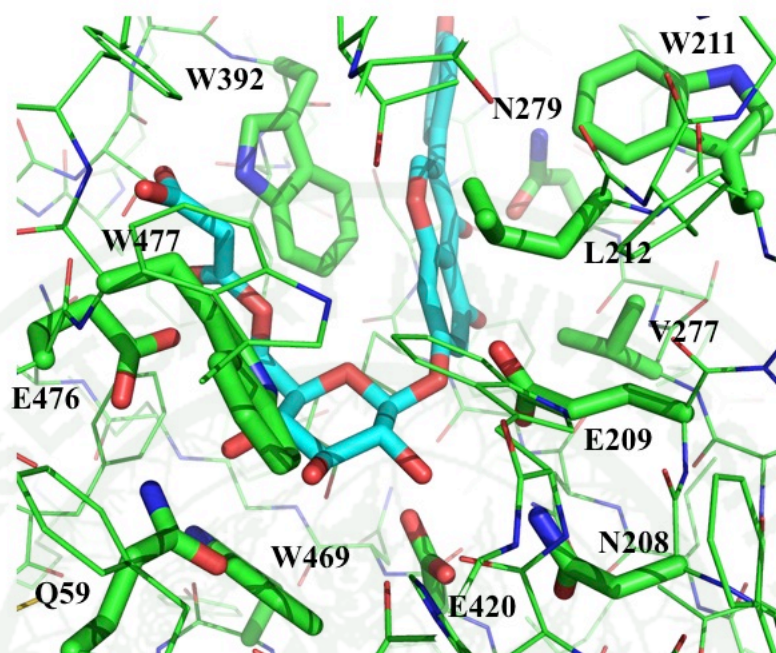


Figure 21 The docking result of malonylgenistin in the GmICHG model. The side-chains of GmICHG that interacted with the ligand are shown in green stick models. The structure of malonylgenistin is shown as a cyan stick model.

Table 27 Summary of distances between residues of dalcochinase and malonylgenistin

Dalcochinase	Malonylgenistin	Distance (Å)
Subsite +1		
N189-Nδ2	Oxygen of aglycone (O-7)	3.7
H252-Nδ1	Hydroxyl of aglycone (O-8)	3.8
W368-Nε1	Carbonyl oxygen (O-10)	3.8
Subsite -1		
E182-Oε1	O-glucosidic linkage	2.6
N181-Nδ2	Glucose O-2	3.9
E396-Oε1	Glucose O-2	3.3
Q36-Oε1	Glucose O-3	2.9
W453-Nε1	Glucose O-3	3.4
Q36-Nε2	Glucose O-4	4.0
W445-Nε1	Glucose O-4	2.5
E452-Oε1	Glucose O-4	2.8
E452-Oε2	Glucose O-6	1.9
Subsite -2		
E452-Oε2	Carboxylate oxygen of (O-12) malonyl group	2.4
E455-Oε1	Carboxylate oxygen of (O-11) malonyl group	2.7

Table 28 Summary of distances between residues of GmICHG and malonylgenistin

Dalcochinase	Malonylgenistin	Distance (Å)
Subsite +1		
N279- Nδ2	Carbonyl oxygen	3.5
Subsite -1		
E209-Oε1	O-glucosidic linkage	2.4
N208-Nδ2	Glucose O-2	3.7
E420-Oε1	Glucose O-2	2.8
Q59-Oε1	Glucose O-3	3.5
W477-Nε1	Glucose O-3	3.1
Q59-Nε2	Glucose O-4	4.0
W469-Nε1	Glucose O-4	2.7
E476-Oε1	Glucose O-4	3.1
E476-Oε2	Glucose O-6	2.5
Subsite -2		
W392-Nε1	Carboxylate oxygen of malonyl group	2.8

In the dalcochinase model, subsite +1, which is the aglycone binding site, consisted of five residues, namely I185, N189, M195, F196, H253, and W368. The side-chains of N189, H253 and W368 appeared to form weak hydrogen bond with the aglycone group, while, in GmICHG, only N279 was hydrogen-bonded with oxygen at the carbonyl group in aglycone of malonylgenistin (Figs. 22A and 22B). The side-chains of W392 of GmICHG and W368 of dalcochinase likely formed π - π interaction between its residue and aromatic face of malonylgenistin (Figs. 22C and 22D). Moreover, the side-chain of W392 of GmICHG also formed hydrogen bond with carboxylate oxygen of substrate. This binding was not observed in dalcochinase.

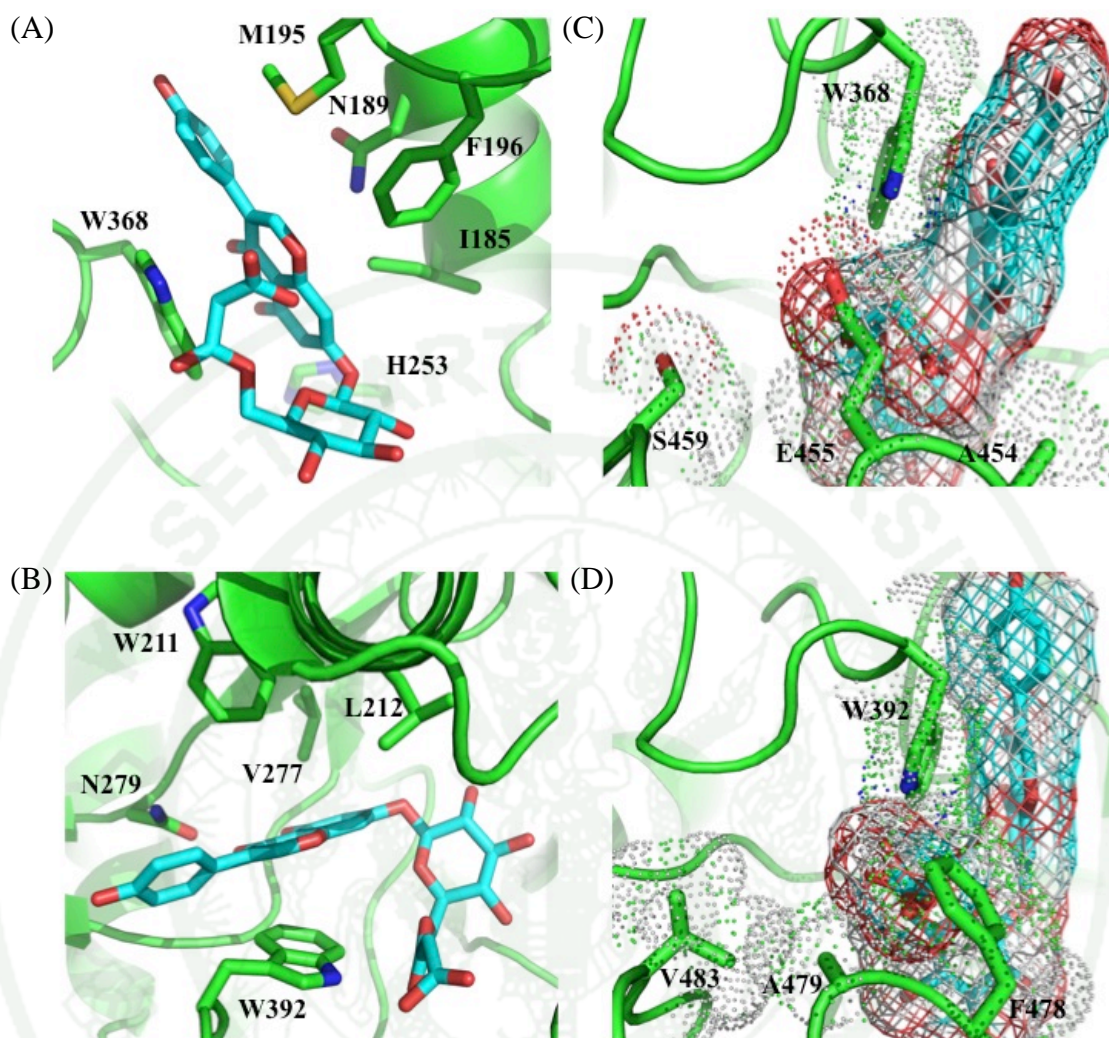


Figure 22 The interactions between malonylgenistin and the residues in the aglycone binding pocket of the wild-type dalcochinase (A) and GmICHG (B), and the π - π interaction between aromatic face of the side-chain of W368 in dalcochinase (C) and the side-chain of W392 in GmICHG (D). The side-chains of dalcochinase that interacted with the ligand are shown in green stick models. The structure of malonylgenistin is shown as a cyan stick model.

Because the GmICHG showed very high hydrolytic efficiency toward malonylgenistin, while the dalcochinase poorly hydrolyzed the modified isoflavone glucosides, the models of these two enzymes docked with malonylgenistin were studied in order to compare the structures of ligand and protein. From the docking

result of malonylgenistin in dalcochinase (Fig. 23A), hydrophobic side of the malonyl group faced to the aglycone group (Saino *et al.*, 2014). From this reason, the carboxylate group of malonylgenistin faced to residue E455 of the wild-type enzyme. The negative charge of E455 may push the malonyl group, resulting in reduction the flexibility of malonylgenistin. On the other hand, the binding pocket of GmICHG contained hydrophobic environment (Fig. 23B). Residues F478, A479, and V483 showed hydrophobic interactions with the malonyl group of malonylgenistin, resulting in flexibility of malonyl group. From these reasons, it is suggested that the negative charge and polar residues in the wild-type dalcochinase resulted in loose binding for malonylgenistin, but the hydrophobic residues in the binding pocket of GmICHG recognized and provided more spaces for the modified group of isoflavone glucosides. So, GmICHG showed very high efficiencies toward malonylated isoflavone glucosides because of reduction in K_m values and increase in k_{cat} values.

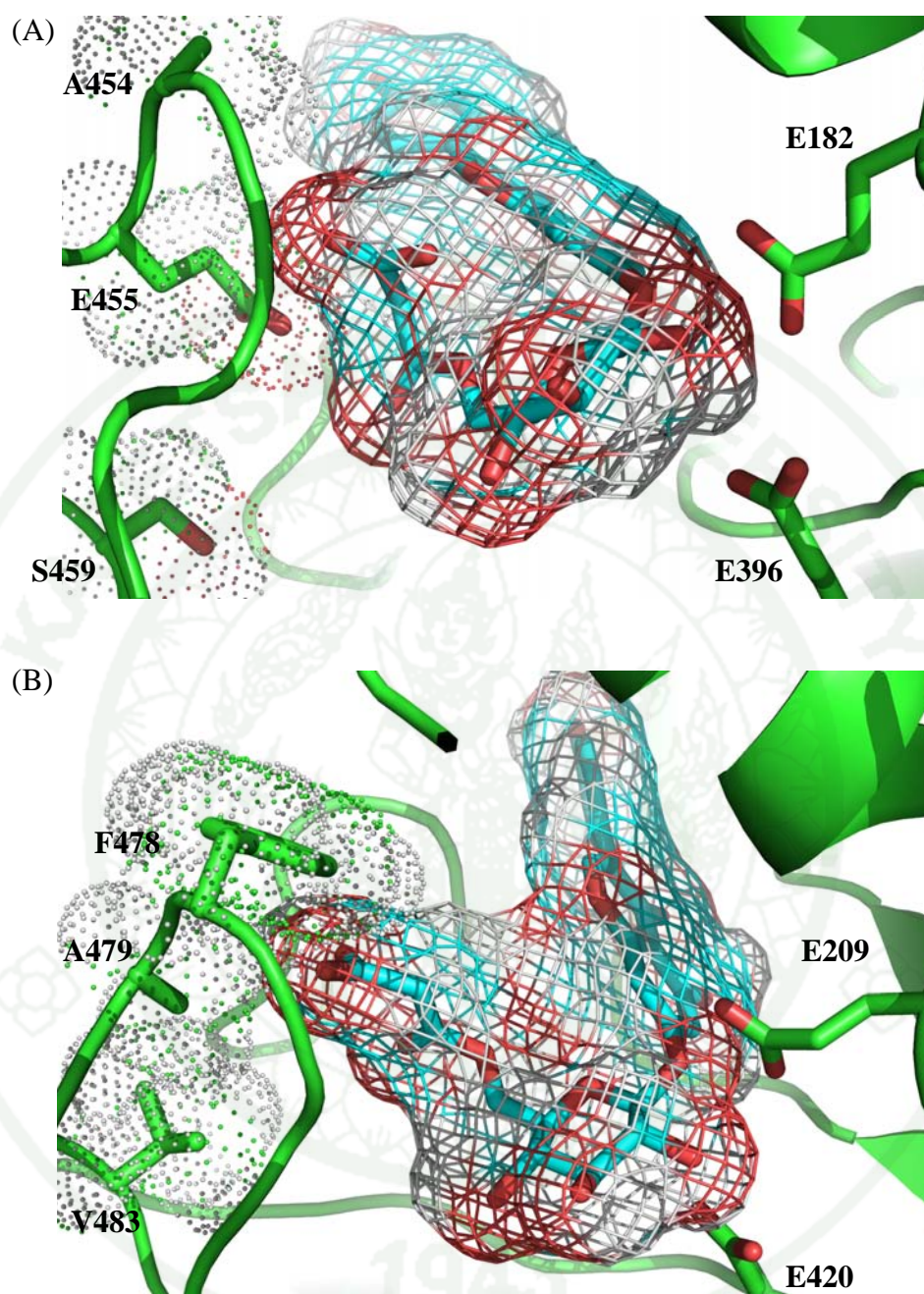


Figure 23 The interactions between malonylgenistin and the residues in the binding pocket of the wild-type dalcochinase (A) and GmICHG (B). The side-chains of dalcochinase that interacted with the ligand are shown in green stick models. The structure of malonylgenistin is shown as a cyan stick model. Mesh and dotted surfaces show the interactions between the substrate and the side-chains, respectively.

Moreover, the A454F/E455A mutant also showed high hydrolytic efficiency toward malonyldaidzin. So, the molecular docking of malonyldaidzin in this mutant was performed. From the result, replacing the negative charge of E455 with A increased the binding surface in the binding pocket, while F454 helped to stabilize the malonyl group of substrate (Fig. 24).

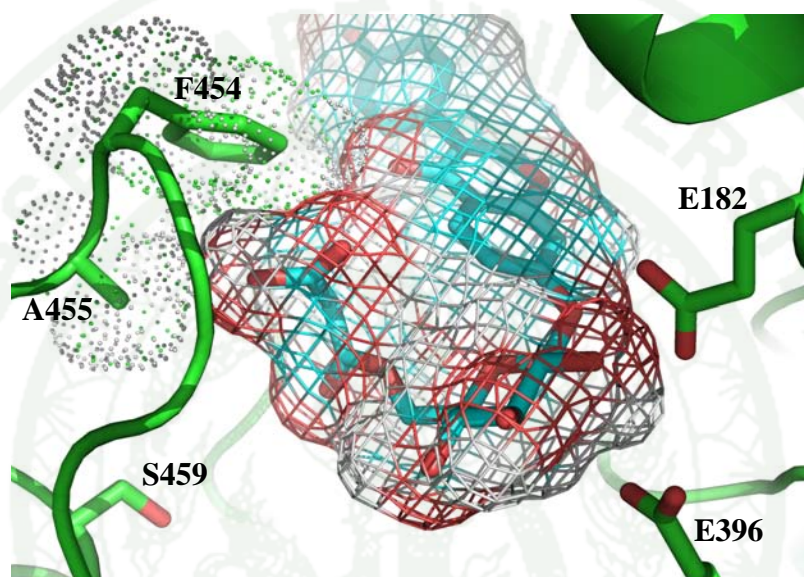


Figure 24 The interactions between malonyldaidzin and the residues in the binding pocket of the A454F/E455A mutant. The side-chains of the A454F/E455A mutant that interacted with the ligand are shown in green stick models. The structure of malonyldaidzin is shown as a cyan stick model. Mesh and dotted surfaces show the interactions between the substrate and the side-chains, respectively.

Amino acid sequence of dalcochinase was compared with other GH1 β -glucosidases, whose structures have been solved. The dalcochinase shared 44 %, 45 %, and 53 % sequence identities with *Zea mays* (maize) β -glucosidase, *Sorghum bicolor* dhurrinase-1, and *Camellia sinensis* β -primeverosidase, respectively. Residues in the glycone binding site (subsite -1) were fully conserved, but some residues in the aglycone binding site (subsite +1) were conserved in some enzymes (Fig 25). Moreover, S473 and Q477 of β -primeverosidase, corresponding to residues E455 and S459 of dalcochinase, respectively, formed hydrogen bonds with its

substrate in the subsite -2, and were responsible for recognition of disaccharide of its substrate (Saino *et al.*, 2014). It is possible that the hydrophobic residues in the binding pocket of GmICHG may recognize the modified isoflavone glucosides.

Dal	ET--ITEVPPFNRSCEFSDFI [□] FGTASSSYQYEGE---GRVPSIWDNFTHQYPEKIADRS	62
MBg	GVQMLSPSEIPQRDWFPSDFTFGAATSAYQIEGAWNEDGKGESNWDHFCNHHPERILDGS	68
DN	GIHRLSPWEIPRRDWFPPSFLFGAATSAYQIEGAWNEDGKGPSTWDHFCNHPEWIVDRS	120
PD	EVAI [□] AAQISSFNRTSFPDGFVFGAASSAYQFEGAAKEGGKGN [□] IWDTFTH [□] EPFGKISNGS	83
Dal	NGDVAVDQFHRYK [□] KDIAIMKDMNLDAYRMSISWPRILPTGRVSGGINQTGV [□] DYYNRLINE	122
MBg	NSDIGANSYHMYKTDVRL [□] LKEMGMDAYRFSISWPRILPKGTKEGGINPDGIKYYRNLINL	128
DN	NGDVAADSYHMYAEDVRL [□] LKEMGMDAYRFSISWPRILPKGTLAGGINEKRV [□] EYYNKLIDL	180
PD	TGDVADDFYHRYKEDVKVLKFI [□] GLDGF [□] RMSISWARVLP [□] RKGLSGGVNKEGIAFYNNVIND	143
Dal	SLANGITPFVTIFHWDLPQALEDEYGGFLNHS---VVNDFQDYADLCFQLFGDRVKHWIT	179
MBg	LLENGIEPYVTIFHWDVPQALEEKYGGFLDKSHKSI [□] VEDYTYFAKVCDFNFGDKVKNWLT	188
DN	LLENGIEPYITIFHWDTPQALVDAYGGFLDER---IIKDYTDFAKVCFEKFGKTVKNWLT	237
PD	LLSKGIQPFITIFHWDLPQALEDEYGGFLSPH---IVNDFRDFAE [□] LCFKEFGDRVKHWIT	200
Dal	LNEPSIFTANGYAYGMFAPGRCS [□] PSYNPTCTGGDAGTETYLVAHN [□] LILSHAATVQVYK [□] RK	239
MBg	FNEPQTF [□] TSFSYGTGVFAPGRCS [□] PGLDCAYPTGNSLVEPYTAGHNILLAHAEAVDLYN-K	247
DN	FNEPETFCSVSYGTGV [□] LAPGRCS [□] PGVSCAVPTGNSLSEPYIVAHNLLRAHAETVDIYN-K	296
PD	MNEPWSYSYGGYDAGLLAPGRCS-AFMAFCPKGNSGTEPYIVTHNLLLSHAAAVKLYKEK	259
Dal	YQEHQKGTIGISLHV [□] VVWV [□] IPLSNSTSDQ [□] NATQRYLDFTCGWFM [□] DPLTAGRYPDSMQYLVG	299
MBg	HYKRDDTRIGLAFDVMGRVPYGT [□] SFLDKQAEERSWDINL [□] GWFL [□] EPVVRGDY [□] PFMSRSLAR	307
DN	YHKGADGRIGLALNVFGRVPY [□] TNTFLDQQAQERSMDKCLGWFL [□] EPVVRGDY [□] PFMSRV [□] SAR	356
PD	YQAYQKQIGITLVTYWMIPYSNSKADK [□] DAQRALDFMYGWFIEPLSFGEYPKSMRRLVG	319
Dal	DRLPKFTTDQAKLVKGSFDFIGLNYTTNYATKSDASTCCPPSYLTD [□] PQVTL [□] LQQR--NG	357
MBg	ERLPFFKDEQKEKLAGSYNMLG [□] LNYYTSRFSKNIDISPNYSPV [□] LNTDDAYASQEVNGPDG	367
DN	DRV [□] PFKEKEQEKLVGSYDMIGINYYTSTFSKHIDLSPNNSPVLNTDDAYASQETKGPDG	416
PD	KRLPRFTKEQAMLVKGSFDFLGLNYYIANVVLNVPTSN [□] SVNLSYTTDSL [□] SNQTAFR--NG	377
Dal	VFIGPVT [□] PSG [□] WMC [□] IYPKGLRDL [□] LLYFKEKYN [□] NPLVYIT [□] ENGID--EKNDASLSLEESLID	415
MBg	KPIGPPMGNPWIYMYPEGLKDLLMIMKNKYGN [□] PP [□] IYITENGIGVD [□] TKETPLPMEALND	427
DN	NAIGPPTGN [□] AWINMYPKGLHDILMTMKNKYGN [□] PP [□] MIYITENGMDIDKGD--LPKPVALED	474
PD	VAIGRPTGVP [□] AFMYPKGLKDLLVYTK [□] EYNDPVIYITENG [□] MG--DNN--NVTTEEGIKD	433
Dal	TYRIDSYYRHLFYVRYAIRSGANVKGFFAW [□] SLLDN [□] FEWAEGYTSRFGLYFVNYTT-LNRY	474
MBg	YKRLDYIQRHIALKESIDLGSN [□] VQGYFAWSLLDN [□] FEW [□] FAGFTERYGIVYVDRNNNCTRY	487
DN	HTRLDYIQRHLSVLKQSIDLGADV [□] RGYFAWSLLDN [□] FEWSSGYTERF [□] GIVYVDRENGCERT	534
PD	PQRVYFYNQHL [□] LSLKN [□] IAAGVKVKG [□] YFTWAF [□] LDN [□] FEWLSGYTQRF [□] GIVYVDFKDKL [□] KRY	493
Dal	PKLSATWFKYFLARDQESAKLEILAPKARWSLSTMIKEEKTKPKRGIEGF	524
MBg	MKESAKWLKEFN-TAKP-SKKILTPA-----	512
DN	MKRSARWLQEFNGAAKVENNKILTPAGQLN-----	565
PD	PKHSALWFKKFLK-----	507

Figure 25 Sequence alignment of four β -glucosidases. The catalytic residues are indicated by filled triangles above the sequence. The residues in the glycone and aglycone binding sites are indicated by blue and red boxes, respectively. The residues of dalcochianse that were mutated to the corresponding residues of GmICHG were underlined. Dal: Dalcochianse, MBg: Maize β -glucosidase, DN: Dhurrinase-1, and PD: β -primeverosidase.

CONCLUSION

The dalcochinase mutants, A454F/E455A, A454F/S459V, E455A/S459V, and A454F/E455A/S459V, were successfully generated by using site-directed mutagenesis methods. All double and triple dalcochinase mutants were then expressed in *P. pastoris* system, and purified by phenyl sepharose and Ni²⁺ sepharose chromatography. The purified dalcochinase mutants showed the molecular mass of 66 kDa and their identities were also detected by using western blot analysis. The activities of all dalcochinase mutants were also tested by non-denaturing PAGE using 4MU-Glc as a substrate.

The kinetic studies of all dalcochinase mutants were determined toward *p*NP-Glc, dalcochinin-8'-*O*-β-D-glucoside and four soybean isoflavone glucosides. For hydrolysis of *p*NP-Glc and dalcochinin-8'-*O*-β-D-glucoside, all double mutants showed improved efficiencies, while the triple mutants showed a decrease in efficiency toward *p*NP-Glc, when compared with the wild-type enzyme and their corresponding single mutants. However, the E455A/S459V mutant showed the highest efficiency for hydrolysis of *p*NP-Glc, while the A454F/E455A mutant exhibited the highest efficiency for hydrolysis of dalcochinin-8'-*O*-β-D-glucoside. For hydrolysis of daidzin, the efficiency of the A454F/E455A mutant was similar to the wild-type dalcochinase but lower than its corresponding single mutants, while other mutants showed decreases in the efficiencies toward daidzin when compared with the wild-type enzyme. For hydrolysis of genistin, the A454F/E455A and E455A/S459V mutants exhibited high efficiencies when compared with the wild-type enzyme, but did not improve the efficiencies when compared to the corresponding single mutants. For hydrolysis of malonyldaidzin, all double mutants showed improved efficiencies when compared with the wild-type enzyme and their corresponding single mutants. The A454F/E455A mutant exhibited the highest efficiency for hydrolysis of malonyldaidzin. For hydrolysis of malonylgenistin, all double mutants showed increases in efficiencies when compared with the wild-type dalcochinase, but did not show improved efficiencies when compared to their corresponding single mutants.

In these cases, these results suggested that the interactions in all double mutants may have synergism for hydrolysis of *p*NP-Glc, dalcochinin-8'-*O*- β -D-glucoside, and malonyldaidzin, and antagonism for hydrolysis of daidzin, genistin, and malonylgenistin. However, the triple mutant did not show improved efficiencies toward all substrates tested. So, these results suggested that it might be antagonistic interaction in the triple dalcochinase mutant for all substrates tested.

In the hydrolysis of soybean isoflavone glucosides in soybean flour extracts, the E455A/S459V mutant could completely hydrolyzed malonyldaidzin within 4 h of the reaction of soybean flour extracts. Therefore, these mutants may be applied in the food industry in order to release free isoflavone aglycones, which will increase the nutritional values in soybean food products.

LITERATURE CITED

- Andres, S., K. Abraham, K.E. Appel and A. Lampen. 2011. Risks and benefits of dietary isoflavones for cancer. **Crit. Rev. Toxicol.** 41(6):463-506.
- Barrett, T., C.G. Suresh, S.P. Tolley, E.J. Dodson and M.A. Hughes. 1995. The crystal structure of a cyanogenic beta-glucosidase from white clover, a family 1 glycosyl hydrolase. **Structure** 3(9):951-960.
- Behloul, N. and G. Wu. 2013. Genistein: A promising therapeutic agent for obesity and diabetes treatment. **Eur. J. Pharmacol.** 698(1-3):31-38.
- Chen, K.-I., M.-H. Erh, N.-W. Su, W.-H. Liu, C.-C. Chou and K.-C. Cheng. 2012. Soyfoods and soybean products: from traditional use to modern applications. **Appl. Microbiol. Biotechnol.** 96(1):9-22.
- Chiou, T.-Y., Y.-H. Lin, N.-W. Su and M.-H. Lee. 2010. β -Glucosidase Isolated from Soybean Okara Shows Specificity toward Glucosyl Isoflavones. **J. Agric. Food Chem.** 58(15):8872-8878.
- Chuankhayan, P., Y. Hua, J. Svasti, S. Sakdarat, P.A. Sullivan and J.R. Cairns. 2005. Purification of an isoflavonoid 7-O-beta-apiosyl-glucoside beta-glycosidase and its substrates from *Dalbergia nigrescens* Kurz. **Phytochem.** 66(16):1880-1889.
- Chuankhayan, P., T. Rimlumduan, J. Svasti and J.R. Cairns. 2007a. Hydrolysis of soybean isoflavonoid glycosides by *Dalbergia* beta-glucosidases. **J. Agric. Food Chem.** 55(6):2407-2412.
- Chuankhayan, P., T. Rimlumduan, W. Tantanuch, N. Mothong, P.T. Kongsaree, P. Methenukul, J. Svasti, O.N. Jensen and J.R. Cairns. 2007b. Functional and structural differences between isoflavonoid beta-glycosidases from *Dalbergia* sp. **Arch. Biochem. Biophys.** 468(2):205-216.
- Coward, L., M. Smith, M. Kirk and S. Barnes. 1998. Chemical modification of isoflavones in soyfoods during cooking and processing. **Am. J. Clin. Nutr.** 68(6 Suppl):1486S-1491S.

- Czjzek, M., M. Cicek, V. Zamboni, D.R. Bevan, B. Henrissat and A. Esen. 2000. The mechanism of substrate (aglycone) specificity in beta -glucosidases is revealed by crystal structures of mutant maize beta -glucosidase-DIMBOA, - DIMBOAGlc, and -dhurrin complexes. **Proc. Nati. Acad. Sci. U.S.A.** 97(25):13555-13560.
- Eisenberg, D., R. Luthy and J.U. Bowie. 1997. VERIFY3D: assessment of protein models with three-dimensional profiles. **Methods Enzymol.** 277:396-404.
- Henrissat, B. 1991. A classification of glycosyl hydrolases based on amino acid sequence similarities. **Biochem. J.** 280 (Pt 2):309-316.
- Higgins, D.R.a.J.M.C. 1998. **Pichia Protocols.** Humana Press, New Jersey.
- Hooft, R.W., G. Vriend, C. Sander and E.E. Abola. 1996. Errors in protein structures. **Nature** 381(6580):272.
- Horii, K., T. Adachi, T. Matsuda, T. Tanaka, H. Sahara, S. Shibasaki, C. Ogino, Y. Hata, M. Ueda and A. Kondo. 2009. Improvement of isoflavone aglycones production using β -glucosidase secretory produced in recombinant *Aspergillus oryzae*. **J. Mol. Catal. B: Enzym.** 59(4):297-301.
- Hsieh, M.C. and T.L. Graham. 2001. Partial purification and characterization of a soybean beta-glucosidase with high specific activity towards isoflavone conjugates. **Phytochem.** 58(7):995-1005.
- Ismail, B. and K. Hayes. 2005. β -Glycosidase Activity toward Different Glycosidic Forms of Isoflavones. **J. Agric. Food Chem.** 53(12):4918-4924.
- Jones, G., P. Willett and R.C. Glen. 1995. Molecular recognition of receptor sites using a genetic algorithm with a description of desolvation. **J. Mol. Biol.** 245(1):43-53.
- Ketudat Cairns, J.R., V. Champattanachai, C. Srisomsap, B. Wittman-Liebold, B. Thiede and J. Svasti. 2000. Sequence and expression of Thai Rosewood beta-glucosidase/beta-fucosidase, a family 1 glycosyl hydrolase glycoprotein. **J. Biochem.** 128(6):999-1008.
- Ketudat Cairns, J.R. and A. Esen. 2010. beta-Glucosidases. **Cell. Mol. Life Sci.** 67(20):3389-3405.

- Kim, B.-N., S.-J. Yeom, Y.-S. Kim and D.-K. Oh. 2011a. Characterization of a β -glucosidase from *Sulfolobus solfataricus* for isoflavone glycosides. **Biotechnol. Lett.** 34(1):125-129.
- Kim, Y.-S., S.-J. Yeom and D.-K. Oh. 2011b. Characterization of a GH3 Family β -Glucosidase from *Dictyoglomus turgidum* and Its Application to the Hydrolysis of Isoflavone Glycosides in Spent Coffee Grounds. **J. Agric. Food Chem.** 59(21):11812-11818.
- Klin-khumhom, C. 2012. **Hydrolysis of Soybean Isoflavone Glucosides by Novel β -Glucosidase.** Special Problem Report. Kasetsart University.
- Kuo, L.-C. and K.-T. Lee. 2008. Cloning, Expression, and Characterization of Two β -Glucosidases from Isoflavone Glycoside-Hydrolyzing *Bacillus subtilis* natto. **J. Agric. Food Chem.** 56(1):119-125.
- Laskowski, R.A., D.S. Moss and J.M. Thornton. 1993. Main-chain bond lengths and bond angles in protein structures. **J. Mol. Biol.** 231(4):1049-1067.
- Magee, P.J. and I.R. Rowland. 2004. Phyto-oestrogens, their mechanism of action: current evidence for a role in breast and prostate cancer. **Br. J. Nutr.** 91(4):513-531.
- Marazza, J.A., M.S. Garro and G.S. de Giori. 2009. Aglycone production by *Lactobacillus rhamnosus* CRL981 during soymilk fermentation. **Food Microbiol.** 26(3):333-339.
- Noguchi, A., A. Saito, Y. Homma, M. Nakao, N. Sasaki, T. Nishino, S. Takahashi and T. Nakayama. 2007. A UDP-glucose:isoflavone 7-O-glucosyltransferase from the roots of soybean (*Glycine max*) seedlings. Purification, gene cloning, phylogenetics, and an implication for an alternative strategy of enzyme catalysis. **J. Biol. Chem.** 282(32):23581-23590.
- Pyo, Y.-H., T.-C. Lee and Y.-C. Lee. 2005. Enrichment of bioactive isoflavones in soymilk fermented with β -glucosidase-producing lactic acid bacteria. **Food Res. Int.** 38(5):551-559.
- Saha, B.C. and R.J. Bothast. 1996. Production, purification, and characterization of a highly glucose-tolerant novel beta-glucosidase from *Candida peltata*. **Appl. Environ. Microbiol.** 62(9):3165-3170.

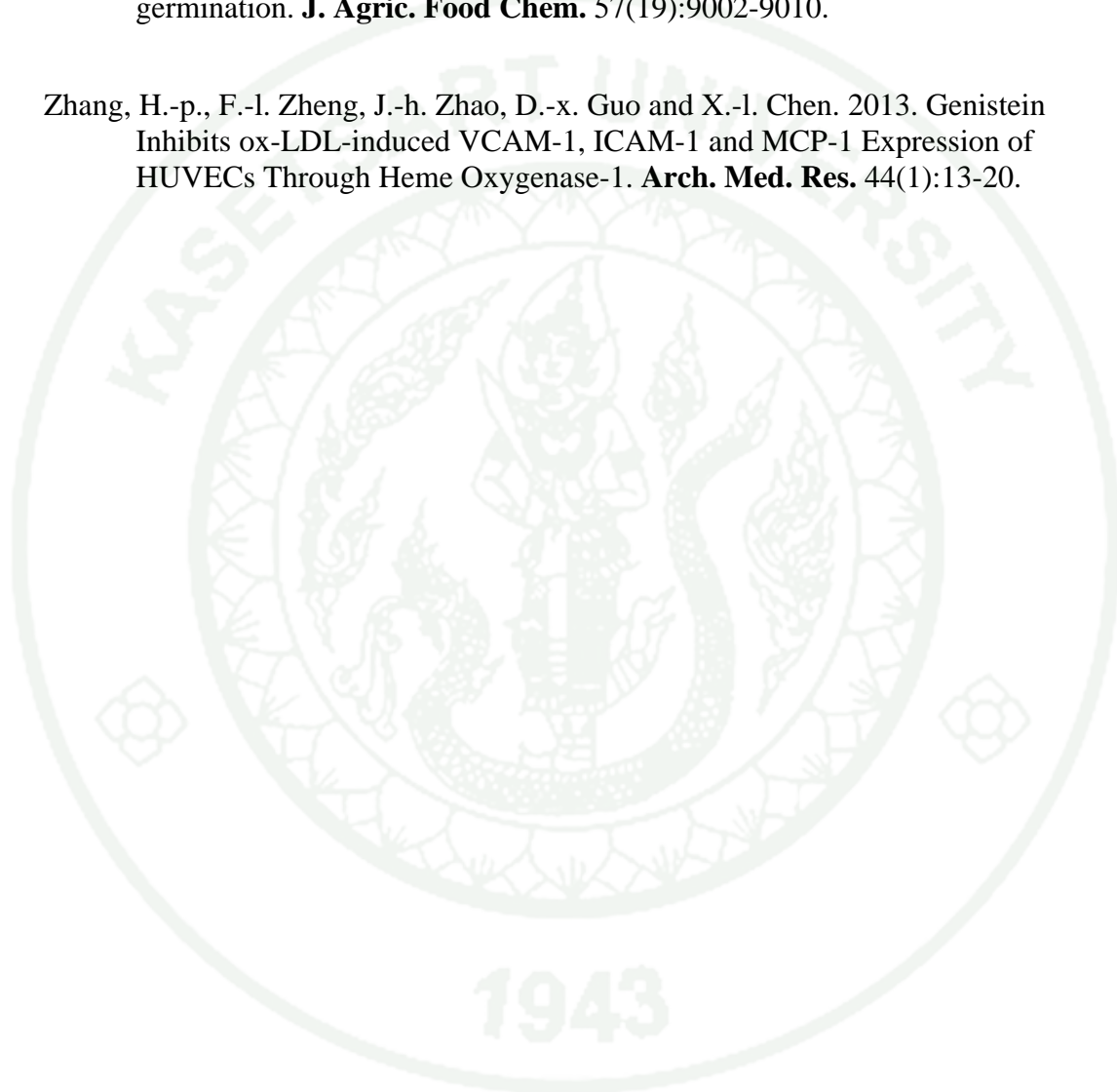
- Saino, H., T. Shimizu, J. Hiratake, T. Nakatsu, H. Kato, K. Sakata and M. Mizutani. 2014. Crystal Structures of β -Primeverosidase in Complex with Disaccharide Amidine Inhibitors. **J. Biol. Chem.** 289(24):16826-16834.
- Sakamoto, T., H. Horiguchi, E. Oguma and F. Kayama. 2010. Effects of diverse dietary phytoestrogens on cell growth, cell cycle and apoptosis in estrogen-receptor-positive breast cancer cells. **J. Nutr. Biochem.** 21(9):856-864.
- Sippl, M.J. 1993. Recognition of errors in three-dimensional structures of proteins. **Proteins** 17(4):355-362.
- Somphao, J. 2011. **Protein Engineering in β -Glucosidase for Hydrolysis of Soybean Isoflavone Glucosides**. M.S. Thesis, Kasetsart University.
- Song, X., Y. Xue, Q. Wang and X. Wu. 2011. Comparison of Three Thermostable β -Glucosidases for Application in the Hydrolysis of Soybean Isoflavone Glycosides. **J. Agric. Food Chem.** 59(5):1954-1961.
- Srisomsap, C., J. Svasti, R. Surarit, V. Champattanachai, P. Sawangareetrakul, K. Boonpuan, P. Subhasitanont and D. Chokchaichamnankit. 1996. Isolation and characterization of an enzyme with beta-glucosidase and beta-fucosidase activities from *Dalbergia cochinchinensis* Pierre. **J. Biochem.** 119(3):585-590.
- Surarit, R., H. Matsui, S. Chiba, J. Svasti and C. Srisomsap. 1997. Evidence for a Single Active Site in β -D-Glucosidase/ β -D-Fucosidase from *Dalbergia cochinchinensis* Seeds. **Biosci. Biotechnol. Biochem.** 61(1):93-95.
- Suzuki, H., S. Takahashi, R. Watanabe, Y. Fukushima, N. Fujita, A. Noguchi, R. Yokoyama, K. Nishitani, T. Nishino and T. Nakayama. 2006. An isoflavone conjugate-hydrolyzing beta-glucosidase from the roots of soybean (*Glycine max*) seedlings: purification, gene cloning, phylogenetics, and cellular localization. **J. Biol. Chem.** 281(40):30251-30259.
- Svasti, J., C. Srisomsap, S. Techasakul and R. Surarit. 1999. Dalcochinin-8'-O- β -D-glucoside and its β -glucosidase enzyme from *Dalbergia cochinchinensis*. **Phytochem.** 50(5):739-743.
- Takahashi, R., R. Ohmori, C. Kiyose, Y. Momiyama, F. Ohsuzu and K. Kondo. 2005. Antioxidant Activities of Black and Yellow Soybeans against Low Density Lipoprotein Oxidation. **J. Agric. Food Chem.** 53(11):4578-4582.

- Tang, S., J. Hu, Q. Meng, X. Dong, K. Wang, Y. Qi, C. Chu, X. Zhang and L. Hou. 2012. Daidzein Induced Apoptosis via Down-Regulation of Bcl-2/Bax and Triggering of the Mitochondrial Pathway in BGC-823 Cells. **Cell Biochem. Biophys.** 65(2):197-202.
- Tikkanen, M.J., K. Wahala, S. Ojala, V. Vihma and H. Adlercreutz. 1998. Effect of soybean phytoestrogen intake on low density lipoprotein oxidation resistance. **Proc. Natl. Acad. Sci. U.S.A.** 95(6):3106-3110.
- Toonkool, P., P. Metheenukul, P. Sujiwattanasat, P. Paiboon, N. Tongtubtim, M. Ketudat-Cairns, J. Ketudat-Cairns and J. Svasti. 2006. Expression and purification of dalcocinase, a beta-glucosidase from *Dalbergia cochinchinensis* Pierre, in yeast and bacterial hosts. **Protein Expression Purif.** 48(2):195-204.
- Verdoucq, L., J. Moriniere, D.R. Bevan, A. Esen, A. Vasella, B. Henrissat and M. Czjze. 2004. Structural determinants of substrate specificity in family 1 beta-glucosidases: novel insights from the crystal structure of sorghum dhurrinase-1, a plant beta-glucosidase with strict specificity, in complex with its natural substrate. **J. Biol. Chem.** 279(30):31796-31803.
- Wang, H.-J. and P.A. Murphy. 1996. Mass Balance Study of Isoflavones during Soybean Processing. **J. Agric. Food Chem.** 44(8):2377-2383.
- Wiederstein, M. and M.J. Sippl. 2007. ProSA-web: interactive web service for the recognition of errors in three-dimensional structures of proteins. **Nucleic Acids Res.** 35(Web Server issue):W407-410.
- Xue, Y., J. Yu and X. Song. 2009. Hydrolysis of soy isoflavone glycosides by recombinant β -glucosidase from hyperthermophile *Thermotoga maritima*. **J. Ind. Microbiol. Biotechnol.** 36(11):1401-1408.
- Yang, L., Z.S. Ning, C.Z. Shi, Z.Y. Chang and L.Y. Huan. 2004. Purification and Characterization of an Isoflavone-Conjugates-Hydrolyzing β -Glucosidase from Endophytic Bacterium. **J. Agric. Food Chem.** 52(7):1940-1944.
- Yang, S., L. Wang, Q. Yan, Z. Jiang and L. Li. 2009. Hydrolysis of soybean isoflavone glycosides by a thermostable β -glucosidase from *Paecilomyces thermophila*. **Food Chem.** 115(4):1247-1252.

Yeom, S.-J., B.-N. Kim, Y.-S. Kim and D.-K. Oh. 2012. Hydrolysis of Isoflavone Glycosides by a Thermostable β -Glucosidase from *Pyrococcus furiosus*. **J. Agric. Food Chem.** 60(6):1535-1541.

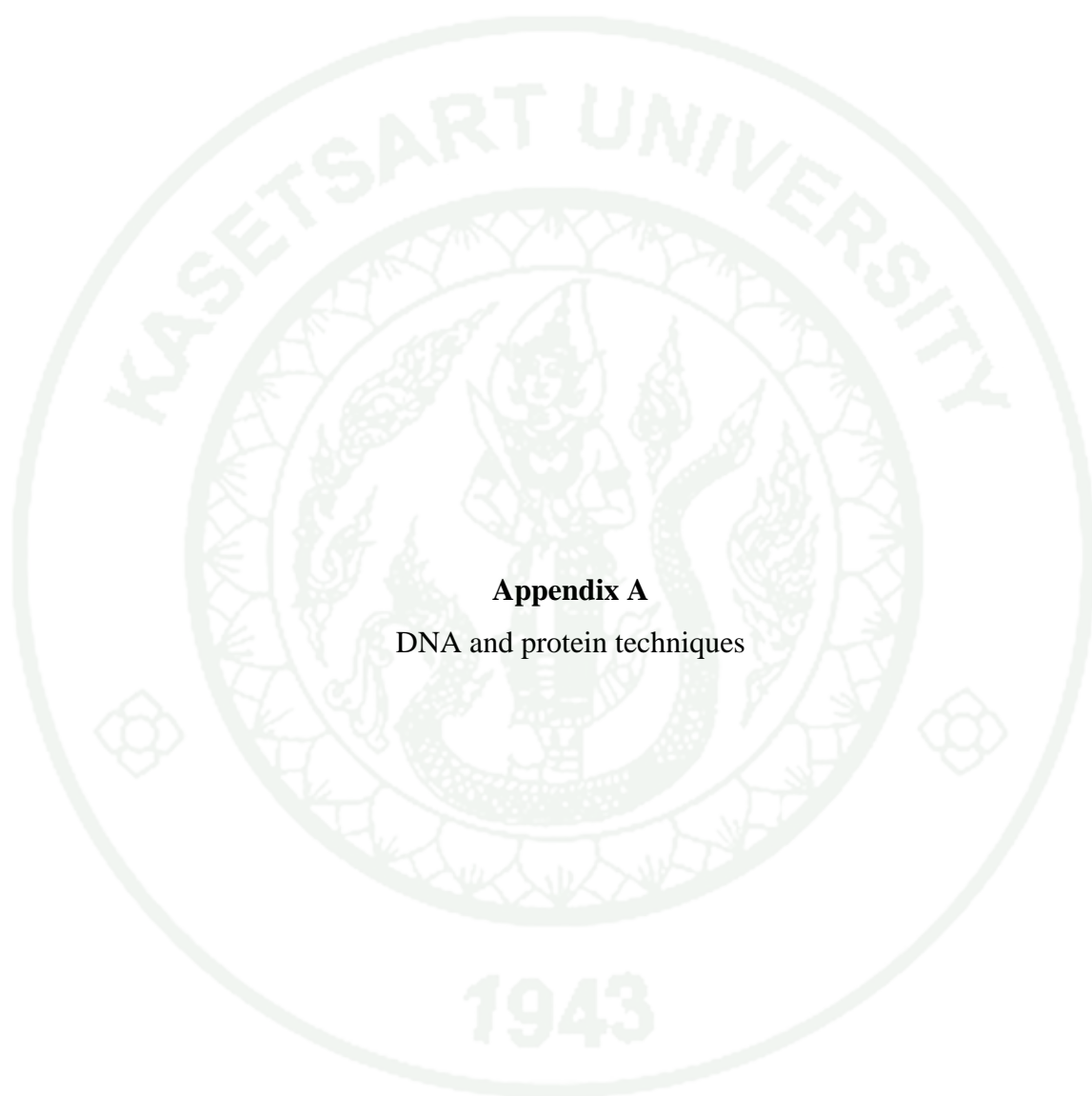
Yuan, J.P., Y.B. Liu, J. Peng, J.H. Wang and X. Liu. 2009. Changes of isoflavone profile in the hypocotyls and cotyledons of soybeans during dry heating and germination. **J. Agric. Food Chem.** 57(19):9002-9010.

Zhang, H.-p., F.-l. Zheng, J.-h. Zhao, D.-x. Guo and X.-l. Chen. 2013. Genistein Inhibits ox-LDL-induced VCAM-1, ICAM-1 and MCP-1 Expression of HUVECs Through Heme Oxygenase-1. **Arch. Med. Res.** 44(1):13-20.





APPENDICES



Appendix A
DNA and protein techniques

1. Agarose gel electrophoresis method

The sizes of DNA fragments were determined by 1 % agarose gel electrophoresis. To prepare 1 % agarose, 0.5 g of agarose was dissolved in 50 ml of 1X TAE buffer [50X TAE stock: 2 M Tris, 5.71 % (v/v) acetic acid, and 0.1 M EDTA, pH 8.5] with heating. The temperature of agarose solution was cooled to lower than 60 °C before pouring into the tray. After complete polymerization, agarose gel was soaked in 1X TAE buffer. DNA samples were mixed with 1X loading buffer [6X stock: 300 mM EDTA, pH 8.0, 0.25 % (w/v) bromphenol blue, 30 % (w/v) glycerol] before loaded into the well. The DNA samples were separated by electrophoresis at 100 volt for 30 min. Then, DNA samples were stained with 1 µg/ml ethidium bromide, and visualized under the ultraviolet light by using gel documentation system.

2. Preparation of competent *E. coli* DH5 α and transformation

E. coli DH5 α was grown on LB agar and incubated at 37 °C for 16 h. One colony was grown in 10 ml LB at 37 °C, 200 rpm. The culture was inoculated in 200 ml LB broth and incubated at 200 rpm, 37 °C until the OD₆₀₀ reached to 0.55-0.65. The culture was cooled at 4 °C for 30 min in order to stop cell growth. Then, cells were collected by centrifugation at 2,000 ×g, 4 °C for 15 min. The cell pellet was washed by 100 ml cold water and then centrifuged at 2,000 ×g, 4 °C for 15 min. Moreover, the cell pellet was washed again by 50 ml cold water, and centrifuged under the same condition. The cell pellet was re-washed with 50 ml of cold 10 % glycerol, centrifuged under the same condition, and re-suspended in 200 µl of cold 10 % glycerol. Eighty microliter of cell suspension in 10 % glycerol was collected in each tube and kept at -80 °C. For DNA transformation into *E. coli* DH5 α , one to ten nanogram of DNA plasmid was mixed 80 µl competent cell and then incubated on ice for 30 sec. The cell-plasmid mixture was gently pipetted into the electro-cuvette without gas bubble. Plasmid was transformed into the bacterial cells via an electric pulse at 25 µF, 200 Ω, and 2.5 V. Then, the transformed cells were rapidly added with 1 ml LB broth, incubated at 200 rpm, 37 °C for 1 h, and plated on LB agar containing

25 µg/ml zeocin. All transformants were grown at 37 °C for 16 h, which is their optimal growth condition.

3. Plasmid extraction by miniprep method and restriction digestion

E. coli DH5α harboring the wild-type or mutant dalcocinase gene in the pPICZαB-His₈-trncTRBG construct was inoculated in 2 ml LB broth containing 25 µg/ml zeocin for 16 h. Cells were collected by centrifugation at 13,000 rpm for 10 min. Cell pellet was re-suspended with 100 µl Solution I [50 mM glucose, 25 mM Tris, pH 8.0 and 10 mM EDTA] and incubated at room temperature for 10 min. Then, cell suspension was gently mixed with 200 µl Solution II [0.2 M sodiumhydroxide and 1 % SDS], incubated on ice for 5 min, and neutralized by adding with 150 µl Solution III [3 M potassiumacetate and 2 M acetic acid]. The cell debris was separated by centrifugation at 13,000 rpm for 10 min. Supernatant were collected, and the DNA was precipitated with 2 volume of absolute ethanol, and incubated at -20 °C for 30 min. The DNA pellet was separated by centrifugation at 13,000 rpm for 10 min. The plasmid was washed by 70% ethanol, dried, and re-suspended with 20 µl TE buffer pH 8.0 [10 mM Tris, pH 8.0, 1 mM EDTA]. The extracted plasmid was digested with *Pst*I and *Xba*I restriction endonucleases in 1X FastDigest Green buffer. The sizes of cut and/or uncut plasmid fragments were analyzed by 1 % agarose gel electrophoresis (Appendix A1).

4. Preparation of competent *P. pastoris* Y11430 and transformation

P. pastoris Y11430 from stock was grown on YPD agar at 30 °C for 4-6 days. Single colony of yeast was inoculated in 5 ml YPD broth to be a starter culture and incubated at 200 rpm, 30 °C for overnight. The starter culture of *P. pastoris* Y11430 was inoculated in 125 ml YPD broth with the initial OD₆₀₀ of 0.1, and then incubated at 200 rpm, 30 °C until the OD₆₀₀ reached 1.3-1.5. The cells were then harvested by centrifugation at 2,000 ×g, 4 °C for 15 min. Cell pellet was re-suspended with 25 ml YPD containing 0.02 M HEPES, pH 8.0. Then, cell suspension was gently added with

DTT to 0.25 M final concentration, and incubated further at 200 rpm, 30 °C for 15 min. After incubation, sterile cold water was added into the cell suspension up to 125 ml, and the cells were collected by centrifugation at 4 °C for 15 min. The cell pellet was re-washed with 62.5 ml sterile cold water under the same condition. Finally, the competent cell was re-suspended with 0.25-0.50 ml of 1 M sorbitol. Forty microliter of cell suspension was collected in each sterile tube, and kept at -80 °C. For transformation, one hundred nanogram of linear DNA plasmid was mixed with competent cell and incubated on ice for 30 sec. Cell suspension containing DNA plasmid was gently pipetted into the electro-cuvette without gas bubble. The plasmid was transformed into the yeast cells via an electric pulse at 25 μ F, 200 Ω , and 1.5 V. Then, the transformants were rapidly added with 1 M sorbitol, incubated at 200 rpm, 30 °C for 1 h, and grown on YPDS agar containing 100 μ g/ml of zeocin. The transformed cells were incubated at 30 °C for 2-4 days.

5. Protein determination by sodium dodecyl sulphate polyacrylamide gel electrophoresis (SDS-PAGE)

10% SDS-polyacrylamide gel was prepared (Appendix Table A1) and soaked in 1X running buffer [10X stock: 250 mM Tris, pH 8.3, 2 M glycine, and 1 % SDS]. After protein purification, one microgram of purified protein sample was mixed with 1X sample buffer [4X stock: 4 % (w/v) SDS, 20 % (v/v) glycerol, 5 % (v/v) β -mercaptoethanol, 0.01 % (w/v) coomassie blue G, and 50 mM Tris, pH 6.8], and heated in boiling water for 5 min. The denatured proteins were centrifuged for 1 min and loaded into the SDS-polyacrylamide gel. All proteins were separated by electrophoresis at 150 volt for 60 min. The gel was stained with staining solution [0.125 % (w/v) coomassie blue R, 45 % (v/v) methanol, and 10 % (v/v) acetic acid] for an hour, and washed twice by de-staining solution [40 % methanol and 10 % acetic acid] for an hour.

Appendix Table A1 Preparation of 10% SDS-polyacrylamide gel

Materials	10 % resolving gel	4 % stacking gel
Sterile distilled water	2050 μ l	3000 μ l
30 % Acrylamide	1600 μ l	650 μ l
1.5 M Tris, pH 8.8	1250 μ l	-
0.5 M Tris, pH 6.8	-	1250 μ l
10 % (w/v) SDS	50 μ l	50 μ l
10% (w/v) Ammonium persulfate	50 μ l	50 μ l
TEMED	8 μ l	8 μ l

6. Protein determination by non-denaturing polyacrylamide gel electrophoresis (Non-denaturing-PAGE)

8 % Non-denaturing polyacrylamide gel was prepared (Appendix Table A2) and soaked in 1X running buffer [10X stock: 250 mM Tris, pH 8.3, 2 M glycine]. After protein purification, 0.1 unit of purified enzymes was mixed with 1X sample buffer [4X stock: 10 % (v/v) glycerol, 12.5 % (w/v) bromophenol blue, and 125 mM Tris, pH 6.8], and loaded into the non-denaturing polyacrylamide gel. All samples were separated by electrophoresis at 150 volt for 60 min. The gel was incubated with 1 mM 4MU-Glc and visualized under the ultraviolet light. Moreover, the gel was washed with sterile water, stained with staining solution (same as section A5) for an hour, and washed twice by de-staining solution (same as section A5) for an hour.

Appendix Table A2 Preparation of 8 % Non-denaturing polyacrylamide gel

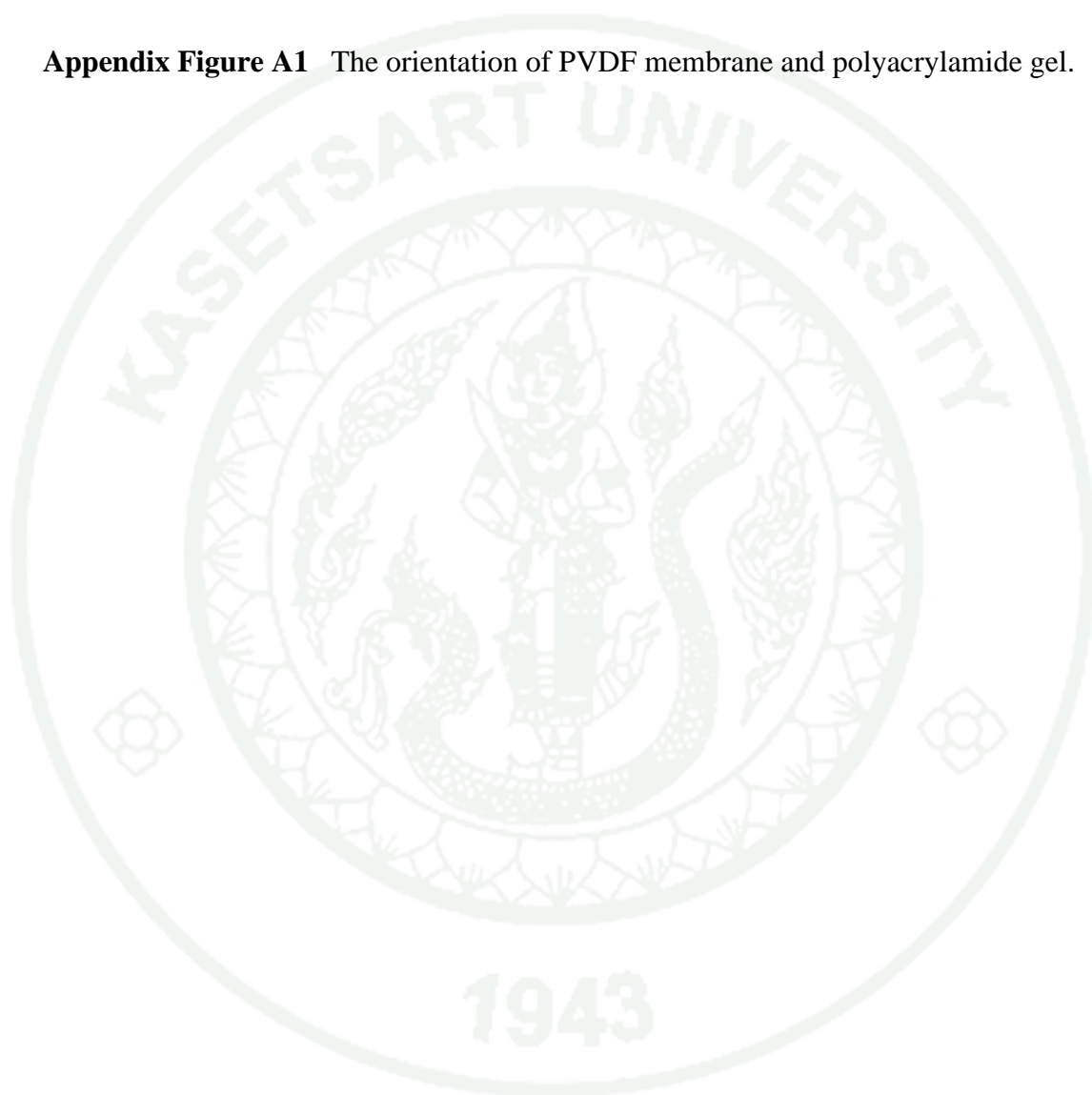
Materials	8 % resolving gel	4 % stacking gel
Sterile distilled water	2248 μ l	2200 μ l
30 % Acrylamide	1250 μ l	500 μ l
1.5 M Tris, pH 8.8	1250 μ l	-
0.5 M Tris, pH 6.8	-	1250 μ l
0.2 M EDTA, pH 6.9	-	50 μ l
10% (w/v) Ammonium persulfate	50 μ l	50 μ l
TEMED	8 μ l	8 μ l

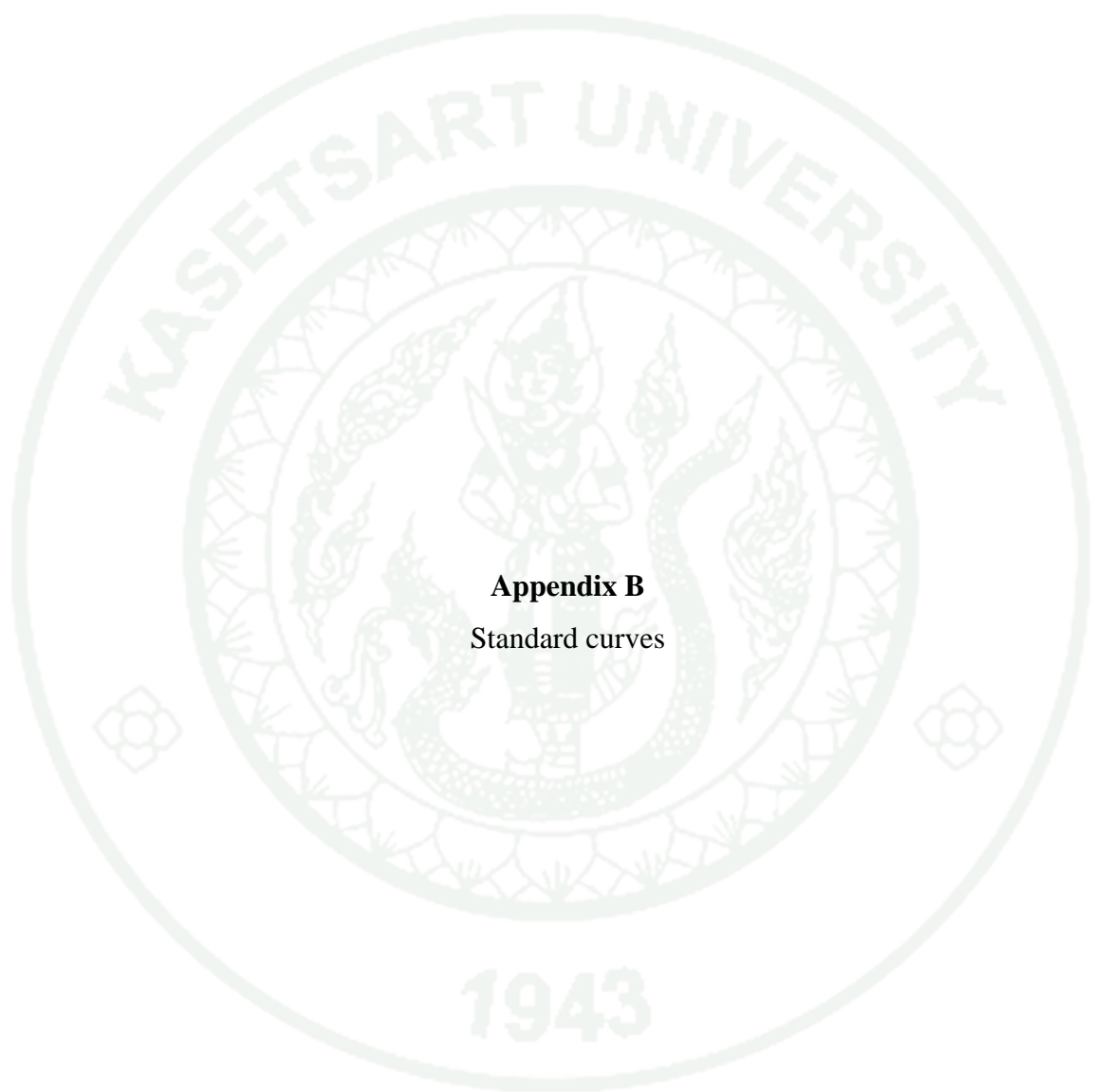
7. Western blotting analysis

After SDS-PAGE, the gel was soaked in the 1X transfer buffer [20X stock: 200 mM Tris and 2 M Glycine] for 20-60 min. The PVDF membrane was previously activated by 100% methanol for 5 s. Then, the PVDF membrane and 6 pieces of filtered paper were also soaked in 1X transfer buffer for 20 min and 10 min, respectively. The protein samples were electrically transferred from the polyacrylamide gel to the PVDF membrane by electrophoresis at 10 V for 30 min (Appendix Figure A1). The membrane was further incubated with 5% non-fat skim milk in 1X PBST [0.08 M Na_2HPO_4 , 0.02 M NaH_2PO_4 , 0.1 M NaCl, and 0.1 % Tween 20] for 1 h. The PVDF membrane was washed twice by 1X PBST and incubated with a mouse monoclonal antibody against natural dalcochinase [1 in 5,000 dilution in 1X PBST] for 1 h. Then, membrane was washed with 1X PBST for 5 min, 3 times and 1X PBST for 15 min with gentle shaking. The membrane was then incubated with a polyclonal rabbit anti-mouse immunoglobulin linked-HRP [1 in 5,000 dilution in 1X PBST] for 1 h. The PVDF membrane was washed again in the same manner, and then incubated with the chemiluminescent substrate (GE healthcare, Sweden) for visualizing the band of dalcochinase samples.



Appendix Figure A1 The orientation of PVDF membrane and polyacrylamide gel.

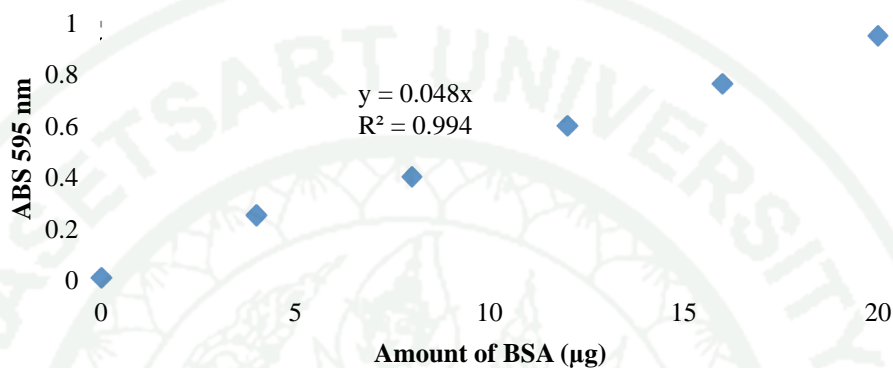




Appendix B
Standard curves

1. Standard curve of protein

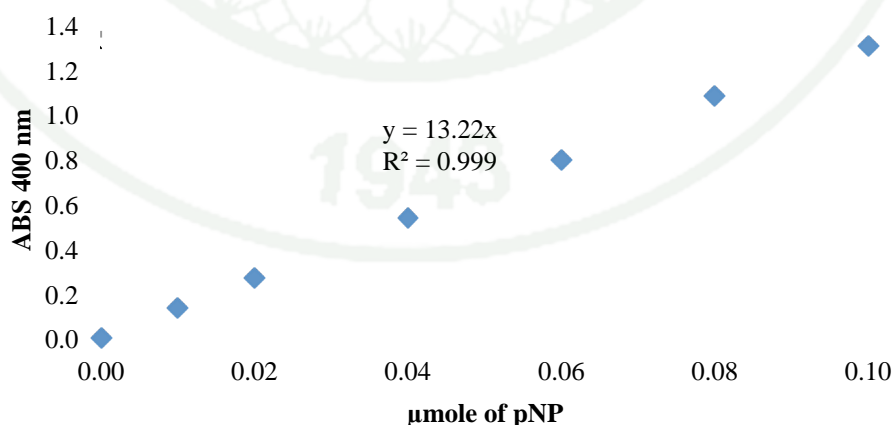
0-20 μg of bovine serum albumin (BSA) in 800 μl water was mixed with 200 μl Bio-Rad protein assay for 5 min. The absorbance of the mixture was measured at 595 nm.



Appendix Figure B1 Standard curve of protein

2. Standard curve of *p*NP (used during protein expression and purification)

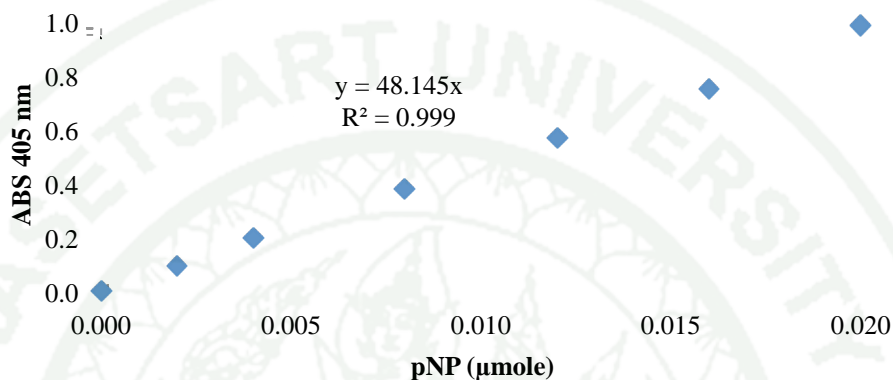
0-0.1 μmol of *p*NP was dissolved in 500 μl of 0.1 M sodium acetate, pH 5.0. The solutions were added with 1 ml of 2 M sodium carbonate, and their absorbance was measured at 400 nm.



Appendix Figure B2 Standard curve of *p*NP for determination of β -glucosidase activities during expression and purification steps

3. Standard curve of *p*NP (used for kinetic study)

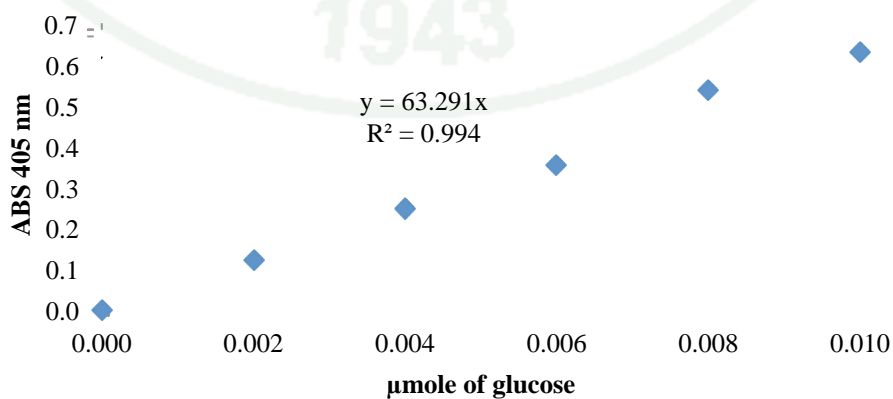
0-0.02 μmol of *p*NP was dissolved in 50 μl of 0.1 sodium acetate, pH 5.0. The solutions were added with 0.1 ml of 2 M sodium carbonate, and their absorbance was measured at 405 nm.



Appendix Figure B3 Standard curve of *p*NP for determination of β -glucosidase activities for kinetic study

4. Standard curve of glucose

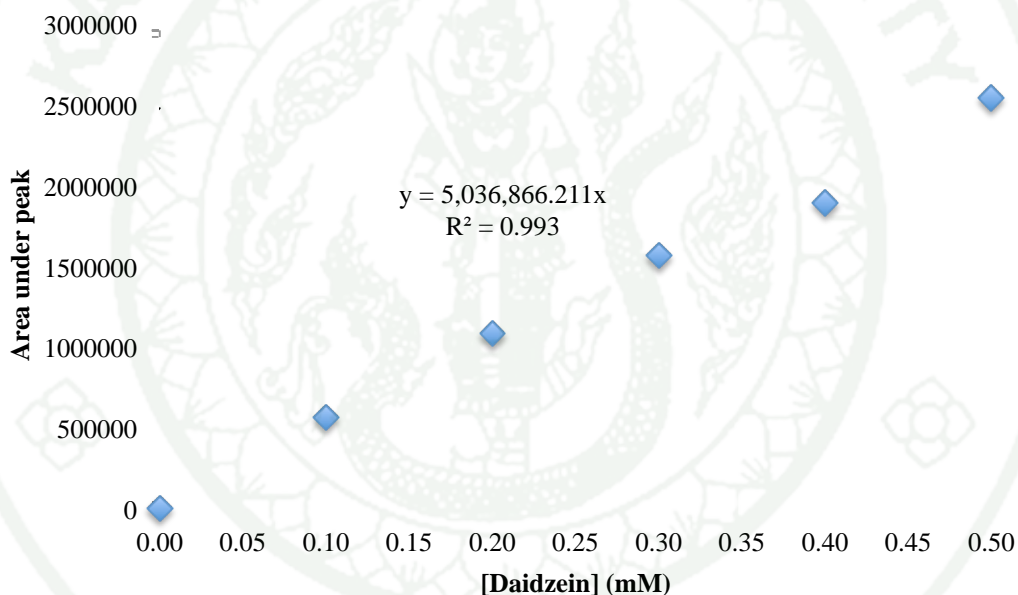
0-0.01 μmol of glucose was dissolved in 50 μl of 0.1 M sodium acetate, pH 5.0. The solutions were added with 0.5 unit glucose oxidase reagent containing 0.5 mg/ml ABTS, and incubated at 37 $^{\circ}\text{C}$ for 15 min. Finally, the absorbance of the reaction products was measured at 405 nm.



Appendix Figure B4 Standard curve of glucose

5. Standard curve of daidzein

0-0.5 mM of daidzein was dissolved in 50 μl of 0.1 M sodium acetate, pH 5.0, containing 5 % DMSO. Then, the samples were dried, and re-suspended in 50 μl of 70 % Solvent A [0.1% phosphoric acid in ultrapure water] 30 % Solvent B [acetonitrile]. Ten μl of the samples were injected into HPLC. The analytes were eluted with the elution gradients described in section 7.3 of Materials and Methods, and detected at 260 nm. The peak of daidzein appeared at 10.5 min after the start of the elution gradient.

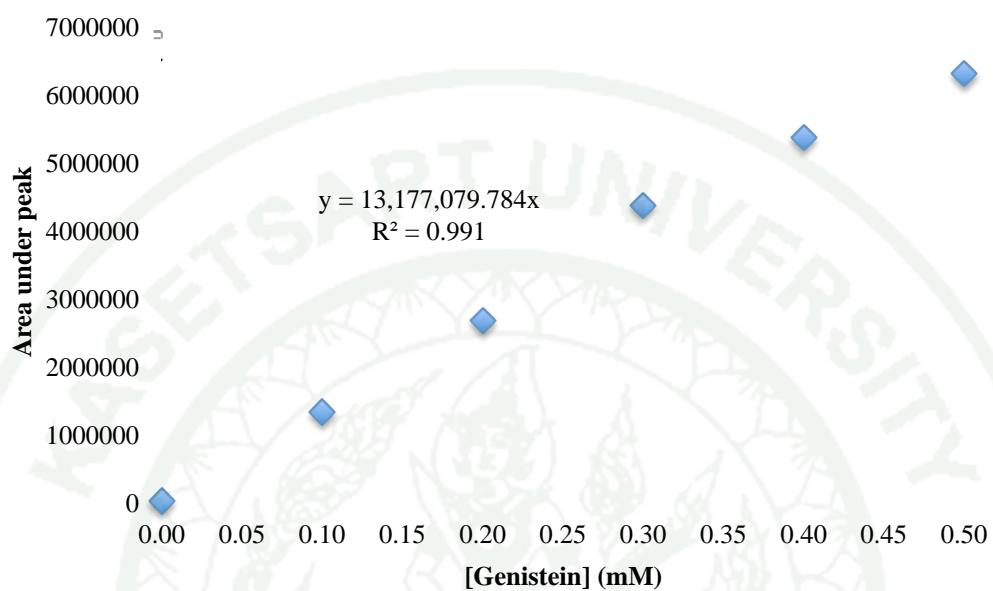


Appendix Figure B5 Standard curve of daidzein

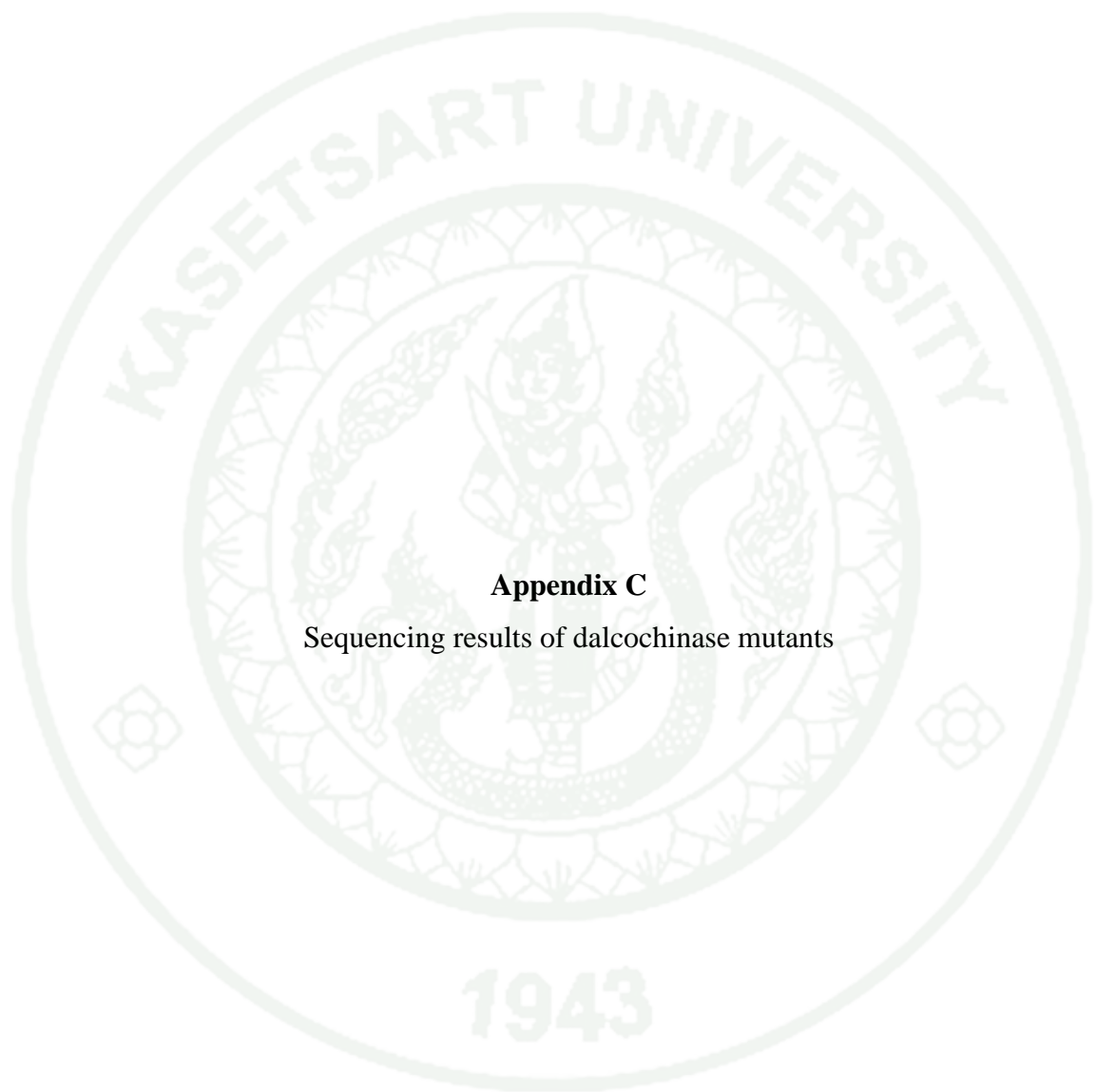
6. Standard curve of genistein

0-0.5 mM of genistein was dissolved in 50 μl of 0.1 M sodium acetate, pH 5.0, containing 5 % DMSO. Then, the samples were dried, and re-suspended in 50 μl of 70 % Solvent A [0.1% phosphoric acid in ultrapure water] 30 % Solvent B [acetonitrile]. Ten μl of the samples were injected into HPLC. The analytes were eluted with the elution gradients described in section 7.3 of Materials and Methods,

and detected at 260 nm. The peak of daidzein appeared at 14.5 min after the start of the elution gradient.



Appendix figure B6 Standard curve of genistein



Appendix C

Sequencing results of dalcochinase mutants

1. Sequencing result of the A454F/E455A dalcochinase mutant using AOXF1 primer
(1,432 bp)

CCGTATTAGACTTTTTTACGACACTTTGAGAAGATCAAAAAACAATAATTATTTCGAAACGATGAGATTTCCCTTCT
ATTTTTACTGCTGTTTTGTTTCGCGCATCTTCTGCATTGGCTGCTCCAGTCAACACTACAACAGAAGATGAAACGG
CACAAATTCGGCTGAAGCTGTCATCGGTTACTCAGATTTAGAAGGGGATTTTCGATGTTGCTGTTTTGCCATTTTC
CAACAGCACAAATAACGGTTATTGTTTTATAAATACTACTATTGCCAGCATGCTGCTAAAGAAGAAGGGGTATCT
CTCGAGAAAAGAGAGGCTGAAGCTGCACATCACCATCACCATCACCATGCTGCAGTTCTCCATTCAACCGAA
GCTGTTTTCTTCAGATTTCATTTTTGGGACAGCATCCTCCTCGTACCAGTATGAAGGTGAGGGCAGAGTACCAAG
TATATGGGATAACTTCACCCACCAATATCCAGAAAAGATAGCGGATAGAAGCAACGGAGATGTTGCAGTTGACCAA
TTTCACCGCTATAAGAAGGATATTGCAATCATGAAGGATATGAACTTGGATGCTTATAGAATGTCCATCTCCTGGC
CTAGAATTCTCCCAACGGGTAGGGTTAGTGGAGGCATAAACCAAACAGGAGTTGACTACTACAACAGGCTCATCAA
TGAGTCACTGGCCAATGGCATAACACCATTTGTAACCATTTTTTCATTGGGATCTTCCACAAGCCTTGGAGGATGAG
TACGGTGGCTTCTTAAATCATAGCGTTGTAATGATTTCCAAGACTATGCGGATCTTTGCTTCCAATTATTTGGAG
ATAGGGTAAAGCATTGGATTACTACTAAATGAGCCATCAATCTTACC CGGAATGGGTATGCATACGGTATGTTTTGC
ACCAGTTCGATGTTCTCCATCGTACAATCCAACCTGCACAGGGTGGGGATGCAGGAACAGAGACTTATCTGGTTGC
GCACAACCTGATCCTTTCTCATGCAGCAACTGTCCAAGTGTACAAAAGGAAGTATCAGGAACATCAGAAAGGTACA
ATAGGCATTTCTTGCACGTAAGTTTGGGTTATAACCGCTTCAAATAGCACATCAGATCAAATGCTACCCAGCGA
TATCTTGACTCTCCATGGGGATGGGTTTATGGACCCCTTACC GCCAGGAAGGGATCCCGATAGCAGGCAATATC
TAGTTGGGAATCGATTGCCCAAATTTACTACCAATCAAGCCAAATAAGTTAAGGGGTCAATTTGGATTTTATTGGAC
TAACCTATTACCCCTAACTATGGTACCAAATCAAATGCGTCCAAATGGTTGCCACCTAGTTACCTCCAGAATCT
CAAGTCATCTTTAAACAACCGCATGGGGTCTTTTATGGTCTTGGCTCCCTCCCAAAGGAGT

2. Sequencing result of the A454F/E455A dalcochinase mutant using TRF 1 primer
(1,396 bp)

GAAATTTTGGGAGCATCCTCCTCGTACAGTATGAAGGTGAGGGCAGAGTACCAAGTATATGGGGATAACTTCACCC
ACCAATATCCAGAAAAGATAGCGGATAGAAGCAACGGAGATGTTGCAGTTGACCAATTTACCGCTATAAGAAGGA
TATTGCAATCATGAAGGATATGAACTTGGATGCTTATAGAATGTCCATCTCCTGGCCTAGAATTTCTCCCAACGGGT
AGGGTTAGTGGAGGCATAAACCAAACAGGAGTTGACTACTACAACAGGCTCATCAATGAGTCACTGGCCAATGGCA
TAACACCATTTGTAACCATTTTTTCATTGGGATCTTCCACAAGCCTTGGAGGATGAGTACGGTGGCTTCTTAAATCA
TAGCGTTGTAATGATTTCCAAGACTATGCGGATCTTTGCTTCCAATTATTTGGAGATAGGGTAAAGCATTGGATT
ACACTAAATGAGCCATCAATCTTACC CGGAATGGGTATGCATACGGTATGTTTGCACCAGGTGCGATGTTCTCCAT
CGTACAATCCAACCTTGCACAGGTGGGGATGCAGGAACAGAGACTTATCTGGTTGCGCACAACTGATCCTTTCTCA
TGCAGCAACTGTCCAAGTGTACAAAAGGAAGTATCAGGAACATCAGAAAGGTACAATAGGCATTTCTTGCACGTA
GTTTGGGTTATAACCGCTTCAAATAGCACATCAGATCAAATGCTACCCAGCGATATCTTGACTTCACATGTGGAT
GGTTTATGGACCCACTTACAGCAGGAAGGTATCCAGATAGCATGCAATATCTAGTTGGAGATCGATTGCCTAAGTT
TACTACAGATCAAGCCAAATAGTTAAGGGTTCATTTGATTTTATTGGACTAAACTATTACACCACTAACTATGCT
ACCAAATCAGATGCGTCAACATGCTGCCACCTAGTTACCTCACAGATCCTCAAGTCACTCTTTACAGCAACGCA
ATGGGGTCTTTATAGGTCAGTGACTCCCTCAAGGATGGATGTGCATTTATCCAAAAGGACTTCGAGATTTGTTGC
TTTACTTCAAGGAAAAGTATAACAATCCTTTGGTTTACATCACTGAAAATGGTATAGATGAAAAGAATGATGCATC

ACTATCACCTTGAGGAATCCTTGATAGAACCTTATAAGAATTGATAGTTATTATCCGTCACCTCTTTTATGTTCCA
 ATTGCAATTAAGTCTGGCGCCAAATGTGAAAAGGATTTTTTGCATGGGGCATGGTTGGACACATTTTAAATGGTTG
 CTGGGTATACCTCACCGATTTGGGATATATTTTTTGAACAACACCACCTTTGGAAAAGAATCCCAAGCTCCCTGCA
 CAATGGTTCAATAATTTCTTTGGCACTG

3. Sequencing result of the A454F/E455A dalcochinase mutant using TRF 2 primer (1,338 bp)

CCTTTACTTTATTTGGGAGATAGGGTAAAAGCATTGGATTACACTAAATGAGCCATCAATCTTCACCGGAATGGG
 TATGCATACGGTATGTTTGCACCAGGTCGATGTTCTCCATCGTACAATCCAACCTTGCACAGGTGGGGATGCAGGAA
 CAGAGACTTATCTGGTTGCGCACAACTGATCCTTTCTCATGCAGCAACTGTCCAAGTGTACAAAAGGAAGTATCA
 GGAACATCAGAAAGGTACAATAGGCATTTCTTGCACGTAGTTTGGGTTATACCGCTTCAAATAGCACATCAGAT
 CAAAATGCTACCCAGCGATATCTTGACTTCACATGTGGATGGTTTATGGACCCACTTACAGCAGGAAGGTATCCAG
 ATAGCATGCAATATCTAGTTGGAGATCGATTGCCTAAGTTTACTACAGATCAAGCCAAATTAGTTAAGGGTTCATT
 TGATTTTATTGGACTAACTATTACACCACTAACTATGCTACCAAATCAGATGCGTCAACATGCTGCCACCTAGT
 TACCTCACAGATCCTCAAGTCACTCTCTTACAGCAACGCAATGGGGTCTTTATAGGTCCAGTACTCCCTCAGGAT
 GGATGTGCATTTATCCAAAAGGACTTCGAGATTTGTTGCTTTACTTCAAGGAAAAGTATAACAATCCTTTGGTTTA
 CATCACTGAAAATGGTATAGATGAGAAGAATGATGCATCACTATCACTTGAGGAATCCTTGATAGACACTTATAGA
 ATTGATAGTTATTATCGTCATCTCTTTTATGTTTCGATATGCAATTAGGTCTGGCGCAAATGTGAAAGGATTTTTTG
 CATGGTCATTGTTGGACAACCTTTGAATGGTTTGTGGTTATACATCACGATTTGGATTATATTTTGTGAACACAC
 TACTTTGAATAGATATCCCAAGCTCTCTGCAACATGGTTCAAGTATTTTCTGGCACGTGATCAAGAGAGTGCTAAA
 TTGGAAATTTTAGCACCAAAGGCAAGATGGAGCTTATCAACGATGATCAAGGAAGAAAAGACAAAACCCAAGTGGG
 GGCATTGAAGGCTTTTGTGCTAGATCTTAATCACTAAGTGAATTCGCGGCCCGCTGCAGTACGTAGAATTCACGTG
 GCCCAGCCGGCCGTCTCGGATCGGTACCCCAAGCCCGGGGGCCGCCAGCTTCTAGAACAAAATCATCTTCAA
 AAAAGATCTTGAATAACGCCCTCGACCATCTCCACATCCACCCTTGGAGTTTGGAGCCCTAAACATAGACGGGTCC
 TCAATTTAAATTTGGGCACTTACCAAAAAACCAGGGCTTGCGGAAT

4. Sequencing result of the A454F/E455A dalcochinase mutant using TRF 3 primer (1,177 bp)

TCTAATAAGAGATATAGCACTTAGTTAAAGGGTTCATTTGATTTTATTGGACTAACTATTACACCACTAACTATG
 CTACCAAATCAGATGCGTCAACATGCTGCCACCTAGTTACCTCACAGATCCTCAAGTCACTCTCTTACAGCAACG
 CAATGGGGTCTTTATAGGTCCAGTACTCCCTCAGGATGGATGTGCATTTATCCAAAAGGACTTCGAGATTTGTTG
 CTTTACTTCAAGGAAAAGTATAACAATCCTTTGGTTTACATCACTGAAAATGGTATAGATGAGAAGAATGATGCAT
 CACTATCACTTGAGGAATCCTTGATAGACACTTATAGAATTGATAGTTATTATCGTCATCTCTTTTATGTTTCGATA
 TGCAATTAGGTCTGGCGCAAATGTGAAAGGATTTTTTGCATGGTCATTGTTGGACAACCTTGAATGGTTTGTGGT
 TATACATCACGATTTGGATTATATTTTGTGAACACTACTTTTGAATAGATATCCCAAGCTCTCTGCAACGTGGT
 TCAAGTATTTTCAGGCACGTGATCCAAAGAGTGCTACATTGCACATTTTAGCACCTAAGGCACGACGGAGCTTATA
 ACCTATCATCAAGCAACACTCGACTACTACCCAGCGACACCCTTGCAGGGCCATAGAGATACCTCCACGTTCCCG
 ACCTGACAACTCCGCCGGTGGCACCACCTAGCTCAGACCCTTGGCGCGTTACCCTCATACCTGCACCACATCTAC

TCCTCTTCCGCAACCGTATCCGCATTCAACATAGCCTCAAGCTGATAGGCTCTCTCCAATTAAGGCAGTACCGCC
 TTATCAACTCGCAAGGTCGCGCCTTTATAGCATCGAACTCCCTCAGGTACAATCGCTGACCGGACTGCGACGATTA
 TCACAGGTGAACGCATCGATACTACGACGTACTAGACGCCGCCTTACGGACCATCGAACTTTAATCAGCCCACATT
 GGCCAGTCTAATTCTACTTCGGCTAAACAGGTTGATCAAGGCAATTAACCCTAGGGTTAAAGGTAAGCCGTTT
 GACCGTTCGAGGAGGTTTACAATCGGGAAAGTTGGGTAAGGGGCCGTTAATCTATTTTCGGCCTTACCACCCGAG
 AAATCCAATTCCATTTCTATTGTTATGGAAAAATAAG

5. Sequencing result of the A454F/S459V dalcochinase mutant using AOXF1 primer (1,092 bp)

CCTTTTTCGACTTTTTTACGACACTTGAGAAGATCAAAAAACAATAATTATTCGAAACGATGAGATTTCTTCTA
 TTTTTACTGCTGTTTTGTTCGCAGCATCTTCTGCATTGGCTGCTCCAGTCAACACTACAACAGAAGATGAAACGGC
 ACAAATTCGGCTGAAGCTGTCATCGGTTACTCAGATTTAGAAGGGGATTTTCGATGTTGCTGTTTTGCCATTTTCC
 AACAGCACAAATAACGGGTTATTGTTTTATAAATACTACTATTGCCAGCATGCTGCTAAAGAAGAAGGGGTATCTC
 TCGAGAAAAGAGAGGCTGAAGCTGCACATCACCATCACCATCATCACCATGCTGCAGTTCCTCCATTCAACCGAAG
 CTGTTTTCTTTCAGATTTCATTTTTGGGACAGCATCCTCCTCGTACCAGTATGAAGGTGAGGGCAGAGTACCAAGT
 ATATGGGATAACTTCACCCACCAATATCCAGAAAAGATAGCGGATAGAAGCAACGGGAGATGTTGCAGTTGACCAAT
 TTCACCGCTATAAGAAGGATATTGCAATCATGAAGGATATGAACTTGGATGCTTATAGAATGTCCATCTCCTGGCC
 TAGAATTCTCCCAACGGGTAGGGTTAGTGGAGGCATAAACCAAACAGGAGTTGACTACTACAACAGGCTCATCAAT
 GAGTCACTGGCCAATGGCATAACACCATTTGTAACCATTTTTTCATTGGGATCTTCACAAGCCTTGGAGGATGAGT
 ACGGTGGCTTCTTAAATCATAGCGTTGTAATGATTTCCAAGACTATGCGGATCTTTGCTTCCAATTATTTGGAGA
 TAGGGTAAAGCATTGGATTACACTAAATGAGCCATCAATCTTCACCGCGAATGGGTATGCATACGGTATGTTTGCA
 CCAGGTCGATGTTCTCCATCGTACAATCCAACCTTGACAGGGTGGGGATGCAGGAACAGAGACTTATCTGGTTGCG
 CACAACCTGATCCTTTCTCATGCAGCAACTGTCCAAGGTACAAAAGGAAGTATCAGGAACATCAGAAAGGTACAA
 TAGGCATTTCTTGCACGTAGTTTTGGG

6. Sequencing result of the A454F/S459V dalcochinase mutant using TRF 1 primer (1,012 bp)

GGGAATTTGGGGAGCATCCTCCTCGTACAGTATGAAGGTGAGGGCAGAGTACCAAGTATATGGGATAACTTCACC
 CACCAATATCCAGAAAAGATAGCGGATAGAAGCAACGGGAGATGTTGCAGTTGACCAATTTCCACCGCTATAAGAAGG
 ATATTGCAATCATGAAGGATATGAACTTGGATGCTTATAGAATGTCCATCTCCTGGCCTAGAATTTCCCAACGGG
 TAGGGTTAGTGGAGGCATAAACCAAACAGGAGTTGACTACTACAACAGGCTCATCAATGAGTCACTGGCCAATGGC
 ATAACACCATTTGTAACCATTTTTTCATTGGGATCTTCACAAGCCTTGGAGGATGAGTACGGTGGCTTCTTAAATC
 ATAGCGTTGTAATGATTTCCAAGACTATGCGGATCTTTGCTTCCAATTATTTGGAGATAGGGTAAAGCATTGGAT
 TACACTAAATGAGCCATCAATCTTCACCGCGAATGGGTATGCATACGGTATGTTTGCACCAGGTCGATGTTCTCCA
 TCGTACAATCCAACCTTGACAGGTGGGGATGCAGGAACAGAGACTTATCTGGTTGCGCACAACTGATCCTTTCTC
 ATGCAGCAACTGTCCAAGGTACAAAAGGAAGTATCAGGAACATCAGAAAGGTACAATAGGCATTTCTTGCACGT
 AGTTTGGGTTATACCGCTTCAAAATAGCACATCAGATCAAAATGCTACCCAGCGATATCTTGACTTCACATGTGGA
 TGGTTTATGGACCCACTTACAGCAGGAAGGTATCCAGATAGCATGCAATATCTAGTTGGAGATCGATTGCCTAAGT
 TTACTACAGATCAAGCCAAATTAGTTAAGGGTTCATTTGATTTTATTGGACTAAACTATTACACCACTAATATGC

TACCAAATCAGATGCGTCAACATGCTGCCACCTAGTTACCTCACAGATCCTCAAGTCACTCTCTTACAGCAACGC
AATGGGGTCTTTATAGGTCCAGT

7. Sequencing result of the A454F/S459V dalcochinase mutant using TRF 2 primer
(1,008 bp)

CCCGTCACTTATTTGGGAGATAGGGTAAAAGCATTGGATTACACTAAATGAGCCATCAATCTTCACCGGAATGGG
TATGCATACGGTATGTTTGCACCAGGTCGATGTTCTCCATCGTACAATCCAACCTTGCACAGGTGGGGATGCAGGAA
CAGAGACTTATCTGGTTGCGCACAACTGATCCTTTCTCATGCAGCAACTGTCCAAGTGTACAAAAGGAAGTATCA
GGAACATCAGAAAGGTACAATAGGCATTTCTTGCACGTAGTTTGGGTTATACCGCTTCAAATAGCACATCAGAT
CAAAATGCTACCCAGCGATATCTTGACTTACATGTGGATGGTTTATGGACCCACTTACAGCAGGAAGGTATCCAG
ATAGCATGCAATATCTAGTTGGAGATCGATTGCCTAAGTTTACTACAGATCAAGCCAAATTAGTTAAGGGTTCATT
TGATTTTATTTGGACTAACTATTACACCACTAACTATGCTACCAAATCAGATGCGTCAACATGCTGCCACCTAGT
TACCTCACAGATCCTCAAGTCACTCTCTTACAGCAACGCAATGGGGTCTTTATAGGTCCAGTGACTCCCTCAGGAT
GGATGTGCATTTATCCAAAAGGACTTCGAGATTTGTTGCTTTACTTCAAGGAAAAGTATAACAATCCTTTGGTTTA
CATCACTGAAAATGGTATAGATGAGAAGAATGATGCATCACTATCACTTGGGAATCCTTGATAGACACTTATAGA
ATTGATAGTTATTATCGTCATCTCTTTTATGTTGATATGCAATTAGGTCTGGCGCAAATGTGAAAGGATTTTTTG
CATGGTCATTGTTGGACAACCTTTGAATGGTTTGGGGTTATACAGTTGATTTGGATTATATTTTGTGAACACAC
TACTTTGAATAGATATCCCAAGCTCTCTGCAACATGGTTCAAGTATTTTCTGGCACGTGATCAAGAGAGTGCTAAA
TTGGAAATTTTAGCACCAA

8. Sequencing result of the A454F/S459V dalcochinase mutant using TRF 3 primer
(1,171 bp)

CCCACTATCAGCCAATTTAGTTAGGGTTCATTTGATTTTATTTGGACTAACTATTACACCACTAACTATGCTACC
AAATCAGATGCGTCAACATGCTGCCACCTAGTTACCTCACAGATCCTCAAGTCACTCTCTTACAGCAACGCAATG
GGGTCTTTATAGGTCCAGTGACTCCCTCAGGATGGATGTGCATTTATCCAAAAGGACTTCGAGATTTGTTGCTTTA
CTTCAAGGAAAAGTATAACAATCCTTTGGTTTACATCACTGAAAATGGTATAGATGAGAAGAATGATGCATCACTA
TCACTTGGGAATCCTTGATAGACACTTATAGAATTGATAGTTATTATCGTCATCTCTTTTATGTTGATATGCAA
TTAGGTCTGGCGCAAATGTGAAAGGATTTTTTGCATGGTCATTGTTGGACAACCTTTGAATGGTTTGGGGTTATAC
AGTTCGATTTGGATTATATTTTGTGAACTACACTACTTTGAATAGATATCCCAAGCTCTCTGCAACATGGTTCAAG
TATTTTCTGGCACGTGATCAAGAGAGTGCTAAATTTGGAAATTTTAGCACCAAAGGCAAGATGGAGCTTATCAACGA
TGATCAAGGAAGAAAAGACAAAACCAAGTGGGGCATTGAAGGCTTTTGTATCTAGATCTTAATCACTAGTGAATTC
GCGGCCGCTGCAGTACGTAGAATTCACGTGGCCAGCCGGCCGTCTCGGATCGGTACCTCGAGCCGCGGCGGCCG
CCAGCTTTCTAGAACAAAACCTCATCTCAGAAGAGGATCTGAATAGCGCCGTCGACCATCATCATCATCATTCG
AGTTTGTAGCCTTAGACATGACTGTTCCCTCAGTTCAAGTTGGGCACTTACGAGAAGACCGGTCTTGCTAGATTCTA
ATCAAGAGGATGTCAGAATGCCATTTGCCTGAGAGATGCAGGCTTCATTTTGTACTTTTTTATTTGTAACCTAT
ATAGTATAGGAATTTTTTTTTGTCATTTGGTTCTTCTCGTACGAGCTTGCTCCTGATCAGCCTATCTCGCAGCTGA
TGAATATCTTGTGGTAGGGGTTTGGGAAAGACCATAAAAGTTGGAGGTTCTACGTGGTATCTCTCTCCCGTGT
AAAGTTATAGAGGAATAAGTTGAAGCTTACG

9. Sequencing result of the E455A/S459V dalcochinase mutant using AOXF1 primer
(1,016 bp)

CCTTTTACGACTTTTTACGACAACTTGAGAAGATCAAAAAACAATAATTATTCGAAACGATGAGATTTCCCTTCT
ATTTTTACTGCTGTTTTGTTTCGCAGCATCTTCTGCATTGGCTGCTCCAGTCAACACTACAACAGAAGATGAAACGG
CACAAATTCGGCTGAAGCTGTCATCGGTTACTCAGATTTAGAAGGGGATTTTCGATGTTGCTGTTTTGCCATTTTC
CAACAGCACAAATAACGGGTTATTGTTTTATAAATACTACTATTGCCAGCATGCTGCTAAAGAAGAAGGGGTATCT
CTCGAGAAAAGAGAGGCTGAAGCTGCACATCACCATCACCATCACCATGCTGCAGTTCCTCCATTCAACCGAA
GCTGTTTTCTTCAGATTTCATTTTTGGGACAGCATCCTCCTCGTACCAGTATGAAGGTGAGGGCAGAGTACCAAG
TATATGGGATAACTTCACCCACCAATATCCAGAAAAGATAGCGGATAGAAGCAACGGAGATGTTGCAGTTGACCAA
TTTCACCGCTATAAGAAGGATATTGCAATCATGAAGGATATGAACTTGGATGCTTATAGAATGTCCATCTCCTGGC
CTAGAATTCTCCCAACGGGTAGGGTTAGTGGAGGCATAAACCAAACAGGAGTTGACTACTACAACAGGCTCATCAA
TGAGTCACTGGCCAATGGCATAACACCATTTGTAACCATTTTTTCATTGGGATCTTCCACAAGCCTTGGAGGATGAG
TACGGTGGCTTCTTAAATCATAGCGTTGTAATGATTTCCAAGACTATGCGGATCTTTGCTTCCAATTATTTGGAG
ATAGGGTAAAGCATTGGATTACTAAATGAGCCATCAATCTTACC CGAATGGGTATGCATACGGGTATGTTTTG
CACCAGTGCATGTTCTCCATCGTACAATCCAACTGCACAGGGTGGGGATGCAGGGAACAGAGACTTATTTCTGG
TTGCGCACAACTGATCCTTTCTCATGC

10. Sequencing result of the E455A/S459V dalcochinase mutant using TRF 1 primer
(964 bp)

GGGAAATTTGGGGAGCATCCTCCTCGTACAGTATGAAGGTGAGGGCAGAGTACCAAGTATATGGGGATAACTTCA
CCCACCAATATCCAGAAAAGATAGCGGATAGAAGCAACGGAGATGTTGCAGTTGACCAATTTACCGCTATAAGAA
GGATATTGCAATCATGAAGGATATGAACTTGGATGCTTATAGAATGTCCATCTCCTGGCCTAGAATTCTCCCAACG
GGTAGGGTTAGTGGAGGCATAAACCAAACAGGAGTTGACTACTACAACAGGCTCATCAATGAGTCACTGGCCAATG
GCATAACACCATTTGTAACCATTTTTTCATTGGGATCTTCCACAAGCCTTGGAGGATGAGTACGGTGGCTTCTTAAA
TCATAGCGTTGTAATGATTTCCAAGACTATGCGGATCTTTGCTTCCAATTATTTGGAGATAGGGTAAAGCATTGG
ATTACTAAATGAGCCATCAATCTTACC CGAATGGGTATGCATACGGTATGTTTGCACCAGGTCGATGTTCTC
CATCGTACAATCCAACTTGCACAGGTGGGGATGCAGGAACAGAGACTTATCTGGTTGCGCACAACTGATCCTTTCT
TCATGCAGCAACTGTCCAAGTGTACAAAAGGAAGTATCAGGAACATCAGAAAGGTACAATAGGCATTTCTTGCAC
GTAGTTTGGGTTATACCGCTTTCAAATAGCACATCAGATCAAAATGCTACCCAGCGATATCTTGACTTCACATGTG
GATGGTTTATGGACCACTTACAGCAGGAAGGTATCCAGATAGCATGCAATATCTAGTTGGAGATCGATTGCCTAA
GTTTACTACAGATCAAGCCAAATTAGTTAAGGGTTCATTTGATTTTTATTGGACTAAACTATTACACCACCTAATAT
GCTACCAAAATCAGATGCGTCAACATGCTGCCACCTAGTTACCTCACAGATC

11. Sequencing result of the E455A/S459V dalcochinase mutant using TRF 2 primer
(997 bp)

CCGTGTCCTTTTTTTGGAGAAGGGGTAAAGCATTGGATTACACTAAATGAGCCATCAATCTTCACCGGAATGGGTA
TGCATACGGTATGTTTGCACCAGGTTCGATGTTCTCCATCGTACAATCCAACCTTGCACAGGTGGGGATGCAGGAACA
GAGACTTATCTGGTTGCGCACAACTGATCCTTTCTCATGCAGCAACTGTCCAAGTGTACAAAAGGAAGTATCAGG
AACATCAGAAAGGTACAATAGGCATTTCTTGCACGTAGTTTGGGTTATACCGCTTTCAAATAGCACATCAGATCA
AAATGCTACCCAGCGATATCTTGACTTCACATGTGGATGGTTTATGGACCCACTTACAGCAGGAAGGTATCCAGAT
AGCATGCAATATCTAGTTGGAGATCGATTGCCTAAGTTTACTACAGATCAAGCCAAATTAGTTAAGGGTTCATTTG
ATTTTATTTGGACTAACTATTACACCACTAACTATGCTACCAAATCAGATGCGTCAACATGCTGCCACCTAGTTA
CCTCACAGATCCTCAAGTCACTCTCTTACAGCAACGCAATGGGGTCTTTATAGGTCCAGTGACTCCCTCAGGATGG
ATGTGCATTTATCCAAAAGGACTTCGAGATTTGTTGCTTTACTTCAAGGAAAAGTATAACAATCCTTTGGTTTACA
TCACTGAAAATGGTATAGATGAGAAGAATGATGCATCACTATCACTTGAGGAATCCTTGATAGACACTTATAGAAT
TGATAGTTATTATCGTCATCTCTTTTATGTTTCGATATGCAATTAGGTCTGGCGCAAATGTGAAAGGATTTTTTGCA
TGGTCAATTGTTGGACAACCTTTGAATGGGCTGCTGGTTATACAGTTTCGATTTGGATTATATTTTGTGAACTACACTA
CTTTGAATAGATATCCCAAGCTCTCTGCAACATGGTTCAAGTATTTTCTGGCACGTGATCAAGAGAGTGCTAAATT
GGAAATTTT

12. Sequencing result of the E455A/S459V dalcochinase mutant using TRF 3 primer
(1,157 bp)

GCCACGTATAGCCAAATTTAGTTTAAAGGGTTCATTTGATTTTATTTGGACTAACTATTACACCACTAACTATGCT
ACCAAATCAGATGCGTCAACATGCTGCCACCTAGTTACCTCACAGATCCTCAAGTCACTCTCTTACAGCAACGCA
ATGGGGTCTTTATAGGTCAGTGACTCCCTCAGGATGGATGTGCATTTATCCAAAAGGACTTCGAGATTTGTTGCT
TTACTTCAAGGAAAAGTATAACAATCCTTTGGTTTACATCACTGAAAATGGTATAGATGAGAAGAATGATGCATCA
CTATCACTTGAGGAATCCTTGATAGACACTTATAGAATTGATAGTTATTATCGTCATCTCTTTTATGTTTCGATATG
CAATTAGGTCTGGCGCAAATGTGAAAGGATTTTTTGCATGGTCATTGTTGGACAACCTTTGAATGGGCTGCTGGTTA
TACAGTTTCGATTTGGATTATATTTTGTGAACTACACTACTTTGAATAGATATCCCAAGCTCTCTGCAACATGGTTC
AAGTATTTTCTGGCACGTGATCAAGAGAGTGCTAAATTTGGAAAATTTTAGCACCAAAGGCAAGATGGAGCTTATCAA
CGATGATCAAGGAAGAAAAGACAAAACCCAAGTGGGGCATGAAGGCTTTTATGATCTAGATCTTAATCACTAGTGAA
TTCGCGGCCCTGCAGTACGTAGAATTCACGTGGCCAGCCGCGCTCTCGGATCGGTACCTCGAGCCGCGCGCGG
CCGCCAGCTTTCTAGAACAAAACTCATCTCAGAAGAGGATCTGAATAGCGCCGTCGACCATCATCATCATCATCA
TTGAGTTTGTAGCCTTAGACATGACTGTTCCCTCAGTTCAAGTTGGGCACTTACGAGAAGACCGGTCTTGCTAGATT
CTAATCAAGAGGATGTCAGAATGCCATTTGCCTGAGAGATGCAGGCTTCATTTTTGATACTTTTTTATTTGTAACC
TATATAGTATAGGATTTTTTTTGGCATTGTTTCTTCTCGTACGAGCTTGCTCCTGATCAGCCTATCTCGCAGCT
GATGAAATCTTGGGGTTAGGGGTTGGGAAATTCCTTCAAGTTTCAAGGTTTCCATGGTTATTCCCATTCCCCTTC
AAAATATAGAAGATAAA

13. Sequencing result of the A454F/E455A/S459V dalcochinase mutant using AOXF1 primer (1,006 bp)

CCGTATACGACTTTTACGAACCACTTGAGAAGATCAAAAAACAATAATTATTCGAAACGATGAGATTTCCCTTCTA
 TTTTTACTGCTGTTTTGTTCGCAGCATCTTCTGCATTGGCTGCTCCAGTCAACACTACAACAGAAGATGAAACGGC
 ACAAATCCGGCTGAAGCTGTCATCGGTTACTCAGATTTAGAAGGGGATTTTCGATGTTGCTGTTTTGCCATTTTCC
 AACAGCACAATAACGGGTTATTGTTTTATAAATACTACTATTGCCAGCATTGCTGCTAAAGAAGAAGGGGTATCTC
 TCGAGAAAAGAGAGGCTGAAGCTGCACATCACCATCACCATCATCACCATGCTGCAGTTCCTCCATTCAACCGAAG
 CTGTTTTCTTCAGATTTCATTTTGGGACAGCATCCTCCTCGTACCAGTATGAAGGTGAGGGCAGAGTACCAAGT
 ATATGGGATAAATTCAACCACCAATATCCAGAAAAGATAGCGGATAGAAGCAACGGAGATGTTGCAGTTGACCAAT
 TTCACCGCTATAAGAAGGATATTGCAATCATGAAGGATATGAACTTGGATGCTTATAGAATGTCCATCTCTGGCC
 TAGAATCTCCCAACGGGTAGGGTTAGTGGAGGCATAAACCAAACAGGAGTTGACTACTACAACAGGCTCATCAAT
 GAGTCACTGGCCAATGGCATAACACCATTTGTAACCATTTTTTCATTGGGATCTTCCACAAGCCTTGGAGGATGAGT
 ACGGTGGCTTCTTAAATCATAGCGTTGTAATGATTTCCAAGACTATGCGGATCTTTGCTTCCAATTTTGGAGA
 TAGGGTAAAGCATTGGATTACACTAAATGAGCCATCAATCTTACCAGGAAATGGGTATGCATACGGGTATGTTTTGC
 ACCAGTTCGATGTTCTCCATCGTACAATCCAACCTGCACAGGGTGGGGATGCAGGGAACAGAGGACTTATCTGGT
 TGCGCACAACCTGATCCT

14. Sequencing result of the A454F/E455A/S459V dalcochinase mutant using TRF 1 primer (1,010 bp)

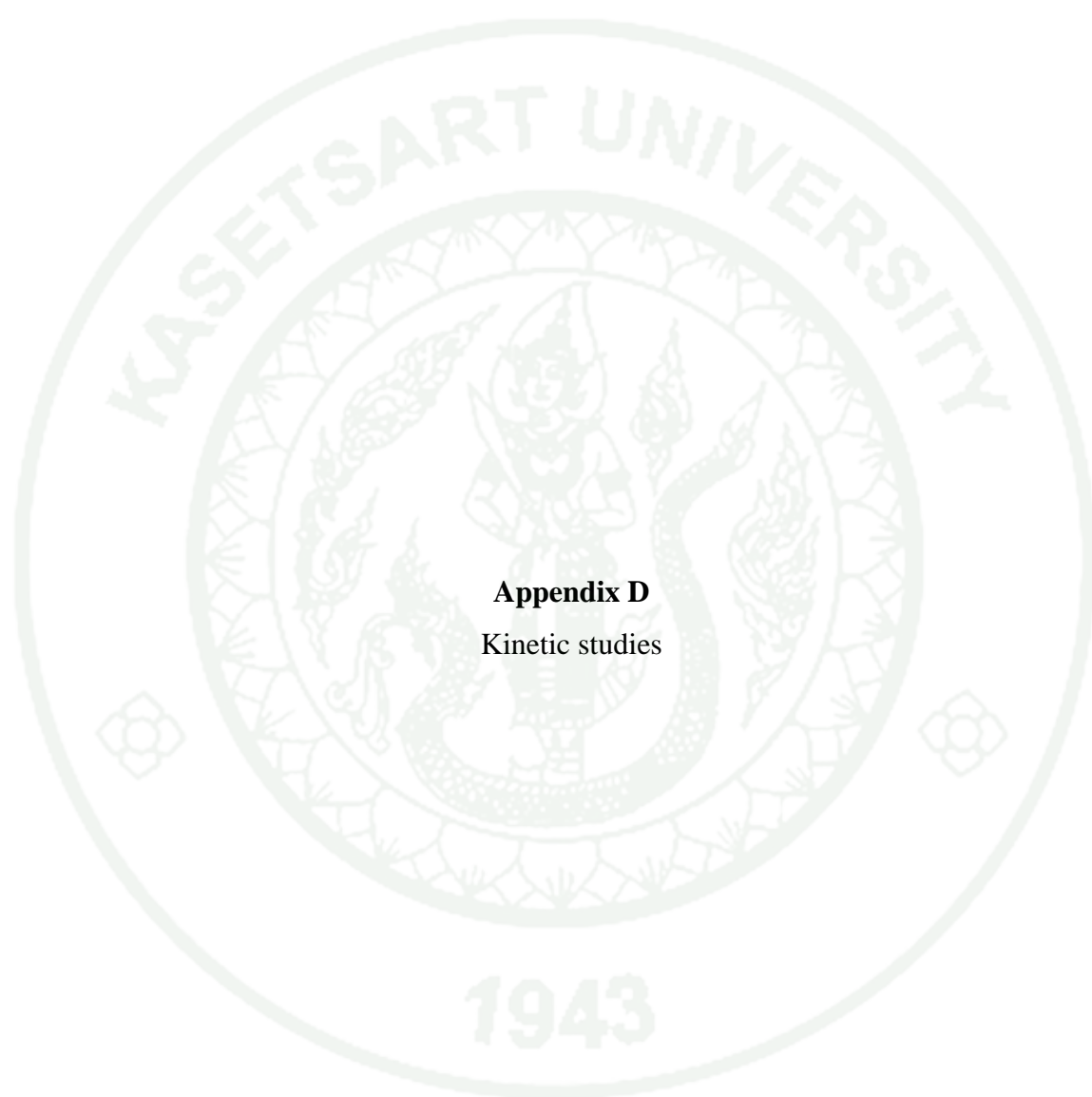
GGAATGTTGGGGAGCATCCTCCTCGTACAGTATGAAGGTGAGGGCAGAGTACCAAGTATATGGGATAACTTCACC
 CACCAATATCCAGAAAAGATAGCGGATAGAAGCAACGGAGATGTTGCAGTTGACCAATTTCCACCGCTATAAGAAGG
 ATATTGCAATCATGAAGGATATGAACTTGGATGCTTATAGAATGTCCATCTCCTGGCCTAGAATTCTCCCAACGGG
 TAGGGTTAGTGGAGGCATAAACCAAACAGGAGTTGACTACTACAACAGGCTCATCAATGAGTCACTGGCCAATGGC
 ATAACACCATTTGTAACCATTTTTTCATTGGGATCTTCCACAAGCCTTGGAGGATGAGTACGGTGGCTTCTTAAATC
 ATAGCGTTGTAATGATTTCCAAGACTATGCGGATCTTTGCTTCCAATTTTGGAGATAGGGTAAAGCATTGGAT
 TACACTAAATGAGCCATCAATCTTACCAGGAAATGGGTATGCATACGGTATGTTTGCACCAGGTCGATGTTCTCCA
 TCGTACAATCCAACCTGCACAGGTGGGGATGCAGGGAACAGAGACTTATCTGGTTGCGCACAACCTGATCCTTTCTC
 ATGCAGCAACTGTCCAAGTGTACAAAAGGAAGTATCAGGAACATCAGAAAGGTACAATAGGCATTTCTTGCACGT
 AGTTTGGGTTATACCGCTTTCAAATAGCACATCAGATCAAAATGCTACCCAGCGATATCTTGACTTCACATGTGGA
 TGTTTTATGGACCCACTTACAGCAGGAAGGTATCCAGATAGCATGCAATATCTAGTTGGAGATCGATTGCCTAAGT
 TTACTACAGATCAAGCCAAATTAGTTAAGGGTTCATTTGATTTTATTGGACTAAACTATTACACCACTAATATGC
 TACCAAATCAGATGCGTCAACATGCTGCCACCTAGTTACCTCACAGATCTCAAGTCACTCTCTTACAGCAACGC
 AATGGGGTCTTTATAGGTCCA

15. Sequencing result of the A454F/E455A/S459V dalcochinase mutant using TRF 2 primer (989 bp)

CGTTATACTTATTTGGAGAAGGGTAAGCATTGGGATTACACTAAATGAGCCATCAATCTTCACCGGAATGGGTAT
GCATACGGTATGTTTGCACCAGGTCGATGTTCTCCATCGTACAATCCAACCTGCACAGGTGGGGATGCAGGAACAG
AGACTTATCTGGTTGCGCACAACTGATCCTTTCTCATGCAGCAACTGTCCAAGTGTACAAAAGGAAGTATCAGGA
ACATCAGAAAGGTACAATAGGCATTTCTTGCACGTAGTTGGGTTATACCGCTTTCAAATAGCACATCAGATCAA
AATGCTACCCAGCGATATCTTGACTTCACATGTGGATGGTTTATGGACCCACTTACAGCAGGAAGGTATCCAGATA
GCATGCAATATCTAGTTGGAGATCGATTGCCTAAGTTTACTACAGATCAAGCCAAATTAGTTAAGGGTTCATTTGA
TTTTATTGGACTAAACTATTACACCACTAACTATGCTACCAAATCAGATGCGTCAACATGCTGCCACCTAGTTAC
CTCACAGATCCTCAAGTCACTCTTACAGCAACGCAATGGGGTCTTTATAGGTCCAGTGACTCCCTCAGGATGGA
TGTGCATTTATCCAAAAGGACTTCGAGATTTGTTGCTTTACTTCAAGGAAAAGTATAACAATCCTTTGGTTTACAT
CACTGAAAATGGTATAGATGAGAAGAATGATGCATCACTATCACTTGAGGAATCCTTGATAGACACTTATAGAATT
GATAGTTATTATCGTCATCTCTTTTATGTTTCGATATGCAATTAGGTCTGGCGCAAATGTGAAAGGATTTTTTGCAT
GGTCATTGTTGGACAACCTTTGAATGGTTTGTCTGGTTATACAGTTCGATTTGGATTATATTTTGTGAACTACACTAC
TTTGAATAGATATCCCAAGCTCTCTGCAACATGGTTCAAGTATTTTCTGGCACGTGATCAAGAGAGTGCTAAATTG
G

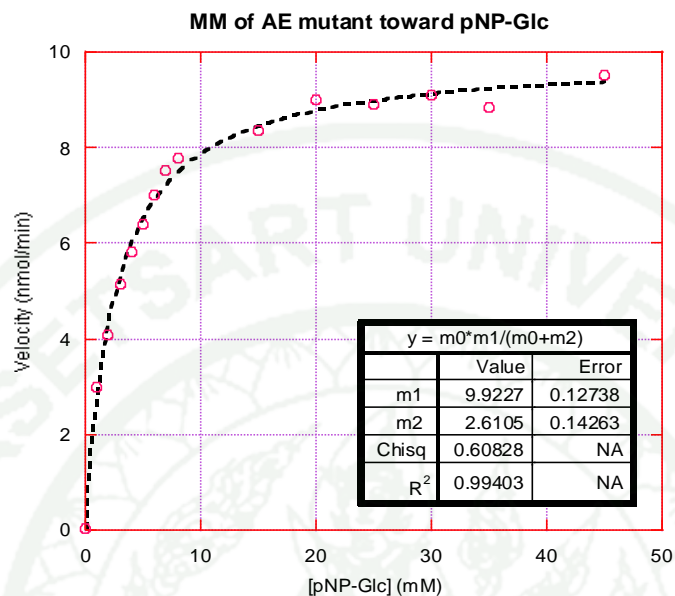
16. Sequencing result of the A454F/E455A/S459V dalcochinase mutant using TRF 3 primer (1,333 bp)

GGGGATATCAGCCAAATTTAGTTTAAAGGGTTCATTTGATTTTATTGGGACTAAACTATTACACCACTAACTATGCT
ACCAAATCAGATGCGTCAACATGCTGCCACCTAGTTACCTCACAGATCCTCAAGTCACTCTCTTACAGCAACGCA
ATGGGGTCTTTATAGGTCAGTGACTCCCTCAGGATGGATGTGCATTTATCCAAAAGGACTTCGAGATTTGTGTCT
TTACTTCAAGGAAAAGTATAACAATCCTTTGGTTTACATCACTGAAAATGGTATAGATGAGAAGAATGATGCATCA
CTATCACTTGAGGAATCCTTGATAGACACTTATAGAATTGATAGTTATTATCGTCATCTCTTTTATGTTTCGATATG
CAATTAGGTCTGGCGCAAATGTGAAAGGATTTTTTGCATGGTCATTGTTGGACAACCTTTGAATGGTTTGTCTGGTTA
TACAGTTCGATTTGGATTATATTTTGTGAACTACACTACTTTGAATAGATATCCCAAGCTCTCTGCAACATGGTTC
AAGTATTTTCTGGCACGTGATCAAGAGAGTGCTAAATTTGAAAATTTTAGCACCAAAGGCAAGATGGAGCTTATCAA
CGATGATCAAGGAAGAAAAGACAAAACCCAAGTGGGGCATTTGAAGGCTTTTGTATCTAGATCTTAATCACTAGTGAA
TTCGCGGCCCGCTGCAGTACGTAGAATTCACGTGGCCAGCCGCGCTCTCGGATCGGTACCTCGAGCCGCGCGCG
CCGCCAGCTTTCTAGAACAAAACTCATCTCAGAAGAGGATCTGAATAGCGCCGTCGACCATCATCATCATCATCA
TTGGAGTTGTAGCCTTAGACATGACTGTTCCCTCAGTTCAAGTTGGGCCTTACGAGAAGACCGGTCTTGCTAGAT
TCTAATCAAGAGGATGTCAGAATGCCATTTGCCTGAGAGATGCAGGCTTCATTTTTGATACTTTTTTATTTGTACC
TATATAGTATAGGGATTTTTTTTGTCAATTTGTTTCTTCTCGTACGAGCTTGCTCCTGATCAGCCTATCTCGCAGC
TGATGAAATCTTGGGGTAGGGGTTTGGGAAAATCATTTCCAAGTTTGATGTTTTTCTTGGTATTTCCCACTCCTC
TTCAAAGTACAGAAGATTAAGTGAGACCTTCGTTTGTGCGGATCCCCACAACCCATAGCTTCAAAGGTGCTAAC
CCCTTTTTAACCTCCCAAATTTTCCCGGACTCCGCCATCCCCGTACACTTTAAAAACCCCAAGCCAGCATA
TAAATTTCCCCCTTTCTCCCTCAGGGGGCGTAAATACCC

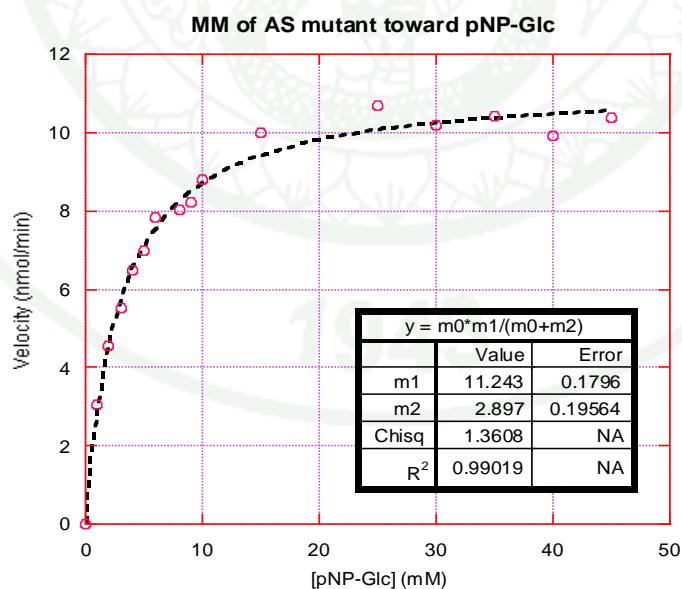


Appendix D
Kinetic studies

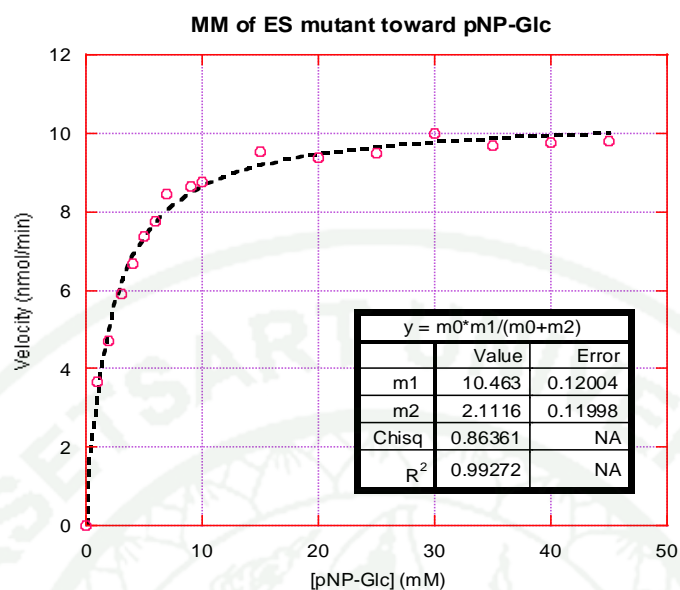
1. Kinetic parameters of dalcochinase wild-type and its mutant forms toward *p*NP-Glc



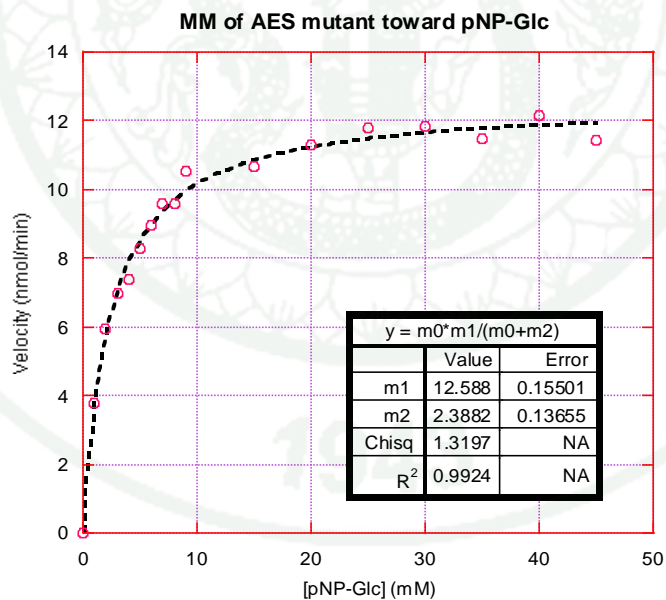
Appendix Figure D1 Michaelis-Menten plot of the A454F/E455A dalcochinase mutant toward *p*-NP-Glc



Appendix Figure D2 Michaelis-Menten plot of the A454F/S459V dalcochinase mutant toward *p*-NP-Glc

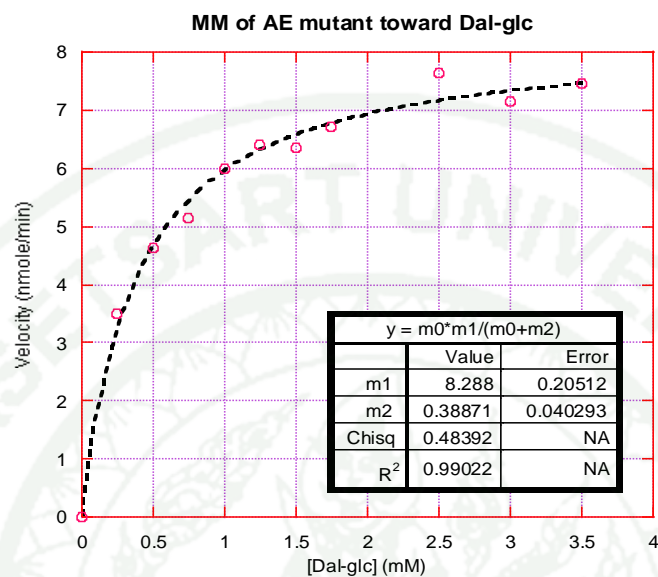


Appendix Figure D3 Michaelis-Menten plot of the E455A/S459V dalcocinase mutant toward *p*-NP-Glc

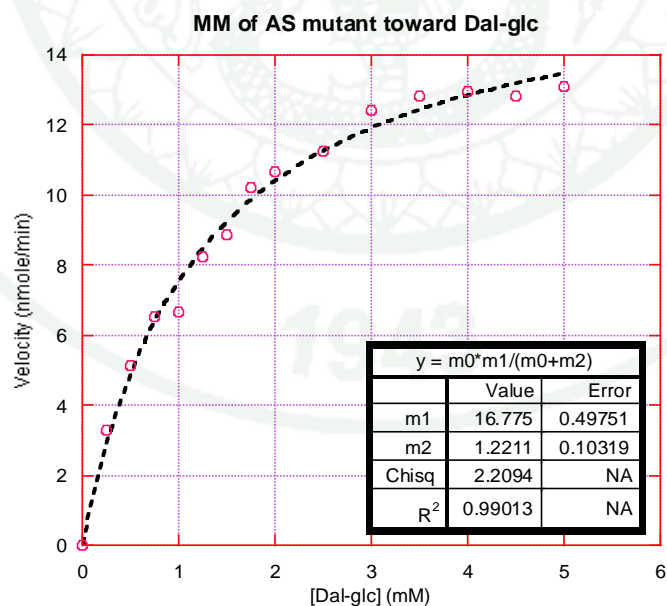


Appendix Figure D4 Michaelis-Menten plot of the A454F/E455A/S459V dalcocinase mutant toward *p*-NP-Glc

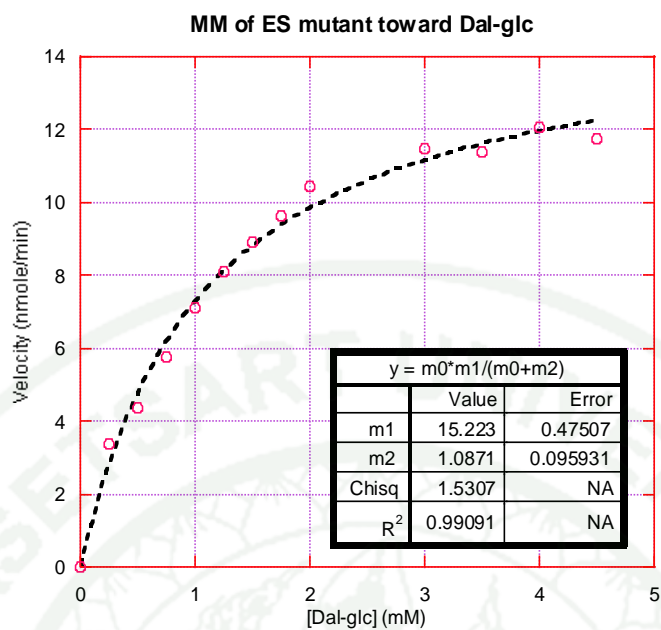
2. Kinetic parameters of dalcocinase wild-type and its mutant forms toward dalcocinin-8'-O-β-D-glucoside



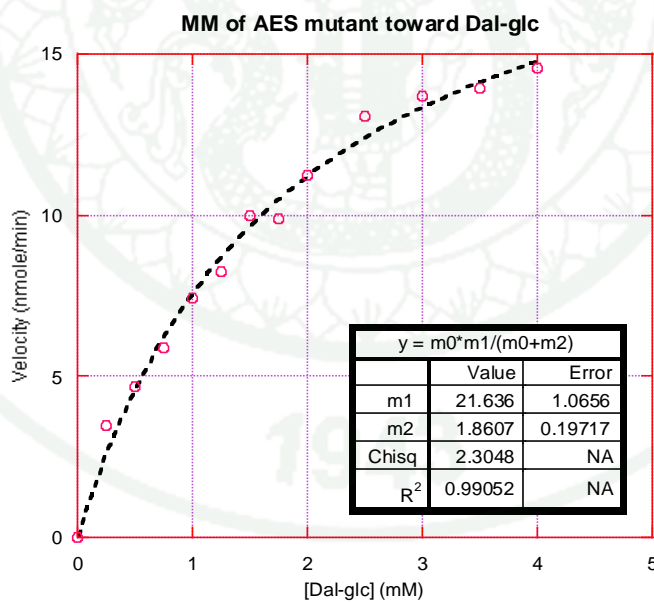
Appendix Figure D5 Michaelis-Menten plot of the A454F/E455A dalcocinase mutant toward dalcocinin-8'-O-β-D-glucoside



Appendix Figure D6 Michaelis-Menten plot of the A454F/S459V dalcocinase mutant toward dalcocinin-8'-O-β-D-glucoside

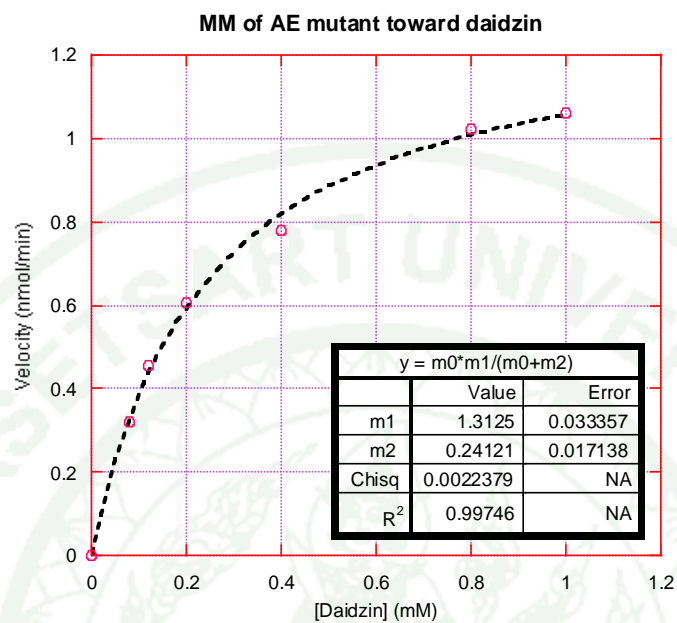


Appendix Figure D7 Michaelis-Menten plot of the E455A/S459V dalcochinase mutant toward dalcochinin-8'-O-β-D-glucoside

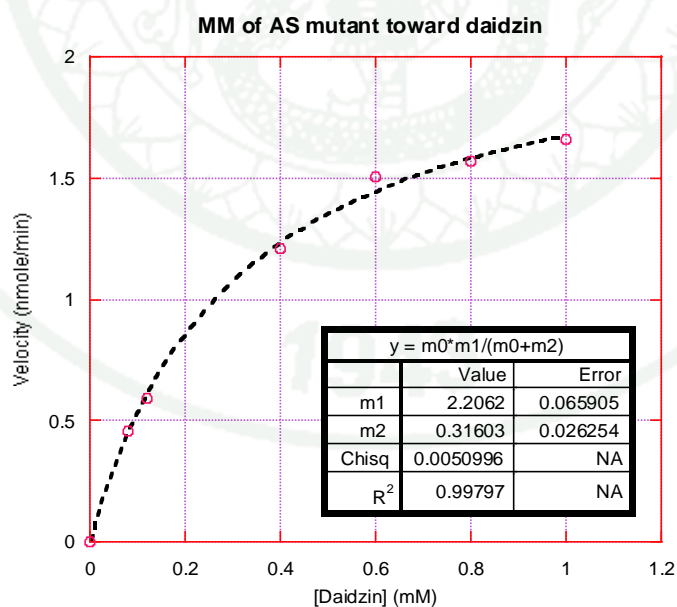


Appendix Figure D8 Michaelis-Menten plot of the A454F/E455A/S459V dalcochinase mutant toward dalcochinin-8'-O-β-D-glucoside

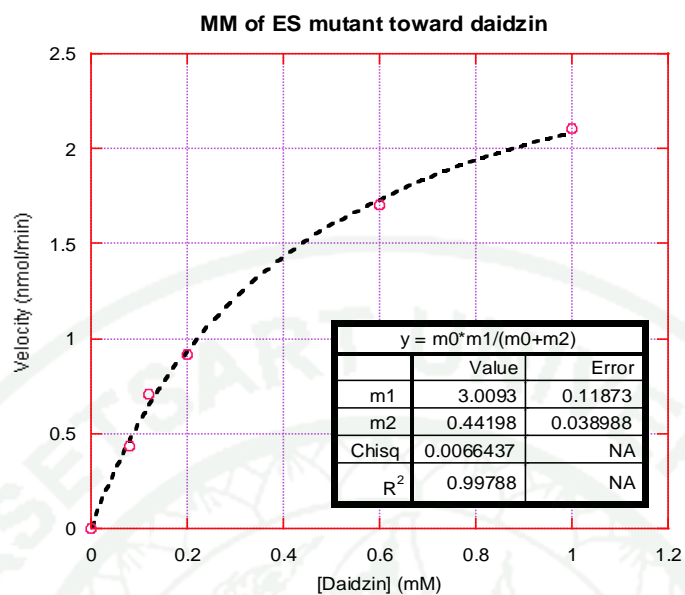
3. Kinetic parameters of dalcochinase wild-type and its mutant forms toward daidzin



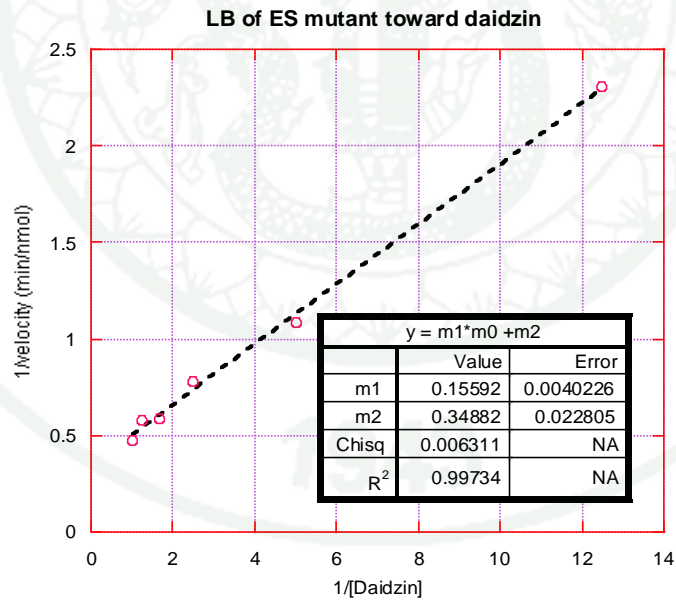
Appendix Figure D9 Michaelis-Menten plot of the A454F/E455A dalcochinase mutant toward daidzin



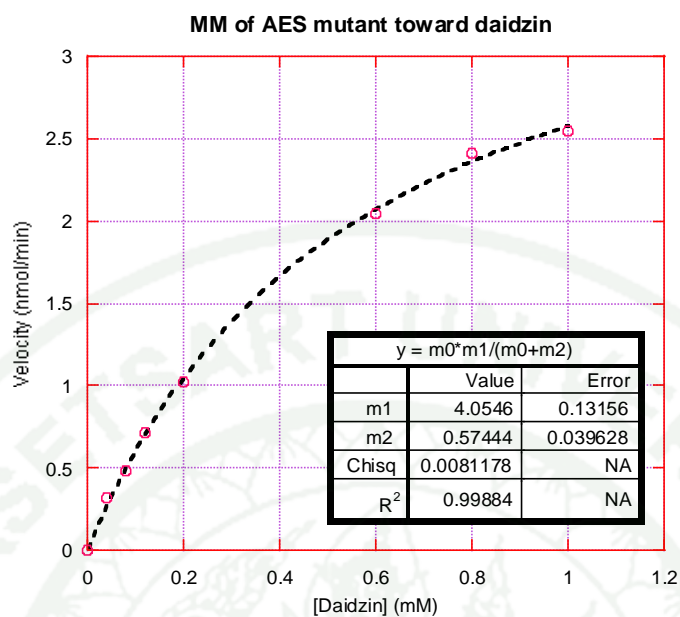
Appendix Figure D10 Michaelis-Menten plot of the A454F/S459V dalcochinase mutant toward daidzin



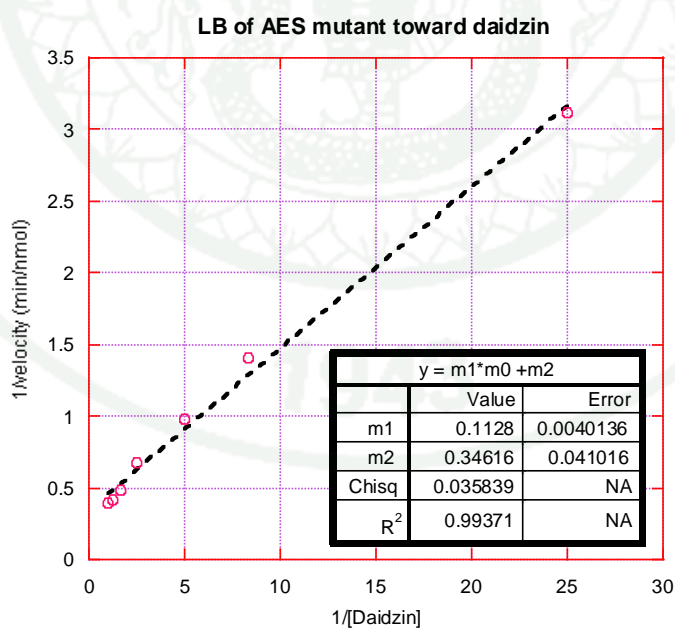
Appendix Figure D11 Michaelis-Menten plot of the E455A/S459V daldochinase mutant toward daidzin



Appendix Figure D12 Lineweaver-Burk plot of the E455A/S459V daldochinase mutant toward daidzin

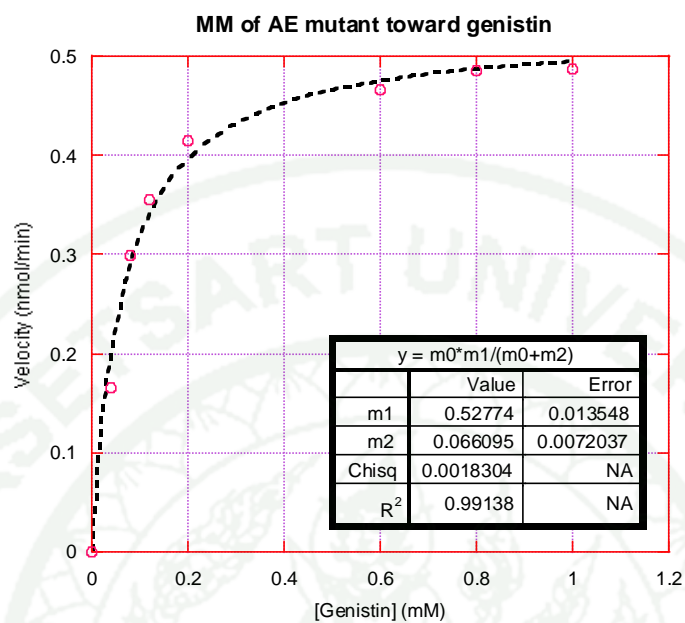


Appendix Figure D13 Michaelis-Menten plot of the A454F/E455A/S459V dalcochinase mutant toward daidzin

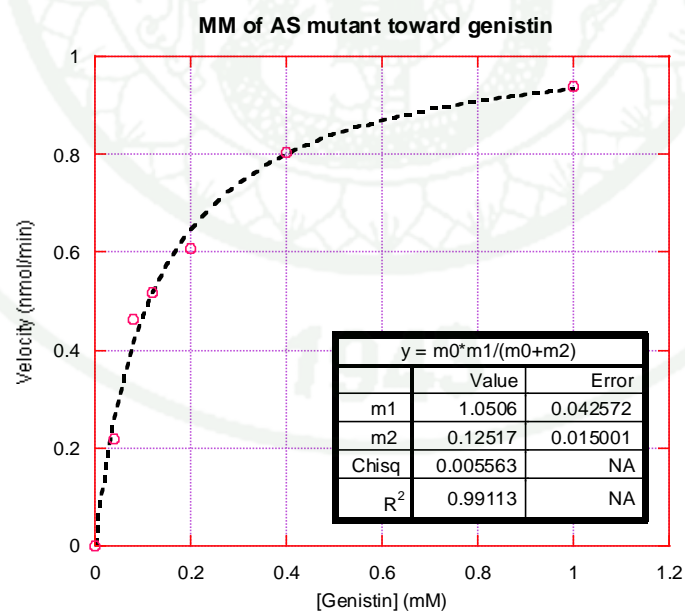


Appendix Figure D14 Lineweaver-Burk plot of the A454F/E455A/S459V dalcochinase mutant toward daidzin

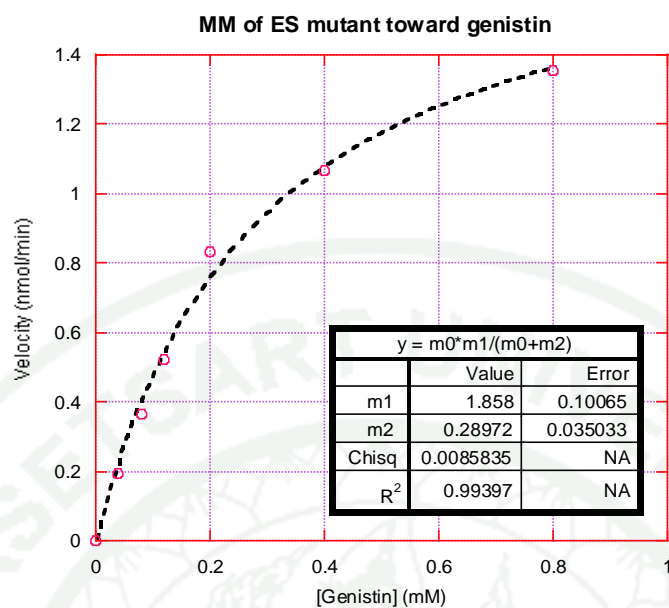
4. Kinetic parameters of dalcochinase wild-type and its mutant forms toward genistin



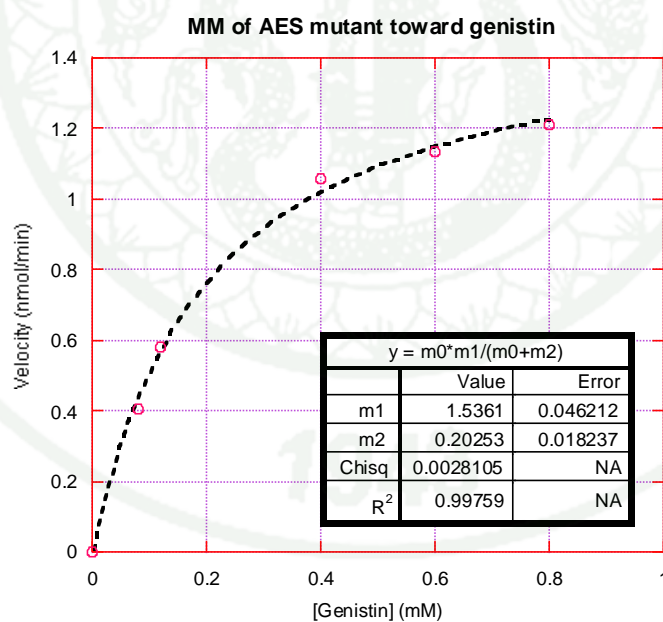
Appendix Figure D15 Michaelis-Menten plot of the A454F/E455A dalcochinase mutant toward genistin



Appendix Figure D16 Michaelis-Menten plot of the A454F/S459V dalcochinase mutant toward genistin

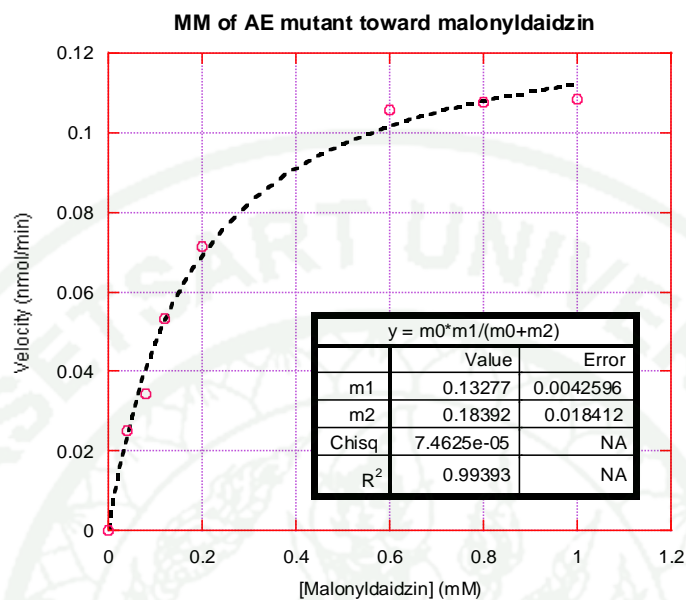


Appendix Figure D17 Michaelis-Menten plot of the E455A/S459V dalcochinase mutant toward genistin

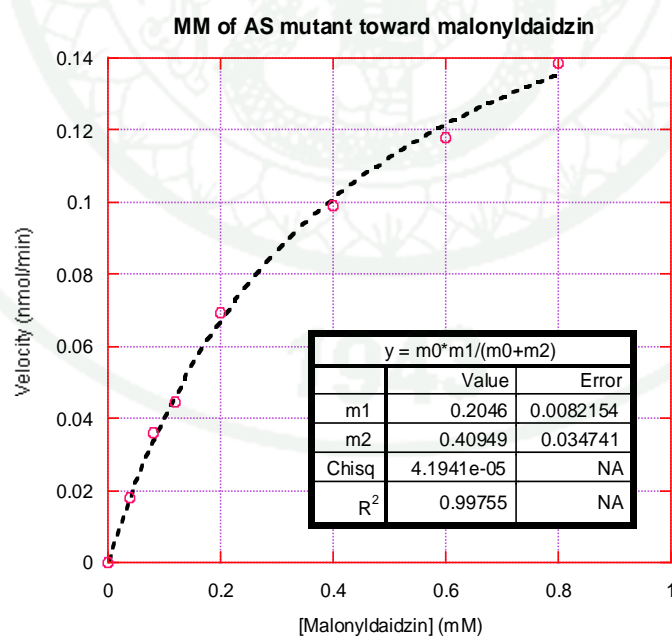


Appendix Figure D18 Michaelis-Menten plot of the A454F/E455A/S459V dalcochinase mutant toward genistin

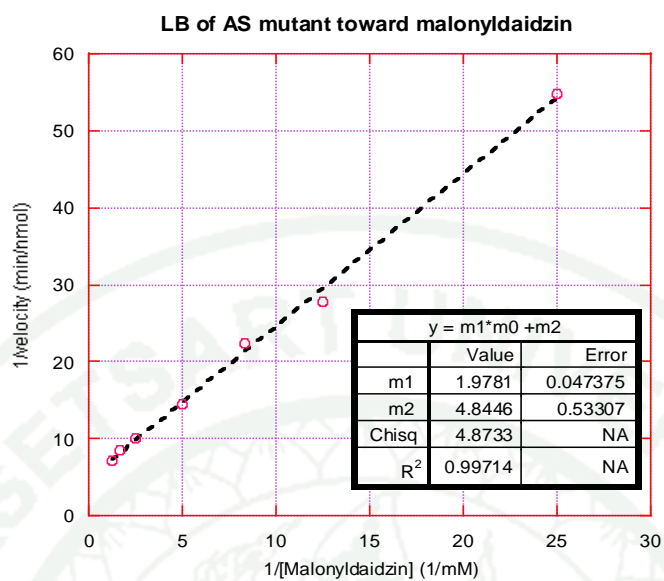
5. Kinetic parameters of dalcochinase wild-type and its mutant forms toward malonyldaidzin



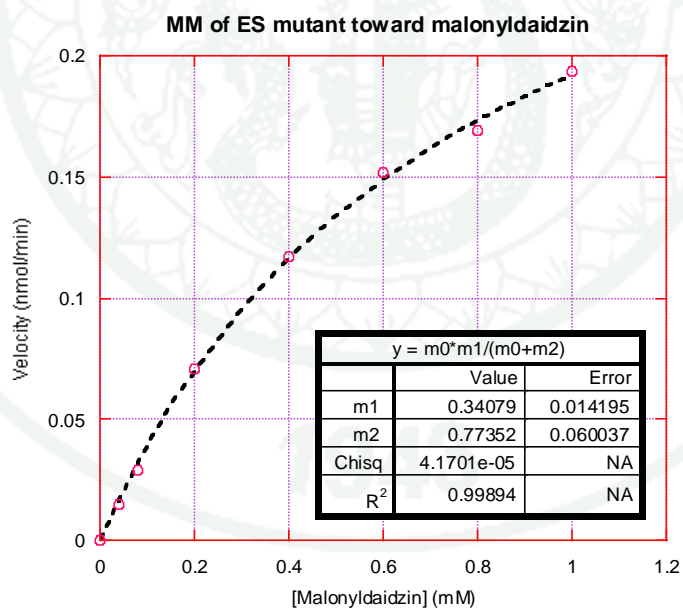
Appendix Figure D19 Michaelis-Menten plot of the A454F/E455A dalcochinase mutant toward malonyldaidzin



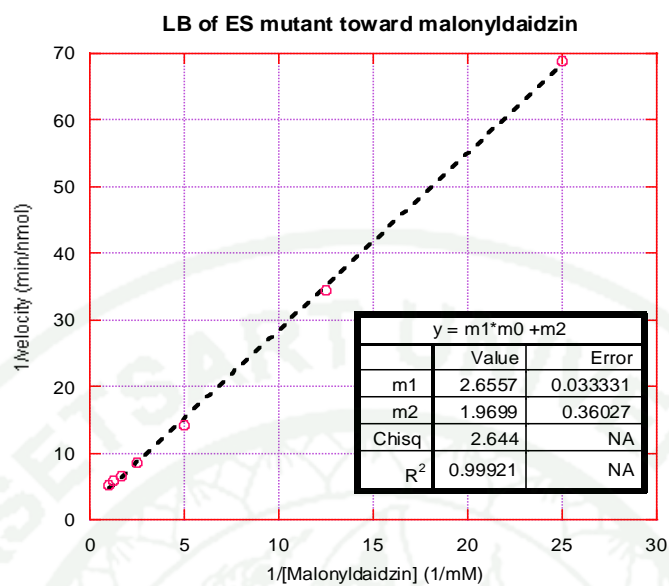
Appendix Figure D20 Michaelis-Menten plot of the A454F/S459V dalcochinase mutant toward malonyldaidzin



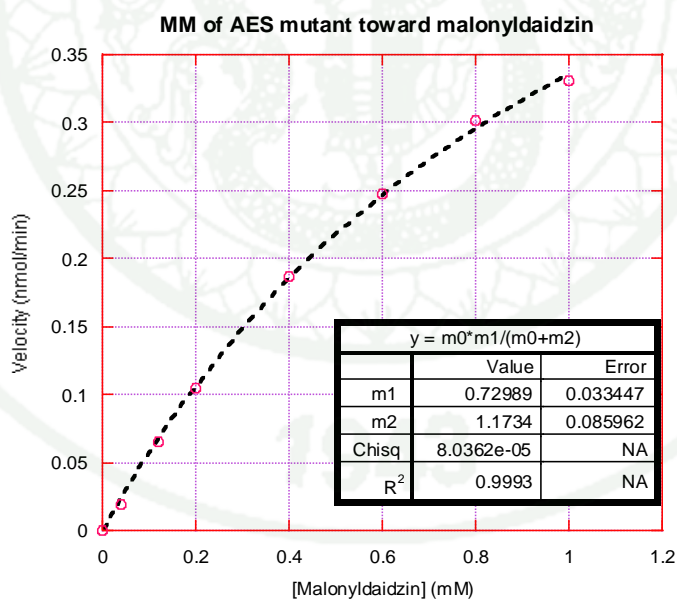
Appendix Figure D21 Lineweaver-Burk plot of the A454F/S459V dalcochinase mutant toward malonyldaidzin



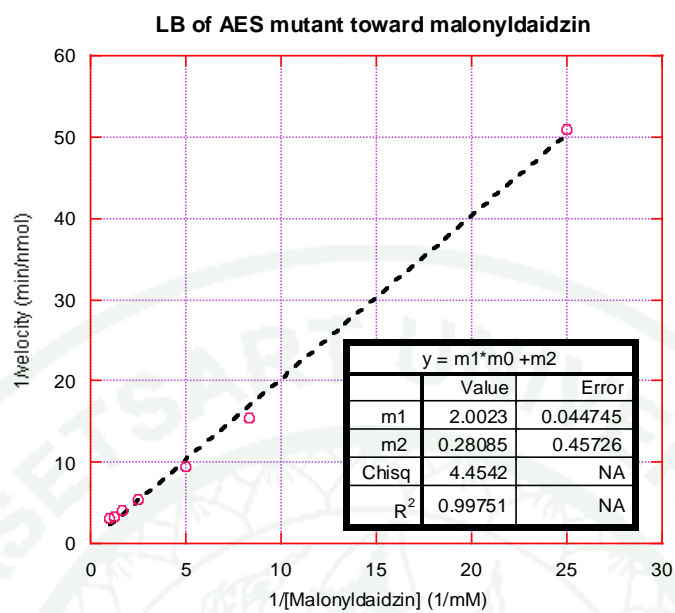
Appendix Figure D22 Michaelis-Menten plot of the A454F/S459V dalcochinase mutant toward malonyldaidzin



Appendix Figure D23 Lineweaver-Burk plot of the E455A/S459V dalcochinase mutant toward malonyldaidzin

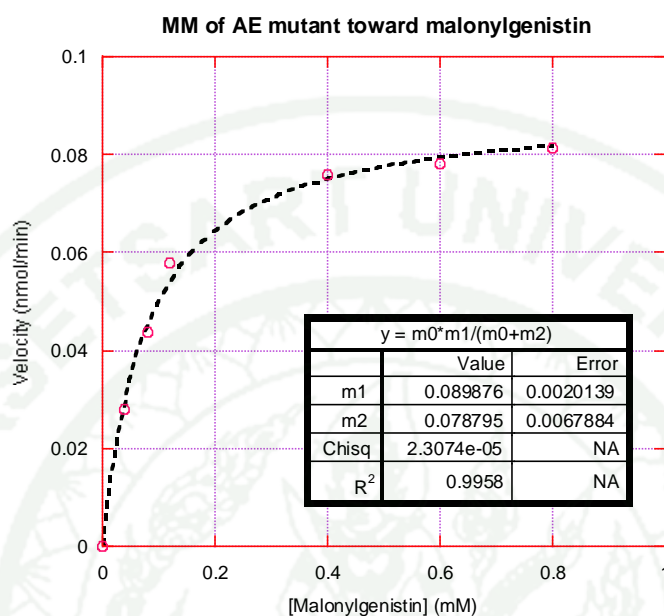


Appendix Figure D24 Michaelis-Menten plot of the A454F/E455A/S459V dalcochinase mutant toward malonyldaidzin

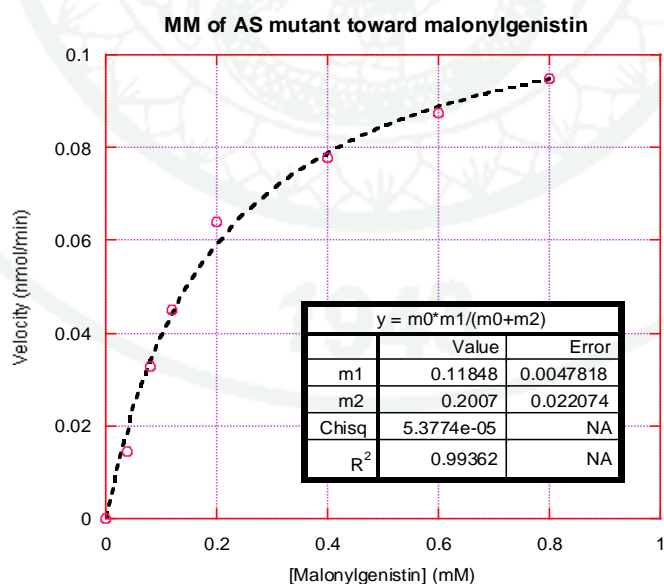


Appendix Figure D25 Lineweaver-Burk plot of the A454F/E455A/S459V dalcochinase mutant toward malonyldaidzin

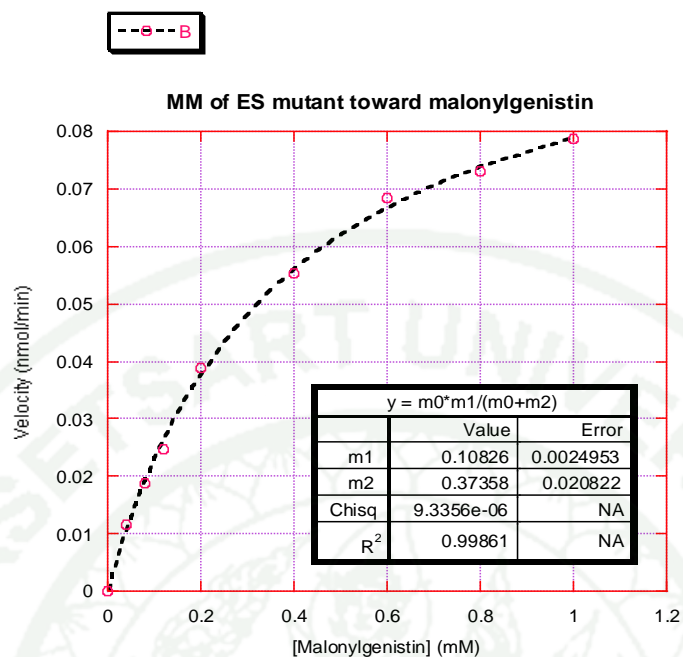
6. Kinetic parameters of dalcochinase wild-type and its mutant forms toward malonylgenistin



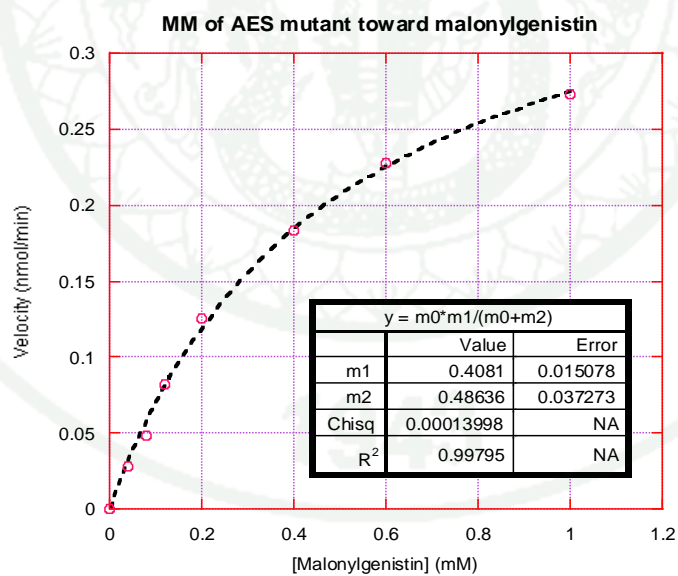
Appendix Figure D26 Michaelis-Menten plot of the A454F/E455A dalcochinase mutant toward malonylgenistin



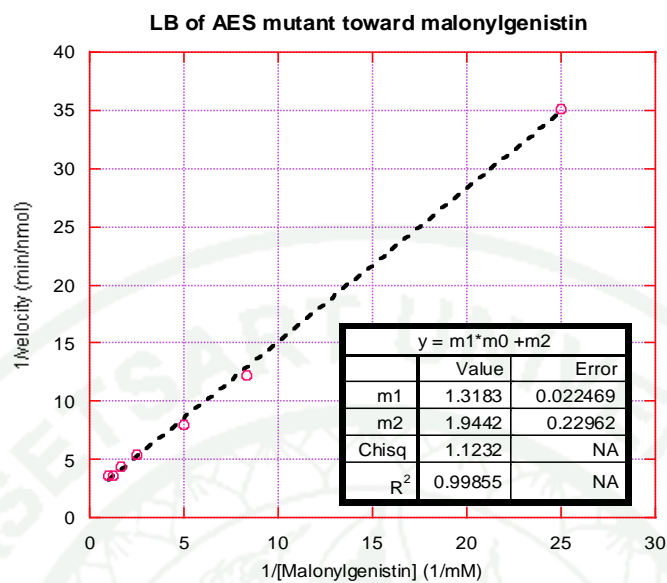
Appendix Figure D27 Michaelis-Menten plot of the A454F/S459V dalcochinase mutant toward malonylgenistin



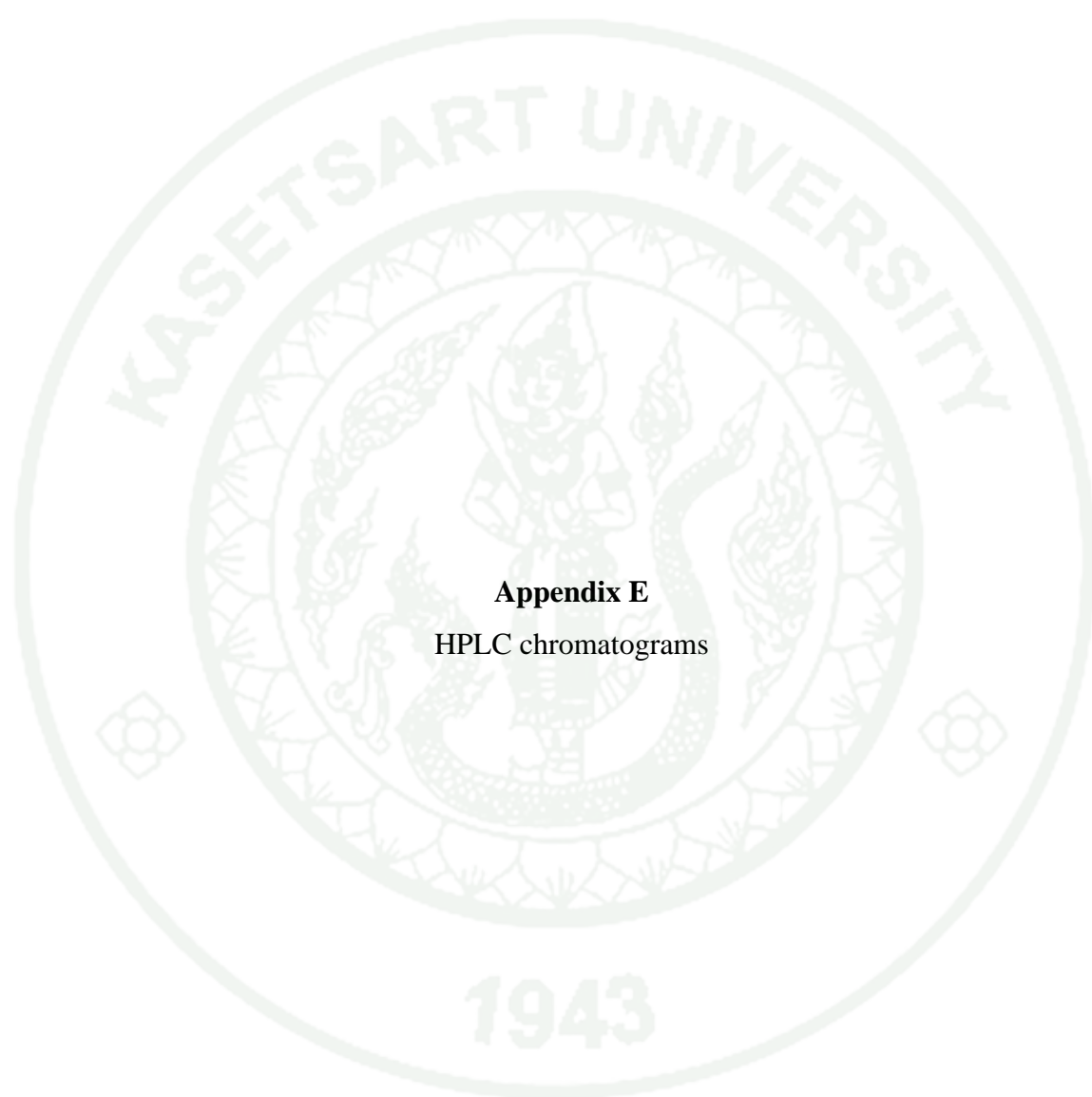
Appendix Figure D28 Michaelis-Menten plot of the E455A/S459V dalcochinase mutant toward malonylgenistin



Appendix Figure D29 Michaelis-Menten plot of the A454F/E455A/S459V dalcochinase mutant toward malonylgenistin



Appendix Figure D30 Lineweaver-Burk plot of the A454F/E455A/S459V dalcochinase mutant toward malonylgenistin

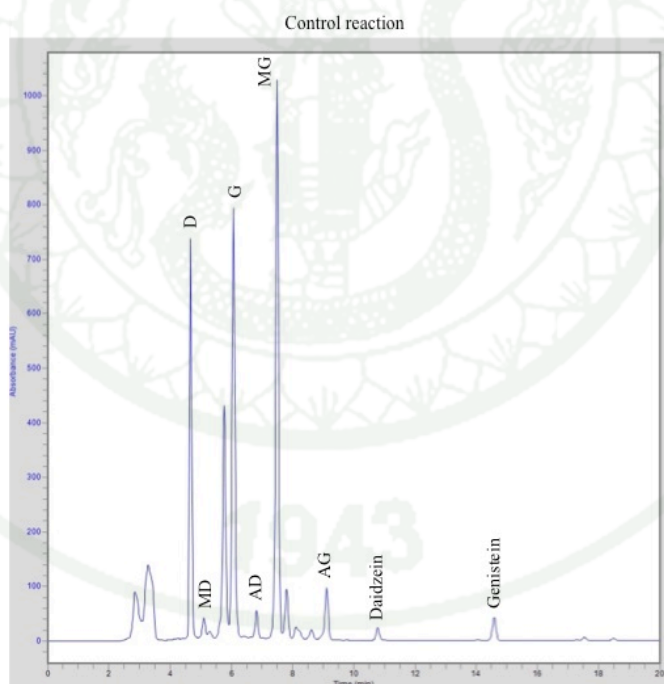


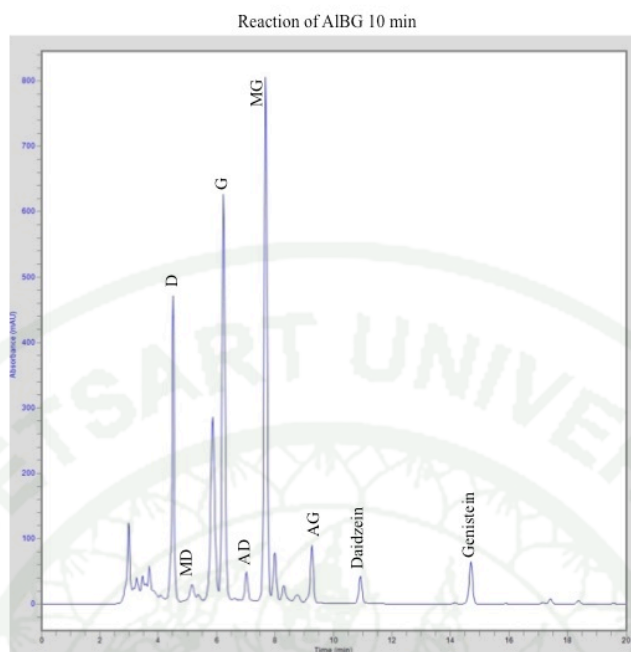
Appendix E
HPLC chromatograms

Appendix Table E1 Area under peaks of the soybean isoflavone glucoside standards.

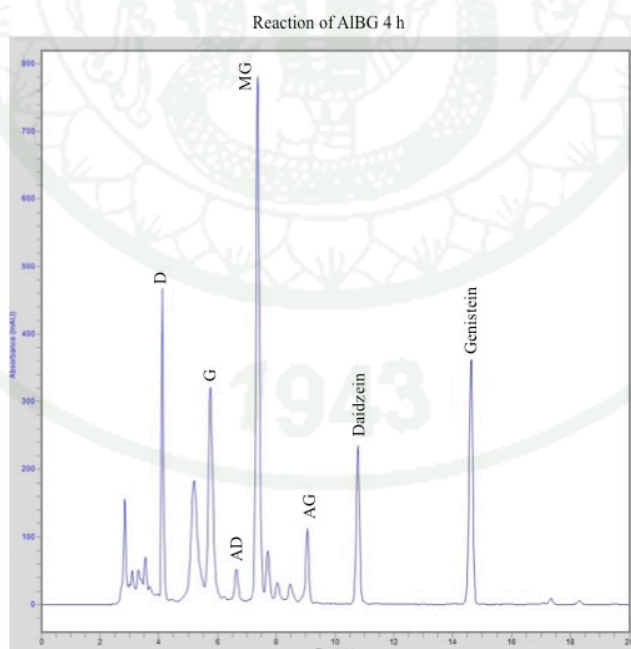
Soybean isoflavones	Retention time (min)	Area under peaks (unit)
Daidzin	4.381	2028624.53
Genistin	6.070	3246779.93
Malonyldaidzin	4.917	921038.69
Malonylgenistin	7.522	3061445.72
Acetyldaidzin	6.833	2295581.03
Acetylgenistin	9.150	3669062.63
Daidzein	10.833	2059426.86
Genistein	14.654	2954286.14

1. Hydrolysis of soybean flour extracts

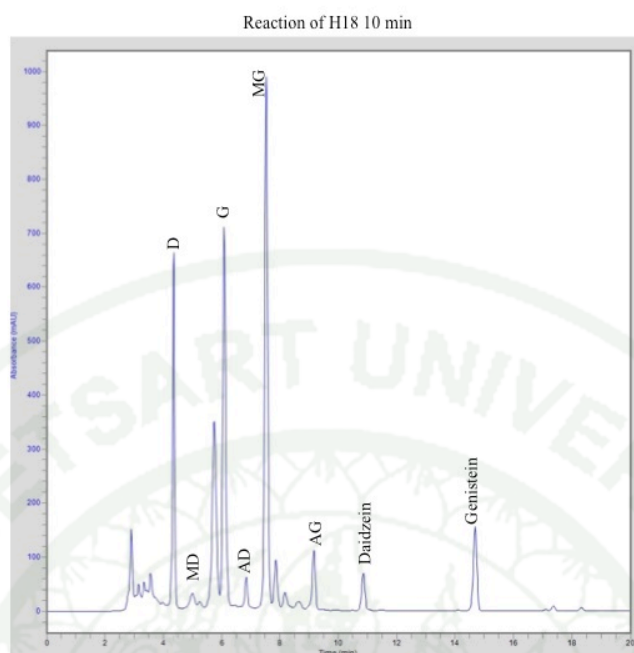
**Appendix Figure E1** HPLC chromatogram of control reaction



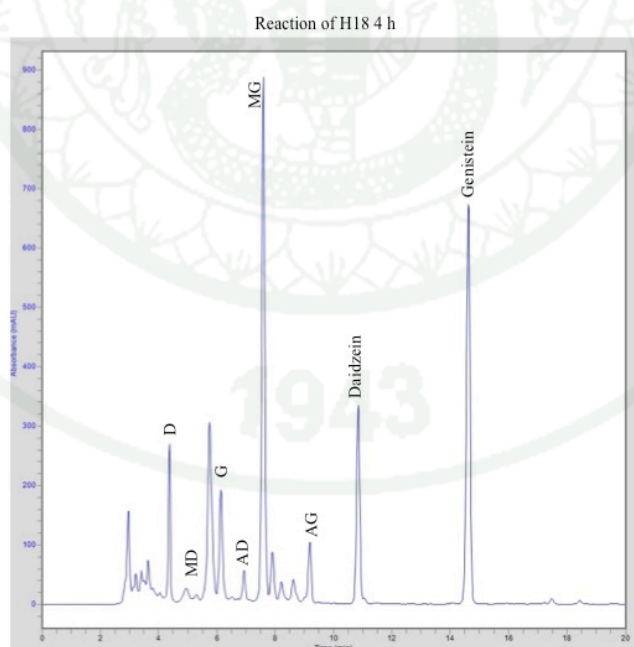
Appendix Figure E2 HPLC chromatogram of reaction incubated with almond β -glucosidase at 10 min.



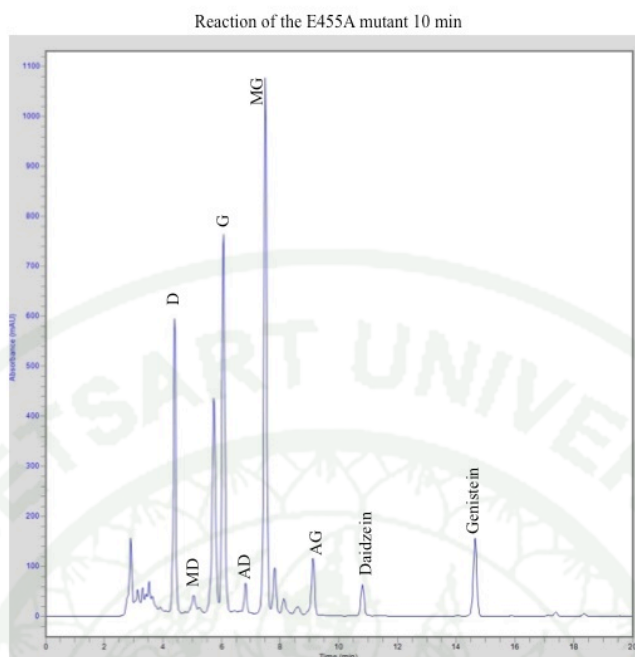
Appendix Figure E3 HPLC chromatogram of reaction incubated with almond β -glucosidase at 4 h.



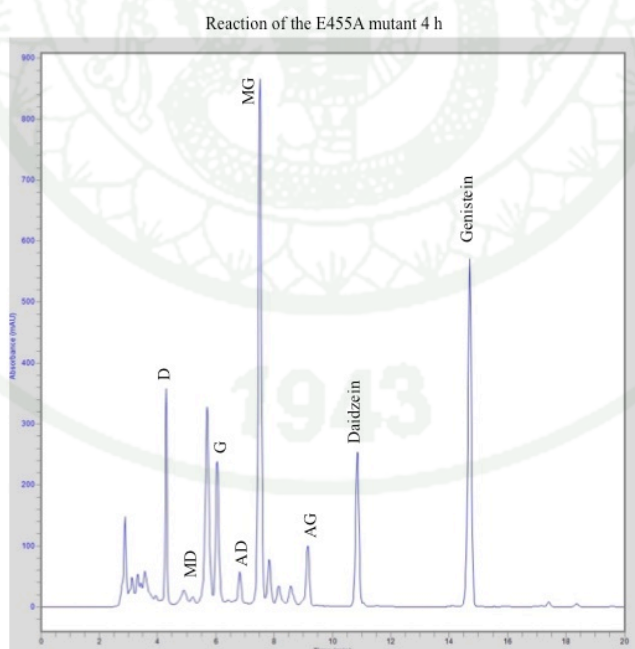
Appendix Figure E4 HPLC chromatogram of reaction incubated with the wild-type dalcochinase at 10 min.



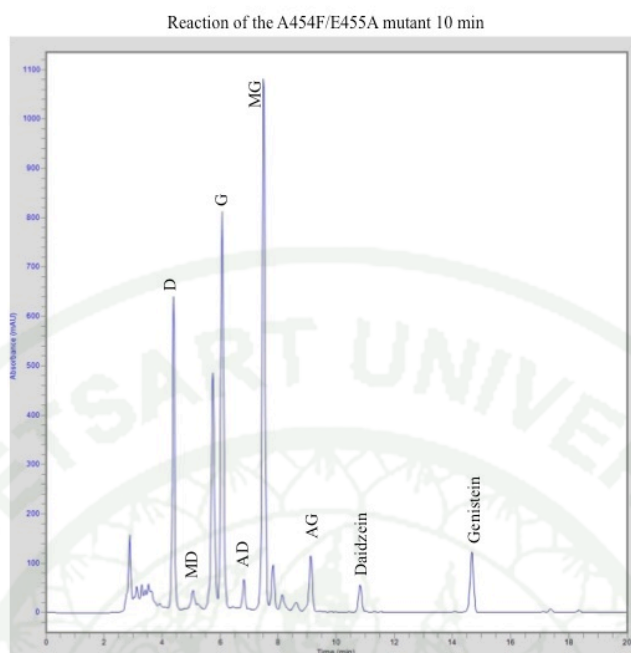
Appendix Figure E5 HPLC chromatogram of reaction incubated with the wild-type dalcochinase at 4 h.



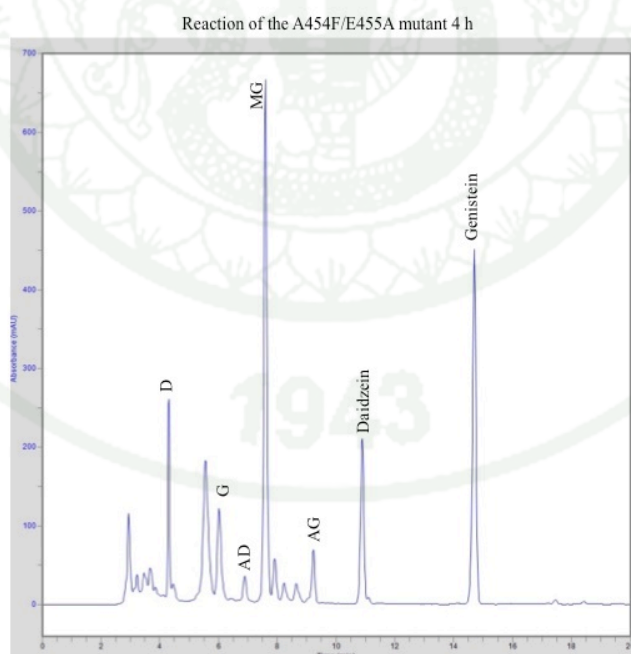
Appendix Figure E6 HPLC chromatogram of reaction incubated with the E455A mutant at 10 min.



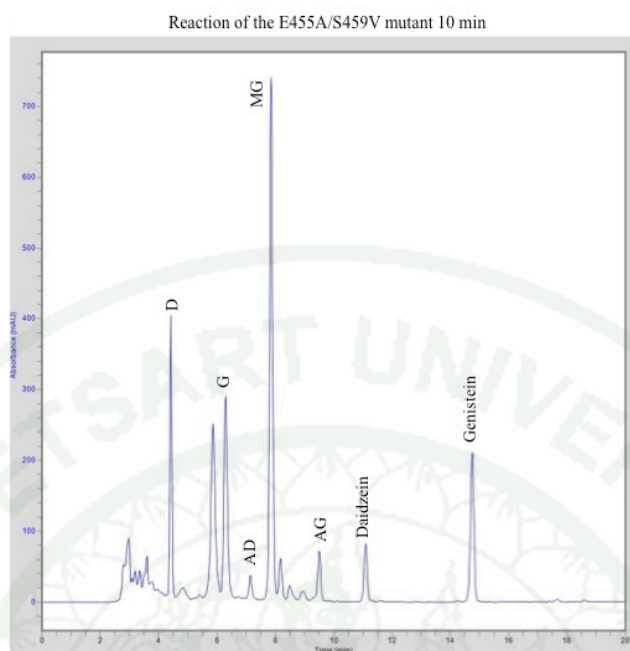
Appendix Figure E7 HPLC chromatogram of reaction incubated with the E455A mutant at 4 h.



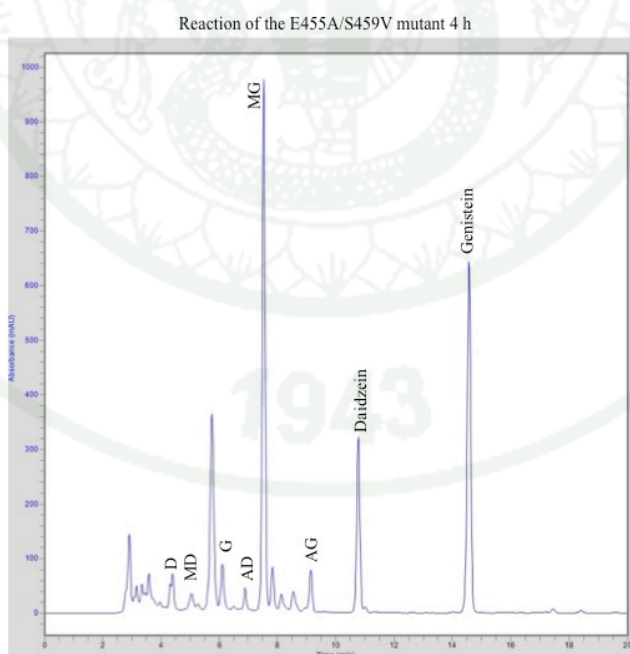
Appendix Figure E8 HPLC chromatogram of reaction incubated with the A454F/E455A mutant at 10 min.



Appendix Figure E9 HPLC chromatogram of reaction incubated with the A454F/E455A mutant at 4 h.



Appendix Figure E10 HPLC chromatogram of reaction incubated with the E455A/S459V mutant at 10 min.



Appendix Figure E11 HPLC chromatogram of reaction incubated with the E455A/S459V mutant at 4 h.

CIRRICULUM VITAE

NAME : Mr. Satrawut Charoenla

BIRTH DATE : January 25, 1989

BIRTH PLACE : Lampang, Thailand

EDUCATION	: <u>YEAR</u>	<u>INSTITUTE</u>	<u>DEGREE/DIPLOMA</u>
	2011	Kasetsart Univ.	B.Sc. Hons II (Biochemistry)

SCHOLARSHIP/AWARD : M.S. scholarship from the Center for Advanced Studies in Tropical Natural Resources under the project of National Research Universities, Kasetsart University, Bangkok, Thailand

CONFERENCES PRESENTATION

1. Satrawut Charoenla and Prachumporn Kongsaree. 2014. Protein Engineering of a β -Glucosidase for Hydrolysis of Soybean Isoflavonoids. The 4th International Biochemistry and Molecular Biology Conference 2014: Bridging ASEAN Biochemical Research Communities. April 2nd-3rd 2014, Rama Gardens Hotel & Resort, Bangkok, Thailand.